GEOCHRONOLOGIC AND ISOTOPIC INVESTIGATION OF THE KOIPATO FORMATION, NORTHWESTERN GREAT BASIN, NEVADA: IMPLICATIONS FOR LATE PERMIAN-EARLY TRIASSIC TECTONICS ALONG THE WESTERN U.S. CORDILLERA

By

Nicholas Quentin Vetz

A thesis

submitted in partial fulfillment

of the requirements for the degree of

Master of Science in Geology

Boise State University

August 2011

BOISE STATE UNIVERSITY GRADUATE COLLEGE

DEFENSE COMMITTEE AND FINAL READING APPROVALS

of the thesis submitted by

Nicholas Quentin Vetz

Thesis Title: Geochronologic and Isotopic Investigation of the Koipato Formation, Northwestern Great Basin, Nevada: Implications for Late Permian-Early Triassic Tectonics along the Western U.S. Cordillera

Date of Final Oral Examination: 04 March 2011

The following individuals read and discussed the thesis submitted by student Nicholas Quentin Vetz, and they evaluated his presentation and response to questions during the final oral examination. They found that the student passed the final oral examination.

Walter S. Snyder, Ph.D.	Chair, Supervisory Committee
Clyde J. Northrup, Ph.D.	Member, Supervisory Committee
Craig M. White, Ph.D.	Member, Supervisory Committee
Mark D. Schmitz, Ph.D.	Member, Supervisory Committee

The final reading approval of the thesis was granted by Walter S. Snyder, Ph.D., Chair of the Supervisory Committee. The thesis was approved for the Graduate College by John R. Pelton, Ph.D., Dean of the Graduate College.

ACKNOWLEDGEMENTS

First, I would like to thank my advisor, Dr. Walter Snyder, for affording me with this opportunity, and for providing the support and help I required over the course of this thesis to finally complete my research. I would like to thank Dr. Mark Schmitz for all the help and guidance with the geochronology and isotopic work required for this study, for being on my committee, and for providing valuable critiques and discussions of my data. I would also like to thank Dr. C.J. Northrup and Dr. Craig White for being on my committee and providing valuable assistance and discussion topics. I would like to thank Jim Crowley for teaching me the many lab procedures, helping me when I forgot them, and for chatting with me when I needed a break from writing my thesis. I would like to thank Ashley Dack for showing me the ropes when I first arrived in Boise, Kyle Tumpane for all the help formatting my thesis and answering any questions I had, Dimitrios Lalos for listening to me rant and for just chatting when I couldn't write any more, A.J. Zenkert for providing me with a place to live and some great entertainment over the past few years, and Jayme Allen for making the last few months of this process much more bearable and enjoyable. Last, but certainly not least, I would like to thank my Mom and Dad for providing me with such great opportunities throughout my life, believing and encouraging me to accomplish my goals, and without whose support I would not be where I am today.

ABSTRACT

The volcanics of the Early Triassic Koipato Formation of central Nevada unconformably overlie the Golconda Allochthon and, classically, this relationship has been used to define the timing of the Sonoma Orogeny as post-Middle Permian to earliest Triassic. However, the Koipato Formation represents a rather isolated magmatic succession, with other western U.S. Early Mesozoic igneous provinces determined to be younger or lacking rocks of Koipato age. This isolation, coupled with the fact that the Koipato Formation does not overlap the Golconda Allochthon, has left open two possible scenarios for its tectonic history: 1) the Koipato Formation represents the earliest, post-Sonoma Orogeny continental margin arc magmatism, which then quickly shifted the locus of magmatism to other locations, or 2) the Koipato Formation was part of an offshore island arc that was deposited on its subduction complex (the eventual Golconda Allochthon), and then this piggyback complex was thrust over the continental margin in post-Koipato time. The Koipato Formation, of central Nevada, is largely composed of Early Triassic, intermediate to felsic, intrusive and volcanic units with minor amounts of sedimentary and metasedimentary rocks, which have been classically subdivided into three units: (in ascending order) the Limerick Greenstone, Rochester Rhyolite, and Weaver Rhyolite. This stratigraphic scheme has been modified by research presented here. The focus of this research has been to help clarify the age and tectonic and magmatic frameworks of the Koipato Formation, in particular as it impacts the

interpretations for the Sonoma Orogeny and the Early Mesozoic Cordilleran magmatic arcs.

New field evidence and geochronology presented in this study demonstrate that the Koipato Formation represents an intermediate to felsic volcanic sequence that documents a short-lived latest Permian to Early Triassic series of magmatic events. Geochronologic data identifies previously unrecognized unconformities within the Koipato Formation and helps to constrain these unconformities and the ones bounding the Koipato Formation.

Field evidence and U-Pb geochronology support the interpretation that the Rochester and lower Weaver Rhyolites are partly coeval units. Also, U-Pb geochronology has proven that the silicic intrusive units observed throughout the Humboldt Range are coeval to the older sequence of the Rochester and the lower Weaver Rhyolites and acted as feeders for these felsic volcanics. Finally, two phases of silicic volcanism are identified within the Koipato Formation, which are separated by a previously unidentified unconformity. This unconformity is documented to have a time span of <350,000 years and separates the older Rochester and Weaver Rhyolites in Troy Canyon and the East and Tobin Ranges from the young Rochester and lower Weaver Rhyolites of Limerick Canyon and the sedimentary and upper Weaver Rhyolites in Troy Canyon. Also, this unconformity records the erosion of the older phase of silicic volcanism from the west side of the Humboldt Range.

U-Pb geochronology shows that the Koipato Formation is predominately late Early Triassic (249.59 to 248.32 Ma), with the majority of volcanism lasting for ~1.2 Ma.

The existence of ~254 Ma inherited zircons within the leucogranite of the Humboldt Range has been inferred to represent the earliest stages of Limerick Greenstone-type Koipato volcanism, which extends the age of Koipato Formation volcanism to the latest Permian. The unconformity between the Limerick Greenstone and Rochester Rhyolite identified by Wilkins (2010) in the East Range has been dated and spans a time gap of ~200,000 years in Troy Canyon and ~1 Ma in Limerick Canyon of the Humboldt Range. Also, this unconformity may have a slight angular component, but this could not be confirmed in the Humboldt Range. This unconformity documents that the transition from intermediate to felsic volcanism was associated with a pause in magmatism and perhaps tectonism. The unconformity between the Golconda Allochthon and the Koipato Formation has been constrained in this study to represent a time gap of ~15 to 6 Ma based on the age of Middle Permian for the youngest unit within the Golconda Allochthon and ~254 Ma from the inherited grains of the leucogranite intrusive. The unconformity between the overlying Prida Formation and the Koipato Formation represents a time gap of ~3 to7 Ma based on an Anisian age of the Prida Formation and the 248.32 Ma obtained from the youngest sample of the Koipato Formation. This time gap would be long enough to allow for a major change from the volcanic setting of the Koipato Formation to a carbonate platform, which is required for deposition of the Prida Formation.

Sr and Nd isotopic investigation of the Koipato Formation demonstrates that intermediate to felsic members exhibit uniformly high $^{87}Sr/^{86}Sr$ (0.7089 – 0.7126) and fairly negative εNd values (-9.73 – -12.89). These compositions require that the volcanics of the Koipato Formation were at least partially sourced from Precambrian continental

crust material. Nd (T_{DM}) isotopic evolution modeling for these samples yield mantle extraction model ages of the source continental crustal material between 1.7 and 2.4 Ga, and indicate that the Koipato Formation was erupted through Paleoproterozoic crust.

These data also imply that the underlying Golconda Allochthon was, at the time of Koipato magmatism, already overlying the continental margin, thus precluding the interpretation that the Koipato Formation and the Golconda Allochthon were emplaced piggyback onto the continental margin in post-Koipato time. These data, however, still leave open the possibility that final emplacement of the Golconda Allochthon, with the Koipato Formation on top, did not occur until a later time in the Mesozoic.

TABLE OF CONTENTS

LIST OF TABLES

LIST OF FIGURES

CHAPTER ONE: INTRODUCTION AND BACKGROUND

Introduction

The Paleozoic-Mesozoic tectonic history of central Nevada is characterized by a series of distinct events that provide the framework for understanding the tectonomagmatic history of the Triassic Koipato Formation. This chapter will present a synthesis both of the previous investigations of the Koipato Formation and an overview of the tectonic history of the western U.S. Cordillera, focusing mainly in the area of central Nevada during the Late Paleozoic to Early Mesozoic. This review is intended to provide a framework for the stratigraphic, geochronologic, and isotopic investigations discussed later in this report.

Koipato Formation

The Koipato Formation, of central Nevada, is largely composed of Early Triassic, intermediate to felsic, intrusive and volcanic units with minor amounts of sedimentary and metasedimentary rocks, which are subdivided into three units: (in ascending order) the Limerick Greenstone, Rochester Rhyolite, and Weaver Rhyolite (Fig. 1.1). The Koipato Formation is restricted to west-central Nevada, primarily in the Humboldt (type locality), East, Sonoma, and Tobin Ranges (Fig. 1.2). The Koipato Formation was first identified and described during the U.S. Geological Survey 40th parallel survey by King (1878). King (1878) describes the Koipato Formation as consisting of metamorphosed

siliceous and argillaceous sediments of probable Triassic age, based on fossil fragments that he found in the Humboldt Range (MacMillan, 1972). King (1878) also noted that the Koipato Formation is conformably overlain by younger Triassic carbonates (MacMillan, 1972). Interestingly, King (1878) makes no mention of volcanic units within the Koipato Formation, which were not recognized until Ransome (1909) noted the predominately volcanic nature of the Koipato Formation (MacMillan, 1972). Knopf (1924) was the first to subdivide the Koipato Formation into separate lithologic units, which he termed the Rochester Trachyte, Nenzel Rhyolite Breccia, and the Weaver Rhyolite. Knopf's (1924) work was also the first to describe the interbedding of sedimentary units with felsic tuffs, which he primarily identified within the Weaver Rhyolite. Jenney (1935) became the first to subdivide the Koipato Formation into a semblance of the modern terminology by naming the subunits the Limerick Keratophyre, Rochester Rhyolite, and Weaver Rhyolite. However, nowhere in Jenney's (1935) unit descriptions are any sedimentary layers described. More recent research and geologic mapping of the Humboldt Range by Wallace et al. (1969a, b) expanded on these initial investigations, increased our understanding of, and formalized the stratigraphic succession within the Koipato Formation. Wallace et al. (1969a, b) support the stratigraphic nomenclature of Jenney (1935) and separate the Koipato Formation into the Limerick Greenstone, Rochester Rhyolite, and Weaver Rhyolite (Fig. 1.1). This stratigraphic order is still employed, but the lithologic, geochronologic, and isotopic evidence presented in this thesis demonstrates that this stratigraphic succession is not as straightforward as has been assumed.

Limerick Greenstone

The lowermost unit of the Koipato Formation, the Limerick Greenstone, is probably the least studied of the Koipato Formation subunits, but it has important tectonic implications due to its interpreted position as the basal member of the Koipato Formation (Fig. 1.1). The Limerick Greenstone is primarily exposed and described in the Humboldt Range, with exposures identified, to the east, in the southern East and Tobin Ranges (Fig. 1.2) (Burke, 1973). The base of the Limerick Greenstone is not exposed in the Humboldt Range. Early preliminary research into the Limerick Greenstone identified only one mappable unit, but more recent work by Vikre (1977) separated out three distinct units: 1) biotite-hornblende andesite, 2) schistose metasediments, and 3) intermediate rhyodacite flows, tuffs, and andesitic greenstones. Vikre (1977) postulated that the biotite-hornblende andesite may be an intrusive unit that is younger than the other subunits of the Koipato Formation, but no fossil assemblages have been identified or radiometric ages produced for any part of the Limerick Greenstone. Vikre (1977) noted that the metasediments within the Limerick Greenstone are probably local features that were either coeval or immediately postdated the volcanic assemblages. The last subunit of the Limerick Greenstone identified by Vikre (1977), the intermediate rhyodacite flows, tuffs, and andesitic greenstones, likely were erupted coevally with the deposition of the schistose metasediments, but its relation to the biotite-hornblende andesite sequence is not clear. Extensive hydrothermal alteration has completely altered the original mineral assemblages of most of the Limerick Greenstone (Burke, 1973; Vikre, 1977). This alteration is evident in the albitization of feldspar and by mafic minerals having been

replaced by calcite, chlorite, and epidote group minerals (Burke, 1973). This pervasive alteration destroyed much of the original texture and mineralogy of the Limerick Greenstone, which makes determining its original composition extremely difficult. In the Humboldt Range, a series of silicic intrusions cut through the Limerick Greenstone and may be a source of some of the alteration observed within the Limerick Greenstone. Based on its lithology, Burke (1973) and Vikre (1977) have interpreted the Limerick Greenstone to have been deposited within a volcanic arc that was either already attached to the continent or some distance offshore.

Rochester Rhyolite

The Rochester Rhyolite is interpreted to conformably overlie the Limerick Greenstone (Wallace et al., 1969a; Vikre, 1977), but recent research by Wilkins (2010) has postulated the existence of an angular unconformity between the Limerick Greenstone and Rochester Rhyolite in the East Range (Fig. 1.2). The upper contact between the Rochester Rhyolite and the overlying Weaver Rhyolite is less clearly defined. The Rochester Rhyolite consists of banded rhyolite flows and rhyolite tuffs with minor amounts of tuff breccias and sedimentary units (Vikre, 1977). Burke (1973) noted that some of the tuffs and sedimentary deposits contain lithic clasts of hornfelsed Limerick Greenstone. This relationship indicates that Rochester Rhyolite deposition postdates deposition of the Limerick Greenstone and confirms the existence of an unconformity between the two units. Compared to the Limerick Greenstone, the units of the Rochester Rhyolite are relatively unaltered even though some show albitization has occurred (Burke, 1973; Vikre, 1977). Also, feldspar grains within the Rochester Rhyolite

exhibit sericite alteration and the formation of clay minerals, which are attributed to the same processes and conditions that affected the Limerick Greenstone (Burke, 1973). The leucogranite and rhyolite porphyry dikes that intruded the Limerick have been shown to intrude the Rochester Rhyolite, but some of these intrusive units were possibly feeders for the Rochester Rhyolite and were emplaced coevally with the Rochester Rhyolite volcanics (Wallace et al., 1969a, b; Silberling, 1973; Vikre, 1977). Burke (1973) and Vikre (1977) deduced that the Rochester Rhyolite was likely deposited under the same tectonic regime as the Limerick Greenstone, with the only major difference that the volcanic arc erupted more compositionally mature material.

Weaver Rhyolite

Overlying the Rochester Rhyolite is the Weaver Rhyolite, which is the uppermost unit within the Koipato Formation and is exposed from the Humboldt Range to the southern Tobin Range (Fig. 1.2). The Rochester Rhyolite-Weaver Rhyolite contact was interpreted by Vikre (1977) to possibly represent an angular unconformity. The upper contact with the Star Peak Group is considered an unconformity that marks the end of Early Triassic silicic volcanism in the area. The Weaver Rhyolite is composed of numerous rhyolite flows, ignimbrites, and tuffs, with sedimentary units increasingly more abundant towards the top of the stratigraphic section (Vikre, 1977). The Weaver Rhyolite has a similar felsic composition to the Rochester Rhyolite, but the two units have been separated based on the presence of ignimbrites in the lower sections and the prevalence of sedimentary units within the upper portions of the Weaver Rhyolite (Vikre, 1977). Burke (1973) described, in the southern Tobin Range, the two rhyolite units as impossible to

distinguish due to their similar compositions. Vikre (1977) mentioned that parts of the lower Weaver Rhyolite intertongue with tuffs and volcaniclastic strata from the upper Rochester Rhyolite. Vikre (1977) previously noted the presence of an angular unconformity between the Rochester and Weaver Rhyolites, but the presence of intertonguing between the two units seems to contradict the notion of an unconformity. Also, this intertonguing could point to the possibility of the coeval deposition of these two currently separate units, which may redefine the current stratigraphic picture of the Koipato Formation.

Significant alteration of the Weaver Rhyolite has not been observed, but within some samples feldspar grains exhibit slight replacement and albitization (Vikre, 1977). The lack of alteration within the Weaver Rhyolite could be due to the fact that the intrusive units observed to intrude Limerick Greenstone and Rochester Rhyolite in the southern Humboldt Range do not intrude into the Weaver Rhyolite, but Wallace et al. (1969a, b) observed that some rhyolite porphyry dikes cross-cut the Weaver Rhyolite (Silberling, 1973). This relationship implies that at least parts of what is mapped as the Weaver Rhyolite is either coeval or older than some of the rhyolite porphyry dikes. Burke (1973) and Vikre (1977) interpreted the lower Weaver Rhyolite as having been deposited as a dominantly volcanic succession, whereas the upper Weaver Rhyolite is composed of increasing sediment and decreasing volcanic material. This may be attributed to the cessation of magmatic activity towards the final stages of Weaver Rhyolite deposition.

Leucogranite and Rhyolite Porphyry Dikes

Leucogranite and rhyolite porphyry dikes are included within the concept of the Koipato Formation (Fig. 1.1). These leucogranites and rhyolite dikes intruded the Limerick Greenstone, Rochester Rhyolite, and possibly the lower sections of the Weaver Rhyolite and, as noted, may be coeval feeders for some of the silicic units (Wallace et al., 1969a, b; Silberling, 1973; Vikre, 1977). The leucogranite is composed of coarse feldspar and quartz grains in a quartz matrix (Vikre, 1977). Vikre (1977) noted that phenocrysts within the leucogranite have been altered to sericite and that secondary tourmaline and pyrite have formed in some sections of the intrusions. The rhyolite porphyry dikes exposed throughout the Humboldt Range are closely associated with the leucogranite, which likely is evidence of a coeval magmatic history for the two sets of intrusives (Vikre, 1977). The composition and texture of the rhyolite porphyry dikes closely mirror that of the Rochester Rhyolite and Weaver Rhyolite flow units as reflected in the predominance of feldspar and quartz (Vikre, 1977). Vikre (1977) described how the dikes that intrude the Rochester Rhyolite are difficult to distinguish from each other due to their similar composition and texture. The dikes display secondary mineral growth that is similar to the leucogranite, but is considerably less extensive (Vikre, 1977). Silberling (1973) and Vikre (1977) have interpreted the dikes to have been related to the lower flows of the Weaver Rhyolite due to their compositional and textural similarities. Based on these relations, Vikre (1977) suggested that map relationships indicate that the leucogranite and dikes postdated the Limerick Greenstone and Rochester Rhyolite and are coeval with the Weaver Rhyolite. Vikre (1977) also concludes that these intrusive

units were the cause of some of the pervasive hydrothermal alteration seen in the Limerick Greenstone and to a lesser degree in the Rochester Rhyolite.

Geochemistry

Even though pervasive alteration is present in much of the Koipato Formation, major element analyses have been conducted on both the volcanic rocks of the Koipato Formation and their associated intrusives. The lowermost unit of the Koipato Formation, the Limerick Greenstone, is the most pervasively altered. Published major element compositions for the Limerick Greenstone are based on three samples and range from basalt to andesite (Table 1.1) (Kistler and Speed, 2000). The low SiO_2 values, combined with their high alkali ($Na_2O + K_2O$) contents, classify the Limerick Greenstone as tephrite basanite to trachy-andesite on the total alkali-silica (TAS) diagram of Le Bas et al. (1986) (Table 1.1 and Fig. 1.3). The Limerick Greenstone displays the lowest SiO_2 content (47.8-61.6%) of any of the units within the Koipato Formation (Table 1.1 and Fig. 1.3). The Rochester (Vikre, 1977, 1981; Kistler and Speed, 2000) and Weaver (Johnson, 1977; Vikre, 1981; Kistler and Speed, 2000) Rhyolites can be classified as rhyolites based both on their SiO_2 content and on the TAS diagram (Table 1.1 and Fig. 1.3). One main difference in the SiO_2 contents of these two units is that the highest observed SiO_2 value in the Rochester Rhyolite (78.7%) is notably less than some of the SiO_2 contents observed in the Weaver Rhyolite (~83.9%) (Table 1.1 and Fig. 1.3). Also, an important trend to notice across the three units of the Koipato Formation is that upwards in the stratigraphic section the SiO_2 content of the units increases, which may be a product of an evolving magmatic system (Vikre, 1977). The plutons and dikes that intruded the Koipato Formation have also been analyzed for their major oxide

compositions, with results showing that both the leucogranite (Johnson, 1977; Vikre, 1977; Kistler and Speed, 2000) and rhyolite porphyry dikes (Johnson, 1977; Vikre, 1977) are rhyolitic based on their SiO_2 content and on the TAS diagram (Table 1.1 and Fig. 1.3). The SiO_2 and alkali contents of the intrusive units overlap with the values obtained for both the Rochester and Weaver Rhyolites, which may indicate a shared magmatic history with the felsic volcanic units of the Koipato Formation. Kistler and Speed (2000) also analyzed four samples of undifferentiated Koipato Formation from the Stillwater Range, which are classified as rhyolites based on their SiO_2 content and the TAS diagram (Table 1.1 and Fig. 1.3). These four samples overlap with the Rochester and Weaver Rhyolite compositions obtained from the Humboldt Range and are probably eastward extensions of these units.

Age

Interpretations of the age of the Koipato Formation have varied considerably since Ferguson et al. (1952) first described the Koipato Formation as unconformably overlying the highly faulted and folded Pumpernickel and Havallah Formations of the Golconda Allochthon (GA). This unconformable relationship was observed at China Mountain, in Hoffman Canyon of the northern Tobin Range, the easternmost outcrop of the Koipato Formation occurs, where a 400-foot thick succession of rhyolitic units rest unconformably on the Havallah Formation (Fig. 1.4) (Ferguson et al., 1952). They still considered the Koipato Formation at Hoffman Canyon to be Permian in age, based on its correlation to the fossil evidence of Wheeler (1939) from the Humboldt Range (Ferguson et al., 1952). Roberts et al. (1958) supported this view and identified the underlying

angular unconformity between the Koipato Formation and GA in the East Range and noted that the Koipato Formation spans several ranges in central Nevada. Roberts et al. (1958) also pointed out that only felsic igneous and sedimentary units of the Koipato Formation are present in the East and Tobin Ranges, which they attributed to the observed eastward pinching out of the Koipato Formation. The Koipato Formation units decrease in thickness across the various mountain ranges of central Nevada, thinning from a maximum of 14,000 feet in the Humboldt Range (Knopf, 1924; Wheeler, 1939) to less than 2000 feet in the southern Tobin and Sonoma Ranges and completely disappearing in the northern parts of these ranges (Ferguson et al., 1952; Roberts et al., 1958).

Silberling and Roberts (1962) used these stratigraphic relationships to define the Late Permian to Early Triassic Sonoma Orogeny, with the internal deformation of the GA and the Golconda thrust assigned to this concept of the Sonoma Orogeny. The age of the unconformably overlying Koipato Formation, as seen in Hoffman Canyon (Fig. 1.4), then provides a minimum age for the orogeny.

Wheeler (1939) based his age assignment for the Koipato Formation on the discovery of a *Helicoprion* fossil reported to have come from the Rochester Trachyte. Wheeler (1939) utilized this fossil to assign the Rochester Rhyolite and underlying Limerick Greenstone a Permian age, with the overlying Weaver Rhyolite as having been deposited either in the Late Permian or Early Triassic. Silberling and Roberts (1962) reported Early Triassic fauna within the uppermost sedimentary sections of the Weaver Rhyolite, thereby leaving open the possibility that the Koipato Formation is an entirely

Early Triassic formation. Subsequent research by Silberling (1973) cast some doubt on the Wheeler (1939) age assignment. Silberling (1973) reexamined the fossil found by Wheeler (1939) and came to the conclusion that it most likely was a fossil specimen collected from outside of the Koipato Formation. Based on this and the discovery of a fish tooth fossil in the Rochester Rhyolite, Silberling (1973) assigned an Early Triassic age for the Koipato Formation. An Early Triassic age was also supported by the occurrence of Late Olenekian ammonites in the upper Weaver Rhyolite sedimentary units (Fig. 1.1) (Silberling, 1973). Nichols and Silberling (1977) have reported the occurrence of Anisian ammonites within the lower Prida Formation, which overlies and sets a minimum age for the Koipato Formation (Fig. 1.1). Wallace et al. (1960) obtained Pb-α ages for two samples from the leucogranite and rhyolite porphyry dikes in the Humboldt Range, which were interpreted to intrude the Limerick Greenstone and Rochester Rhyolite of the Koipato Formation. These Pb-α analyses returned ages of 230 ± 40 and 290 ± 45 Ma, but the large uncertainties do not preclude a Permian age for Koipato Formation deposition (Fig. 1.1) (Wallace et al., 1960). Wallace et al. (1960) noted that these intrusive rocks are probable feeders for the overlying Weaver Rhyolite based on stratigraphic and lithologic relationships. Building on the work of Wallace et al. (1960), McKee and Burke (1972) produced a fission-track age on zircon from a welded tuff in the Rochester Rhyolite of 225 ± 30 Ma (Fig. 1.1). McKee and Burke (1972) combined their data with the two ages obtained by Wallace et al. (1960) to produce a combined age of 250 ± 40 Ma for the Koipato Formation. The hope of these researchers was to provide a minimum age for the emplacement of the GA, but the large amount of uncertainty in the dates for the felsic units of the Koipato Formation and a lack of age constraints on the

basal Limerick Greenstone prevent using these data to provide a definitive minimum age of emplacement.

The composition of the Koipato Formation and its ambiguous age assignments have led to a variety of tectonic models to account for the formation of the Koipato Formation and the Late Permian to Early Triassic tectonic events along the continental margin. Early tectonic models for the deposition of the Koipato Formation favored the idea that deposition was entirely post-Sonoma Orogeny and thus emplacement of the GA (Fig. 1.5) (e.g., Silberling and Roberts, 1962; Roberts, 1964; Burchfiel and Davis, 1972, 1981; Silberling, 1973; Vikre, 1977; Schweickert and Snyder, 1981; Speed and Sleep, 1982; Snyder and Brueckner, 1983; Burchfiel et al., 1992; Dickinson, 2004, 2006). This interpretation was based on the observed angular unconformity between the Koipato Formation and underlying Havallah Formation. Burchfiel and Davis (1972) and Vikre (1977) expanded on this view with the idea that the Koipato Formation represents the first vestiges of a newly developing, post-Sonoma Orogeny continental arc, which would be active at various times throughout the Mesozoic and Cenozoic. Vikre (1977) went on to characterize the intermediate Limerick Greenstone as a product of the final stages of melting of oceanic crust beneath the accreted island-arc system and the overlying Rochester and Weaver Rhyolites as the initial products of continental arc volcanism. The idea of the Koipato Formation having been deposited entirely post-tectonic led some researchers to invoke paleotopography and tectonic loading to explain the eastward pinching out of the Koipato Formation described by Roberts et al. (1958). Specifically, Burke (1973) presented the idea that the Koipato Formation was deposited in a tectonic depression that may have been the result of the down warping of the continental crust due

to the emplacement of the GA and associated island arc. In contrast to this interpretation, other researchers have suggested that it is possible that the Koipato Formation was part of an approaching island arc and deposited in part on top of the arc's subduction complex (GA) and then carried piggyback to its final resting place during the final stages of the Sonoma Orogeny (e.g., Dickinson, 1977; Speed, 1977; Snyder and Brueckner, 1983; Burchfiel et al., 1992; Dunston et al., 2001; Wilkins, 2010). Dickinson (1977) and Speed (1977) first suggested that part of the Koipato Formation could have been carried piggyback on the GA. This view of the Koipato Formation having been carried piggyback on the GA is supported by the fact that nowhere has it been confirmed that units of the Koipato Formation overlie the autochthon (Burchfiel et al., 1992). Also, recent research by Wilkins (2010) has revealed that the Rochester Rhyolite in the East Range is cut by the Golconda thrust and must have been deposited before movement along the thrust. If the Koipato Formation is not post-tectonic, then thrusting associated with the Sonoma Orogeny did not finish until after deposition of the Koipato Formation, which could have lasted into the Early Triassic. Some authors have supported the possibility of younger thrusting, with the view that movement along the Golconda thrust occurred into the Jurassic (Ketner, 1984; Snyder and Brueckner, 1989; Northrup and Snyder, 2000; Dunston et al., 2001). Much debate exists about which of these models best describes the deposition of the Koipato Formation.

Late Paleozoic-Early Mesozoic Tectonic Framework

The mountain ranges of central Nevada lie within the Cordillera of North America, which extends from the ranges of northern Alaska through the western

provinces of Canada and the western states of the U.S., finally terminating in southern Mexico (Fig. 1.6). The discussion here focuses on the Late Paleozoic and Early Mesozoic tectonic history of the western U.S. because during this time the majority of tectonic events of interest for the research presented in this report occurred. A brief overview of the pre-Late Paleozoic tectonic events that influenced western North America will be presented in this section. For a more detailed analysis, consult Burchfiel et al. (1992), Dickinson (2004, 2006), and references therein, which offer an extensive overview of the pre-Late Paleozoic tectonic events that transpired along the western North American margin.

The western North American margin initially formed following the breakup of Rodinia between 770-600 Ma (Prave, 1999; Colpron et al., 2002; Dickinson, 2004), and rifted from Siberia (Sears and Price, 2003; Sears et al., 2005), East Antarctica (Dalziel, 1991; Hoffman, 1991; Moores, 1991), or Australia (Brookfield, 1993; Karlstrom et al., 1999). Rifting formed a passive continental margin that accommodated the accumulation of thick stratigraphic sequences in the subsiding continental margin during the Early Paleozoic (Burchfiel and Davis, 1972; Ross, 1991; Burchfiel et al., 1992; Timmons et al., 2001; Dickinson, 2004, 2006). To the west of this continental shelf, an outboard arc system developed (Burchfiel et al., 1992). During the later stages of the Early Paleozoic (Devonian), either east (Burchfiel and Davis, 1972; Burchfiel et al., 1992) or west (Dickinson, 2006) directed subduction of oceanic crust beneath the island arc system was initiated, which brought the so called Antler arc towards the continental margin and closed the Antler Basin (a marginal ocean basin) (Dickinson, 2006). The movement of

the Antler arc towards the continental margin led to the Antler Orogeny, the first of two major Late Paleozoic tectonic events.

The Antler Orogeny is defined and its remnants are best exposed in central Nevada, but similar age tectonic packages have been observed in both the Kootenay terrane of southern Canada (Smith and Gehrels, 1991, 1992; Dickinson, 2004) and the Yukon-Tanana terrane (Hansen, 1988; Dickinson, 2004) of Northwest Canada. In Nevada, it is identified by the development of the Roberts Mountains Allochthon (RMA), a lower Paleozoic structural assemblage that was thrust eastward onto the outer continental shelf along the Roberts Mountains thrust. The Antler Orogeny is interpreted to have occurred during either the Late Devonian to Early Mississippian (e.g., Burchfiel and Davis, 1972; Nilsen and Stewart, 1980; Johnson and Pendergast, 1981; Schweickert and Snyder, 1981; Dickinson, 2004) or exclusively in the Mississippian (e.g., Speed and Sleep, 1982; Royden and Burchfiel, 1989; Turner et al., 1989; Burchfiel and Royden, 1991; Miller et al., 1992). The RMA is composed of shale, sandstone, bedded chert, and basaltic pillow lavas (e.g., Roberts et al., 1958; Burchfiel and Davis, 1972; Burchfiel et al., 1992). Some workers believed the eastward thrusting of the RMA was the result of west-directed subduction of the oceanic lithosphere that separated the approaching Antler island arc from the western continental margin (Fig. 1.7) (Speed and Sleep, 1982; Dickinson et al., 1983; Snyder and Brueckner, 1983). This subduction eventually resulted in an arc-continent collison; remnants of this Antler arc are interpreted to exist in the northern Sierra Nevada Mountains, eastern Klamath Mountains, and in Canada (e.g., Speed, 1979; Oldow, 1984; Speed et al., 1988; Dickinson, 2004). Following the emplacement of the RMA, the Antler arc either went extinct as subduction continued

under a second east-facing island arc (Fig. 1.7) (Schweickert and Snyder, 1981; Speed and Sleep, 1982; Dickinson et al., 1983; Snyder and Brueckner, 1983; Miller et al., 1984) or subduction continued under the Antler arc after it was only partially accreted to the continental margin (Fig. 1.8) (Burchfiel and Davis, 1972, 1975; Silberling, 1973; Vikre, 1977; Miller et al., 1984, 1992). During the Late Paleozoic, subduction of the oceanic lithosphere seperating this second island arc from the continental margin would lead to the Sonoma Orogeny and the emplacment of the GA onto the continental margin (Fig. 1.7).

Evidence for coeval sedimentation within the Havallah Basin, the successor to the Antler Basin, with the Antler Orogeny has led authors to hypothesize that either the Antler Basin only partially closed (Burchfiel and Davis, 1972, 1975; Miller et al., 1984; Oldow et al., 1989; Burchfiel et al., 1992) or that immediately following the Antler Orogeny, and closure of the Antler Basin, spreading within the newly closed back-arc basin formed the initial vestiges of the Havallah Basin where units of the GA would be deposited during the Middle-Late Paleozoic (Burchfiel and Davis, 1972, 1975; Snyder and Brueckner, 1983; Miller et al., 1984; Burchfiel et al., 1992). Nevertheless, subsequent to the Antler Orogeny, the western margin of North America is interpreted to have reverted back to a passive margin with deposition occurring in the newly formed Havallah Basin, which was receiving continental sediment from the east and volcanic arc sediment from the west (Figs. 1.7 and 1.8) (e.g., Snyder and Brueckner, 1983; Miller et al., 1984; Brueckner and Snyder, 1985; Snyder and Brueckner, 1989; Miller et al., 1992).

Recent research has noted the possible occurrence of multiple deformation events during the time span between the Antler and Sonoma Orogenies along the western North American margin (Ketner, 1977; Snyder et al., 2002; Trexler et al., 2004). During this intervening period, east-directed subduction underneath the volcanic arc to the west of the Havallah Basin (Snyder and Brueckner, 1983, 1989) has been interpreted to last until the Late Pennsylvanian, when the subduction zone flipped and west-directed subduction began to consume the oceanic crust that separated the volcanic arc from the continental margin (Speed, 1979; Speed and Sleep 1982; Snyder and Brueckner 1983; Dickinson et al., 1983). While the Havallah Basin was evolving and accumulating sediment to the west of the continental margin, southward translation of tectonic elements along the western Cordilleran margin, including the RMA, during the Early or Middle Pennsylvanian to the late Early Permian is inferred to have occurred along a left-lateral strike-slip fault system (Burchfiel and Davis, 1981; Walker, 1988; Stone and Stevens, 1988; Burchfiel et al., 1992). Late Permian to Early Triassic deformation within units along the southwestern Cordilleran margin is inferred to be associated with the emplacement of Late Permian plutons, which constrain the cessation of translation as before Early Triassic time (Burchfiel and Davis, 1981; Walker, 1988; Burchfiel et al., 1992). This deformation and plutonic emplacement along the southern Cordilleran margin is the southernmost expression of the Sonoma Orogeny, which further north is characterized by the closure of the Havallah Basin and the emplacement of the GA.

At the same time as the events along the southern Cordilleran margin occurred, rocks within the Havallah Basin were thrust eastward as the GA, along the Golconda thrust, over the RMA and its overlap sequences during what would be named the Sonoma

Orogeny (e.g., Silberling and Roberts, 1962; Burchfiel and Davis, 1972, 1981; Schweickert and Snyder, 1981; Speed and Sleep, 1982; Snyder and Brueckner, 1983; Burchfiel et al., 1992; Dickinson, 2004, 2006). The initial evidence for a Late Paleozoic to Early Mesozoic orogeny along the western Cordilleran margin was recognized by Ferguson et al. (1952) in Hoffman Canyon, Tobin Range, Nevada where undeformed volcanic units of the Koipato Formation rest unconformably on highly deformed units of the GA (Figs. 1.2 and 1.4). Silberling and Roberts (1962) were the first to define this and other deformation as the Sonoma Orogeny and assigned it a Late Permian age. This deformation consisted of the folding and thrusting of the Havallah Formation and its emplacement along the Golconda thrust over the Antler overlap sequence. However, the composition of the upper plate and the fact that the Golconda thrust cuts some Middle Mesozoic thrusts led Silberling and Roberts (1962) to leave open the possibility that the thrust is actually a Late Mesozoic event. Burchfiel and Davis (1972), Speed (1977), and Snyder and Brueckner (1983) continued to push the possible age of the Sonoma Orogeny younger by arguing for a Early or even Middle Triassic age of emplacement for the GA. Presently, the Sonoma Orogeny is considered by most researchers to represent an arc-continent collision that resulted in the thrusting of the oceanic GA eastward onto the continental margin in the Late Permian to Early Triassic (e.g., Dickinson, 2004, 2006).

Other research into the Sonoma Orogeny has, however, cast some doubt on this interpretation of the age of the Sonoma Orogeny and has picked up on the idea of Silberling and Roberts (1962) that thrusting along the Golconda thrust could have occurred in the Early Jurassic or even later (Ketner, 1984; Snyder and Brueckner, 1989; Northrup and Snyder, 2000; Dunston et al., 2001). Currently, the best age constraints on

the emplacement of the GA are Upper Triassic (219 Ma) plutonic pins that cross-cut both the deformed GA and undeformed Mesozoic cover in the eastern Sierra Nevada, CA area (Schweickert and Lahren, 1987, 1993; Dickinson, 2006). This discovery signifies that the GA possibly extends to the Sierra Nevada batholith in the west, although the assignment of rocks to the GA there is inferential. Also, the Late Triassic-Early Jurassic Auld Lang Syne Group, stratigraphically above the Koipato Formation in central Nevada, has been correlated with facies across the Golconda thrust on the Colorado Plateau, which adds a further constraint on the timing of initial movement along the thrust (Burke and Silberling, 1973; Lupe and Silberling, 1985; Riggs et al., 1996; Dickinson, 2006). To constrain the timing of the final emplacement of the GA, Skalbeck (1985) conducted a paleomagnetism study of the Koipato Formation and its overlying units, which showed that emplacement of the GA could not pre-date the Early Triassic in central Nevada. These relationships suggest a minimum age constraint on the emplacement of the GA with thrusting occurring in the Early Triassic and possibly lasting until the Middle Triassic. The maximum age for initiation of the Sonoma Orogeny is constrained by the youngest unit (Edna Mountain Formation) in the Antler Overlap sequence, which is dated to be Guadalupian (Roberts, 1951, 1964; Coats and Gordon, 1972; Erickson and Marsh, 1974; Wardlaw et al., 1995). The position of the Koipato Formation between the GA and Auld Lang Syne Group should presumably help to further constrain the minimum age of emplacement of the GA and therefore the timing of the Sonoma Orogeny, but the age, stratigraphic, and structural information about the Koipato Formation must be examined carefully because the volcanic units do not rest on the autochthon and could have been carried piggyback with the GA during its emplacement (e.g., Dickinson, 1977; Speed,

1977; Snyder and Brueckner, 1983; Burchfiel et al., 1992; Dunston et al., 2001; Wilkins, 2010). Speed (1977) and Burchfiel et al. (1992) postulate that Early Triassic magmatism (e.g., Koipato Formation) along the continental margin could have been syntectonic with the closure of the Havallah Basin and conceivably the emplacement of the GA.

Some debate about the exact timing of the Sonoma Orogeny continues to this day along with a discussion about the mechanism that was the driving force behind the orogeny. Two camps exist in this debate with one favoring west-directed subduction underneath the volcanic arc that bounded the Havallah Basin (Fig. 1.7) (Speed, 1977, 1979; Speed and Sleep, 1982; Snyder and Brueckner, 1983, 1989; Brueckner and Snyder, 1985; Wyld, 1991; Burchfiel et al., 1992) and the other supporting the idea that closure of the basin was caused by back-arc thrusting while east-directed subduction continued under the volcanic arc (Fig. 1.8) (Burchfiel and Davis, 1972, 1975; Silberling, 1973; Vikre, 1977; Miller et al., 1984, 1992). The first model for the closure of the Havallah Basin employs a switch in subduction direction in the Late Paleozoic from east- to west-directed underneath the volcanic arc bounding the basin to the west (Speed, 1977, 1979; Speed and Sleep, 1982; Dickinson et al., 1983; Snyder and Brueckner, 1983; Brueckner and Snyder, 1985; Burchfiel et al., 1992). This switch in subduction direction led to the consumption of the oceanic lithosphere of the Havallah Basin and the formation of an accretionary prism composed of scrapped off sediment that had previously been deposited into the basin (Speed, 1977; Brueckner and Snyder, 1985; Burchfiel et al., 1992). A change in subduction direction is not necessary if the Havallah Basin and Sonoma arc are unrelated to Antler events because the basin and arc can be from far outboard of the continental margin and subduction could have continued in the same

westerly direction under the arc (Fig. 1.7). Nevertheless, consumption of oceanic lithosphere continued throughout the latter stages of the Paleozoic and slowly closed the Havallah Basin, which simultaneously brought the volcanic arc closer to the continental margin (Snyder and Brueckner, 1983; Brueckner and Snyder, 1985; Burchfiel et al., 1992). This movement is interpreted to have culminated in an arc-continent collision that emplaced the accretionary prism, known as the GA, onto the continental margin in the Late Permian to Early Triassic (Fig. 1.7) (Snyder and Brueckner, 1983; Brueckner and Snyder, 1985; Burchfiel et al., 1992). Final closure of the Havallah Basin occurred when the buoyant continental lithosphere of North America entered the subduction zone, thus terminating west-directed subduction underneath the volcanic arc (Burchfiel et al., 1992). This event marked the end of the Sonoma Orogeny, which was coeval with the accretion of the volcanic arc onto the continental margin and a jump in subduction to the west of the newly formed continental margin. Following the orogeny, east-directed subduction under the continental margin led to the development of a continental volcanic arc (Burchfiel at al., 1992).

The second theory for the Sonoma Orogeny employs a back-arc thrusting model for the emplacement of the GA. This model postulates that the foreland of the Antler arc was accreted onto the western continental margin during the Antler Orogeny, which was followed by rifting between the volcanic center of the arc and the western margin of North America (e.g., Miller et al., 1984). This rifting generated a wide back-arc basin that facilitated the accumulation of Havallah and Schoonover strata (Fig. 1.8) (e.g., Miller et al., 1984). Throughout the Late Paleozoic, subduction was continuously east-directed underneath the rifted volcanic arc to the west of the continental margin (Burchfiel and

Davis, 1972, 1975; Churkin, 1974; Vikre, 1977; Miller et al., 1984). This situation remained unchanged until the Permian, when continued east-directed subduction led to a weakening of the crustal strength of the oceanic lithosphere of the Havallah Basin along the axis of the spreading center (Burchfiel and Davis, 1972, 1975; Vikre, 1977; Miller et al., 1984). This weakening of the crust and continued east-directed subduction led to the collapse of the oceanic lithosphere and its thrusting eastward onto the continental margin along the Golconda thrust (Fig. 1.8) (Burchfiel and Davis, 1972, 1975; Vikre, 1977; Miller et al., 1984). The culmination of this model and the end of the Sonoma Orogeny occurs when the volcanic arc collided with the continental margin after the complete closure of the Havallah Basin (Vikre, 1977; Miller et al., 1984). Following closure of the basin, subduction continued in an east-directed sense underneath the continental margin, which led to the development of a continental volcanic arc (Miller et al., 1984). One problem with both models for the Sonoma Orogeny is that remnants of the volcanic arc involved in either the Antler or Sonoma orogenies have never been definitively identified.

A great deal of research has been undertaken to identify the volcanic arc that was integral in the events of the Sonoma Orogeny. Most recent work has focused on the northern Sierra Nevada and eastern Klamath Mountains as the probable locality of this volcanic arc, but stratigraphic and structural relations between the arc complex and coeval units within the GA, to the east, are difficult to discern due to younger rocks and Mesozoic plutons that cover the intervening area (Fig. 1.9) (Burchfiel et al., 1992). Units within the northern Sierra Nevada and eastern Klamath Mountains have been identified as Middle and Upper Paleozoic volcanic arc successions, which indicate that, from the

Middle Devonian to the end of the Paleozoic, arc volcanism occurred (Saleeby et al., 1987; Burchfiel et al., 1992). Miller (1987) and Harwood (1988) identified the Late Devonian, Pennsylvanian, and the Early to Middle Permian as times when intense volcanic arc activity occurred within these terranes. However, correlation of units even within the terranes is difficult due to facies changes caused by varying deposition in relation to the terranes position within the volcanic arc (Harwood, 1983; Watkins, 1985; Burchfiel et al., 1992). One link between these terranes is the occurrence of the McCloud fossil assemblage, in the Permian McCloud Limestone, which is a distinctive Late Paleozoic fusulinid and coral grouping (Miller, 1987; Burchfiel et al., 1992). This McCloud assemblage is distinct from other North American or Tethyan faunas and indicates a regional paleogeographic tie between the eastern Klamath and northern Sierra Nevada Mountains and terranes in Canada (Chilliwack and Quesnellia) (Miller, 1987; Burchfiel et al., 1992). Burchfiel et al. (1992) and Miller et al. (1992) equate the Quesnellia arc of Canada with the Klamath Mountains in northern California and postulate that each was part of the fringing arc that accreted onto the continental margin during the Sonoma Orogeny. The occurrence of this fossil assemblage and the timing of magmatism within these terranes points to a probable close relationship with the western Cordilleran margin in the Late Paleozoic.

Following the Sonoma Orogeny and the accretion of the GA, east-directed subduction was initiated beneath the North American continental margin leading to the development of the Cordilleran magmatic arc, which would be active from the Middle Triassic to the Middle Jurassic (Dickinson, 2004). This volcanic arc was not a localized feature and has been identified to the south in eastern Mexico (Dickinson and Lawton,

2001) and northward in the Quesnellia or Nicola arc (Mortimer, 1987) within the Canadian Cordilleran (Dickinson, 2004). The volcanic arc rocks of the eastern Klamath and Quesnellia terranes represent the basement for the continental magmatic arc in the northern part of the Cordilleran, but further south these units are truncated and the magmatic arc is built on cratonal and miogeoclinal units (Saleeby and Busby-Spera, 1992). This abrupt truncation is the result sinstral strike-slip faulting along the California-Coahuila transform, which was active from the Permian to the Middle Triassic (Burchfiel and Davis, 1972; Burchfiel et al., 1992; Miller et al., 1992; Saleeby and Busby-Spera, 1992; Dickinson, 2000, 2004; Dickinson and Lawton, 2001).

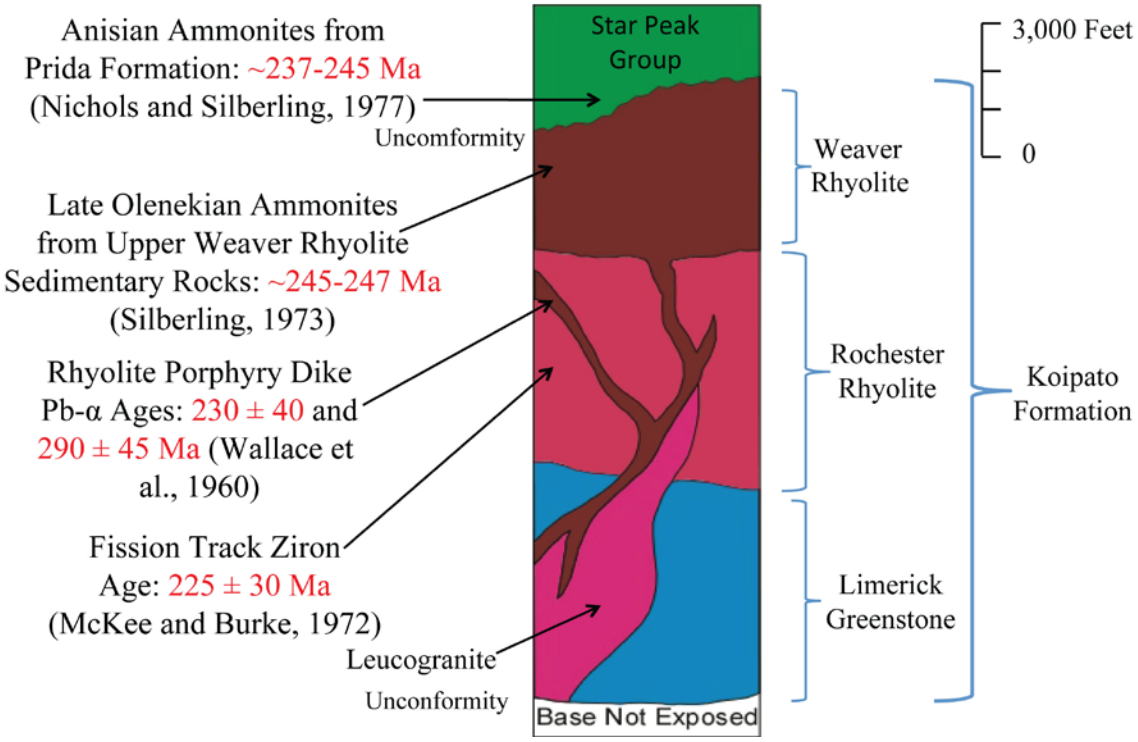

Figure 1.1. Generalized stratigraphic column for the Koipato Formation, in the Humboldt Range, showing previously interpreted stratigraphic relationships and age constraints (paleontological and radiometric). It is important to note that the base of the Koipato Formation in the Humboldt Range is not exposed. Modified from Silberling (1973).

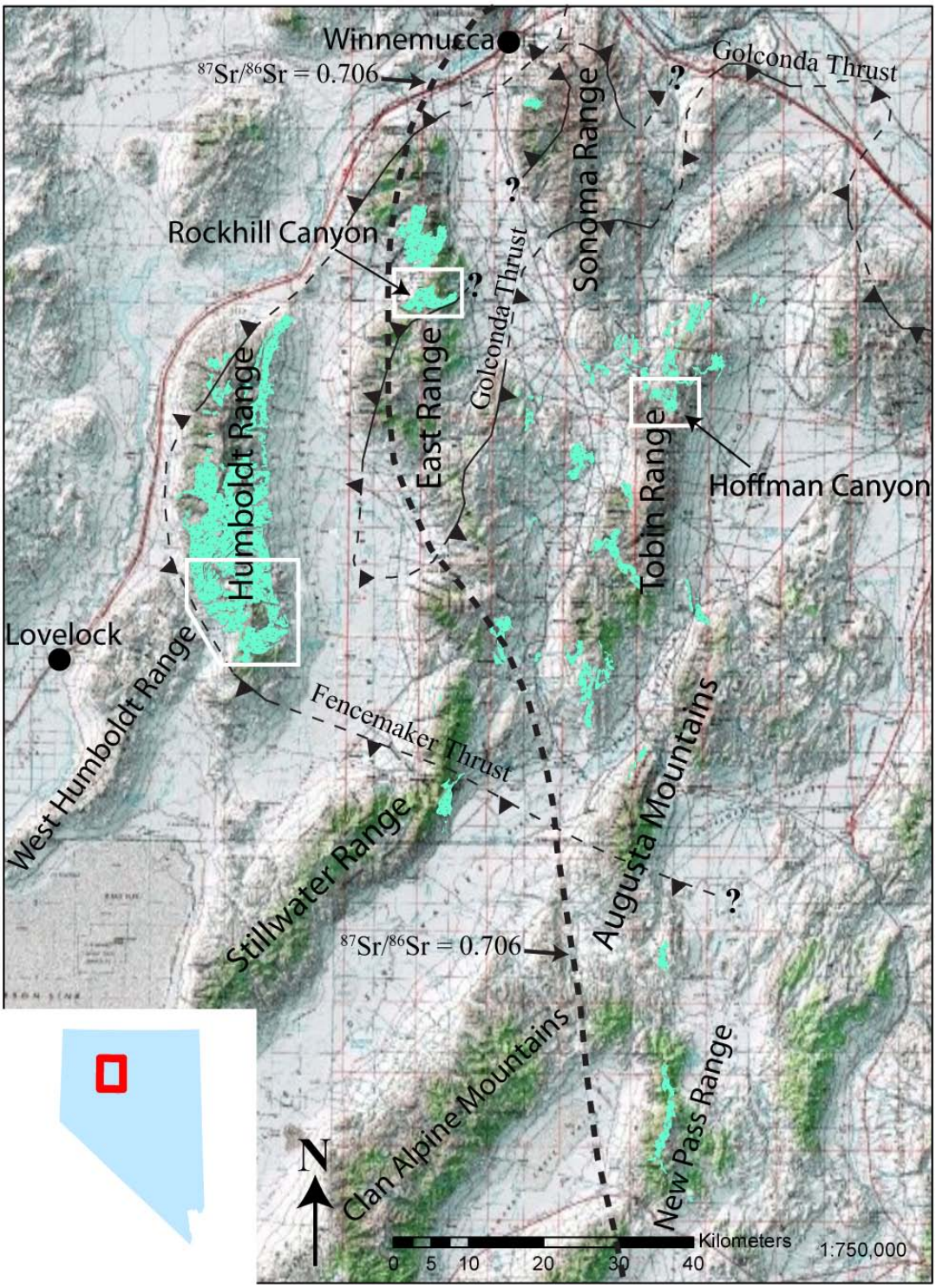

Figure 1.2. Topographic map of central Nevada showing the location of outcrops of the Koipato Formation and related units (bright green). Important mountain ranges and canyons are noted. White boxes outline the main field areas discussed in this report. Golconda and Fencemaker Thrust trends from Wilkins (2010). The $^{87}Sr/^{86}Sr = 0.706$ line is from Elison et al. (1990). Modified from Crafford (2007).

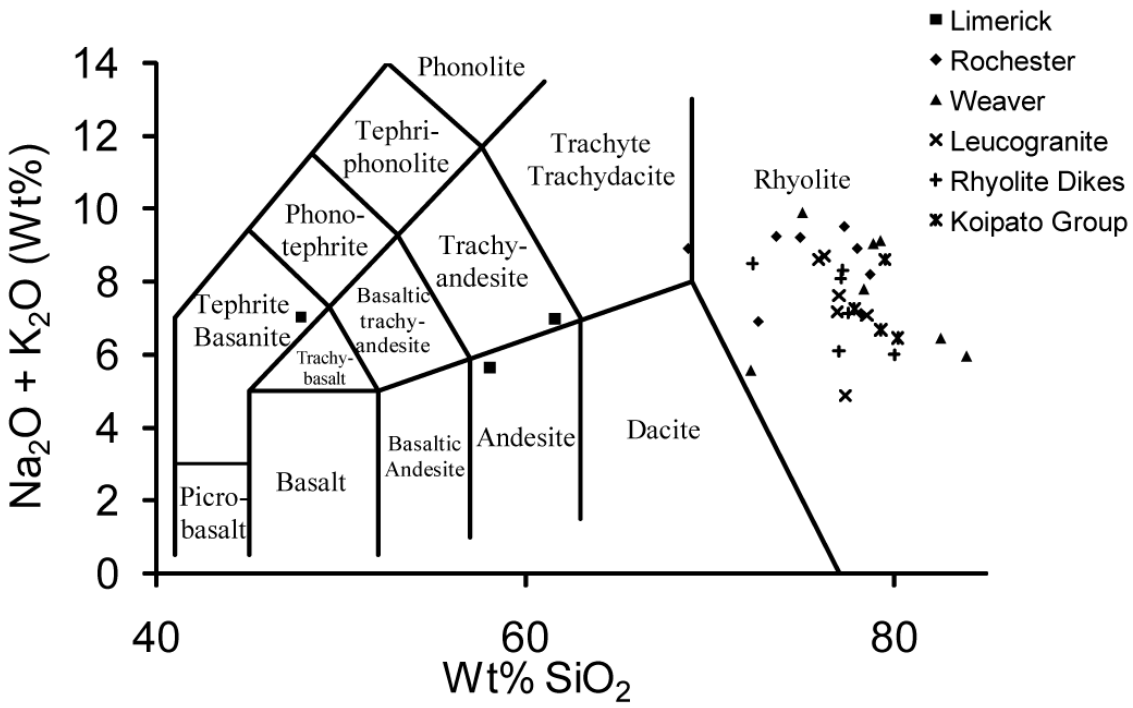

Figure 1.3. Total alkali-silica (TAS) diagram showing chemical classification of units related to the Koipato Formation (after Le Bas et al., 1986). Data are compiled from the work of Johnson (1977), Vikre (1977, 1981), and Kistler and Speed (2000). Consult Table 1.1 for exact concentrations and other major oxides.

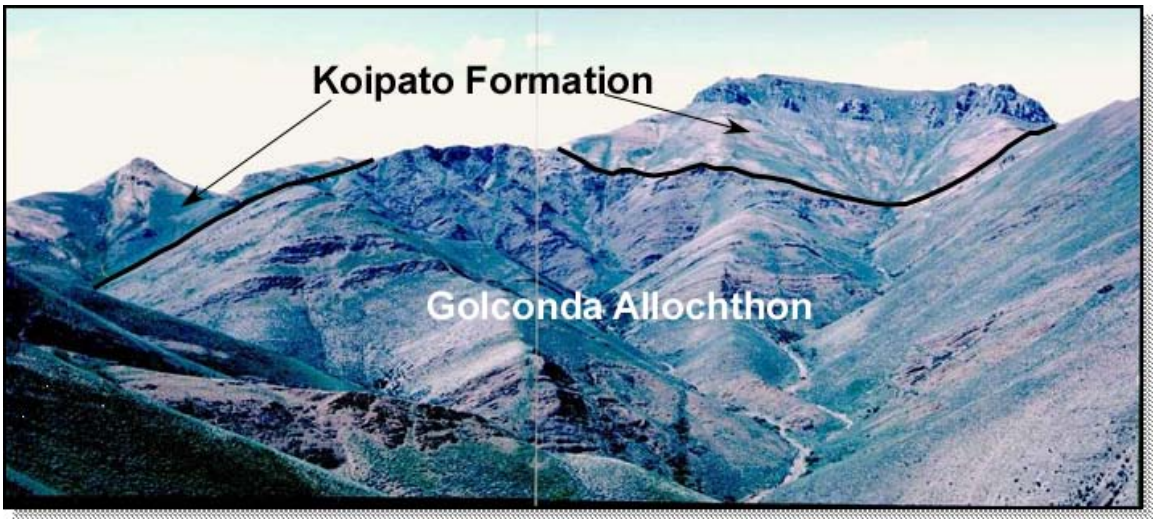

Figure 1.4. View of Hoffman Canyon and China Mountain in the Tobin Range, which is the type locality of the Sonoma Orogeny. Ferguson et al. (1952) noticed that the undeformed Koipato Formation rests on top of the highly deformed Golconda Allochthon with a marked angular unconformity. View to the north. Modified from Walter Snyder (per. comm.).

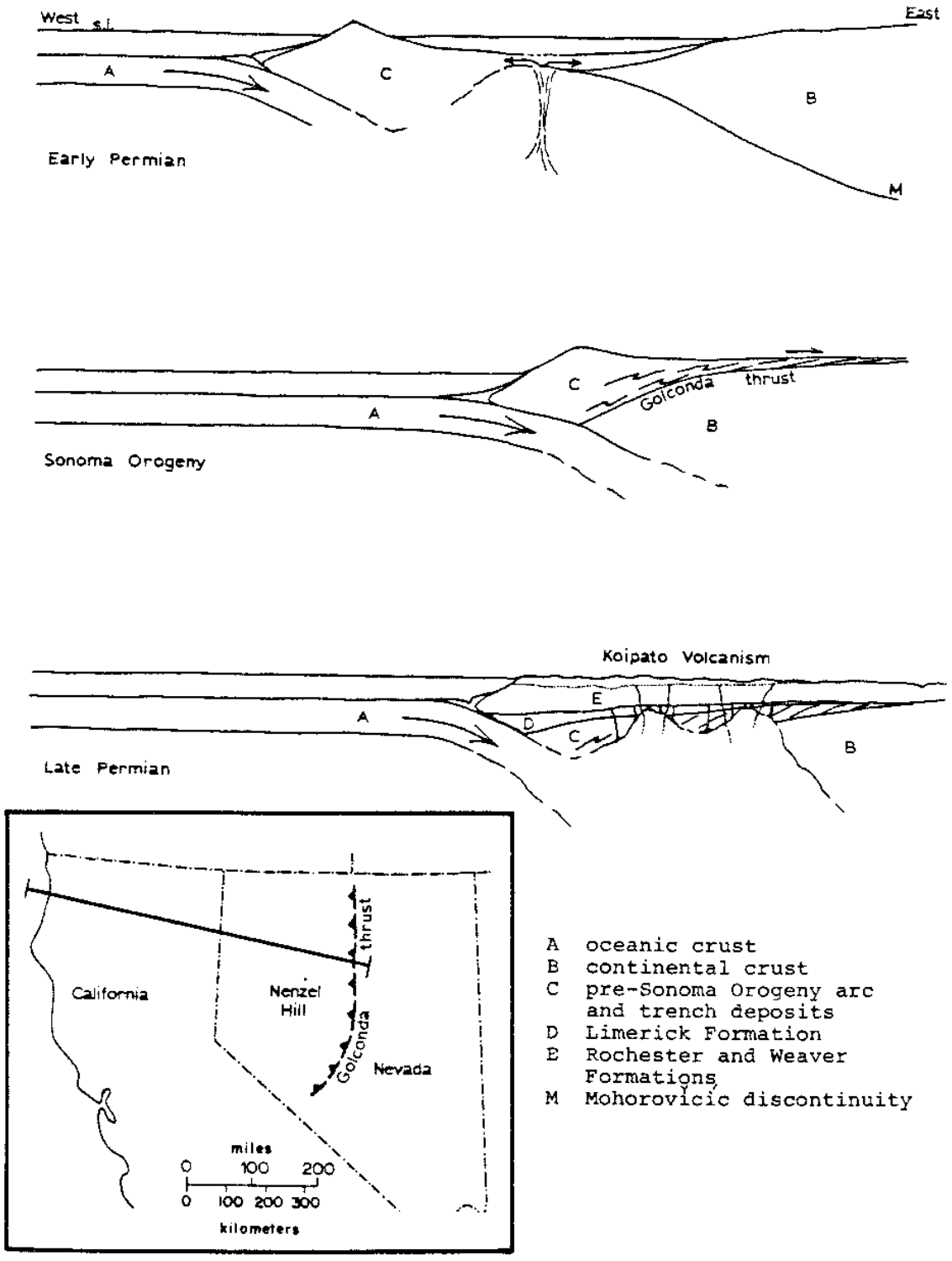

Figure 1.5. Tectonic model for the western North American margin in the Permian depicting the deposition of the Koipato Formation as post-emplacement of the Golconda Allochthon. Index map in bottom-left corner places profiles with respect to the present margin and geography. From Vikre (1977).

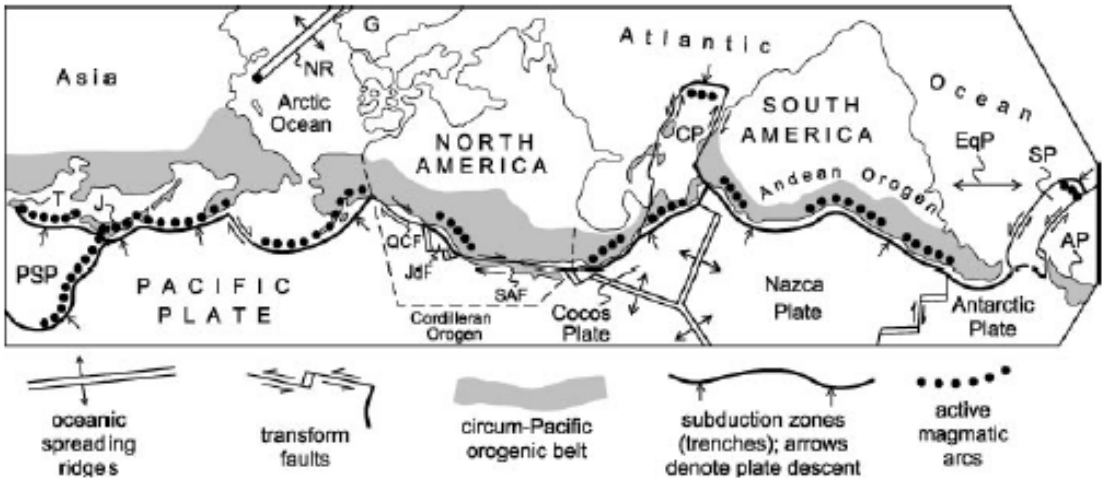

Figure 1.6. Projection displaying the position of the western North American Cordilleran Orogen within the Circum-Pacific orogenic belt. AP-Antarctic Peninsula, C-Cascades volcanic chain, CP-Caribbean plate, G-Greenland, J-Japan, JdF-Juan de Fuca plate, NR-Nansen Ridge (northern extension of Atlantic spreading system), PSP-Philippine Sea plate, QCf-Queen Charlotte fault, SAf-San Andreas fault, SP-Scotia plate, T-Taiwan. From Dickinson (2004).

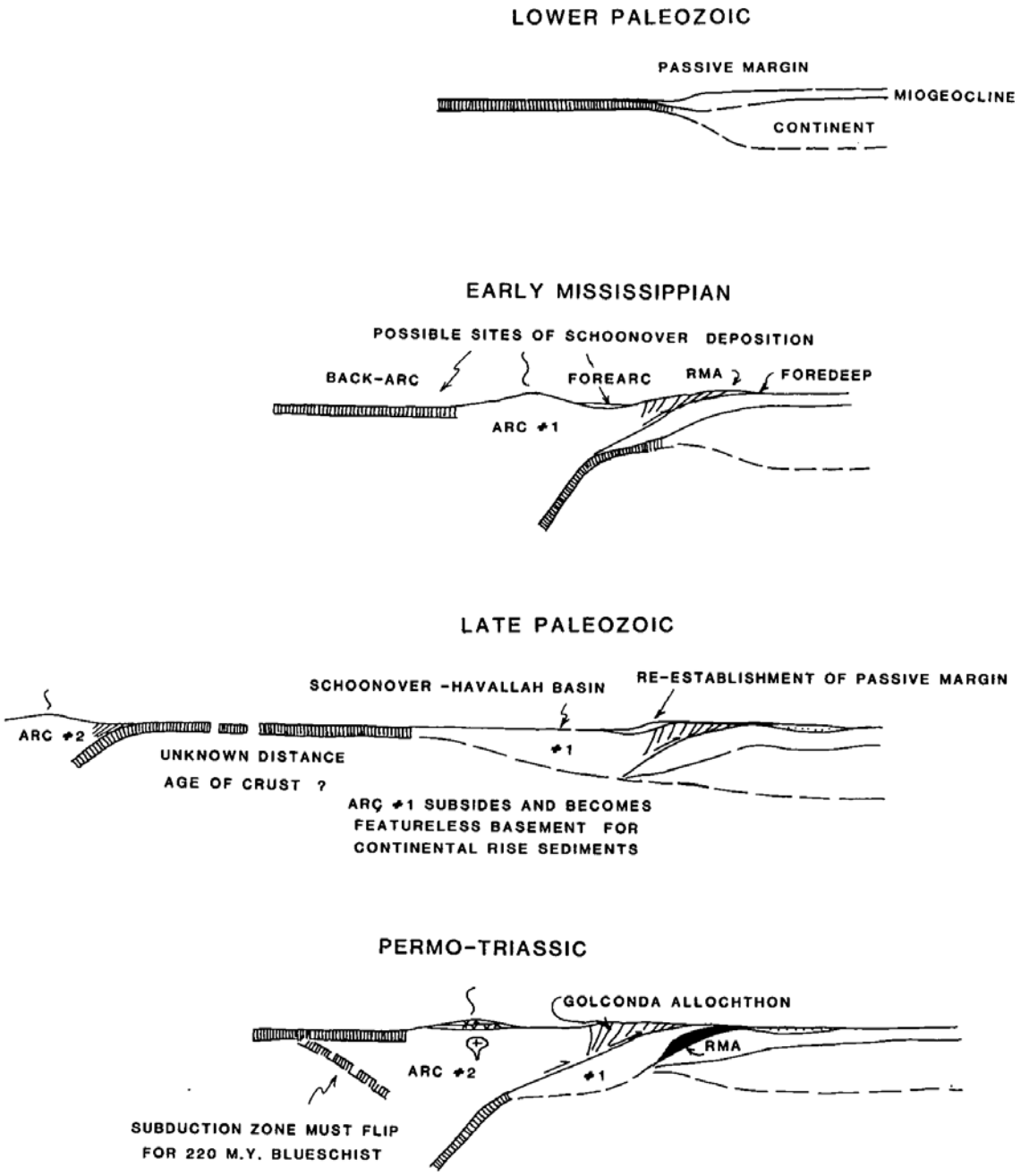

Figure 1.7. Plate tectonic model for the Antler and Sonoma orogenies as proposed by Speed and Sleep (1982), Dickinson et al. (1983), and Snyder and Brueckner (1983). From Miller et al. (1984).

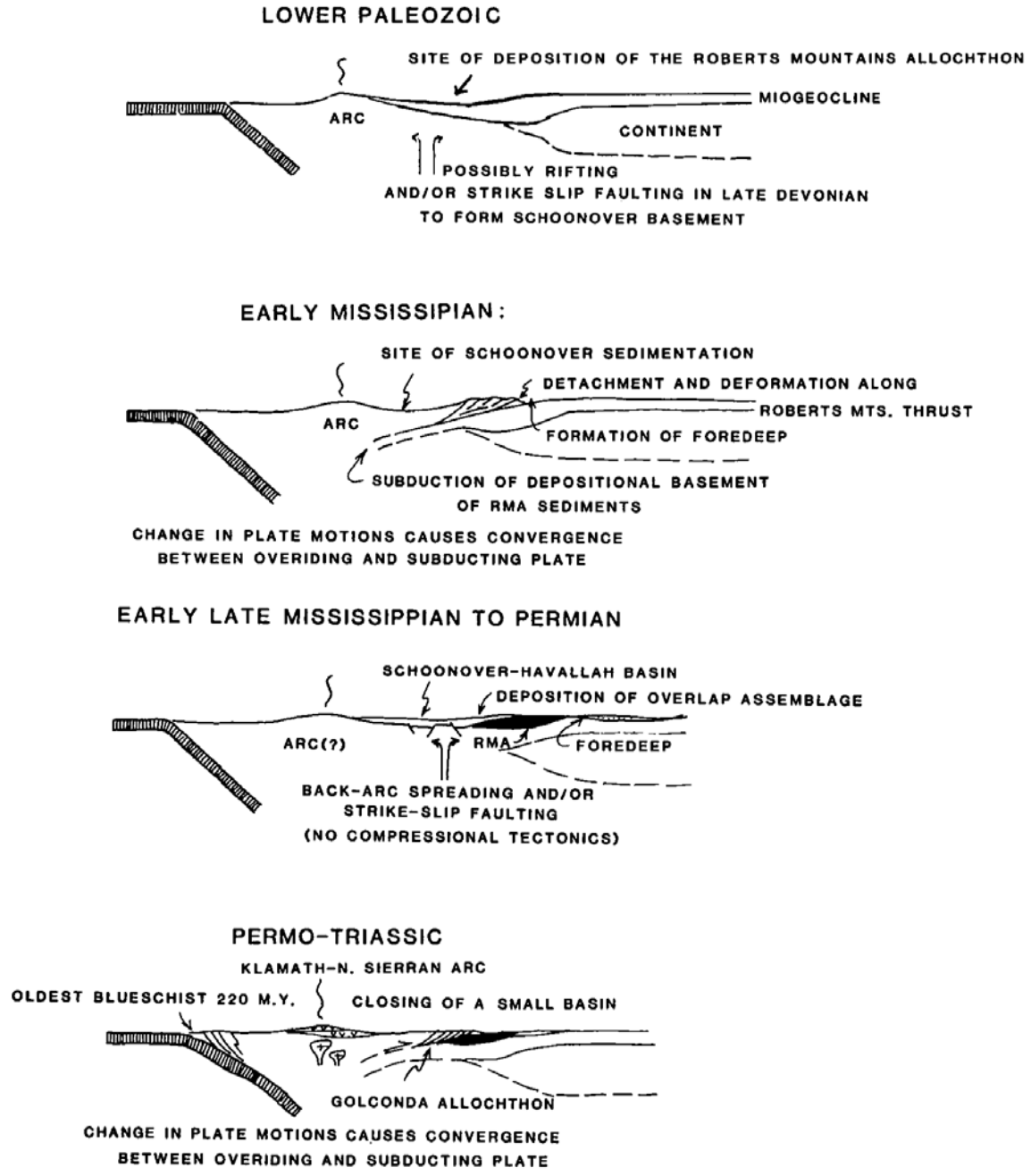

Figure 1.8. Plate tectonic model for the Antler and Sonoma orogenies as proposed by Burchfiel and Davis (1972, 1975), Snyder and Brueckner (1983), and Miller et al. (1984). From Miller et al. (1984).

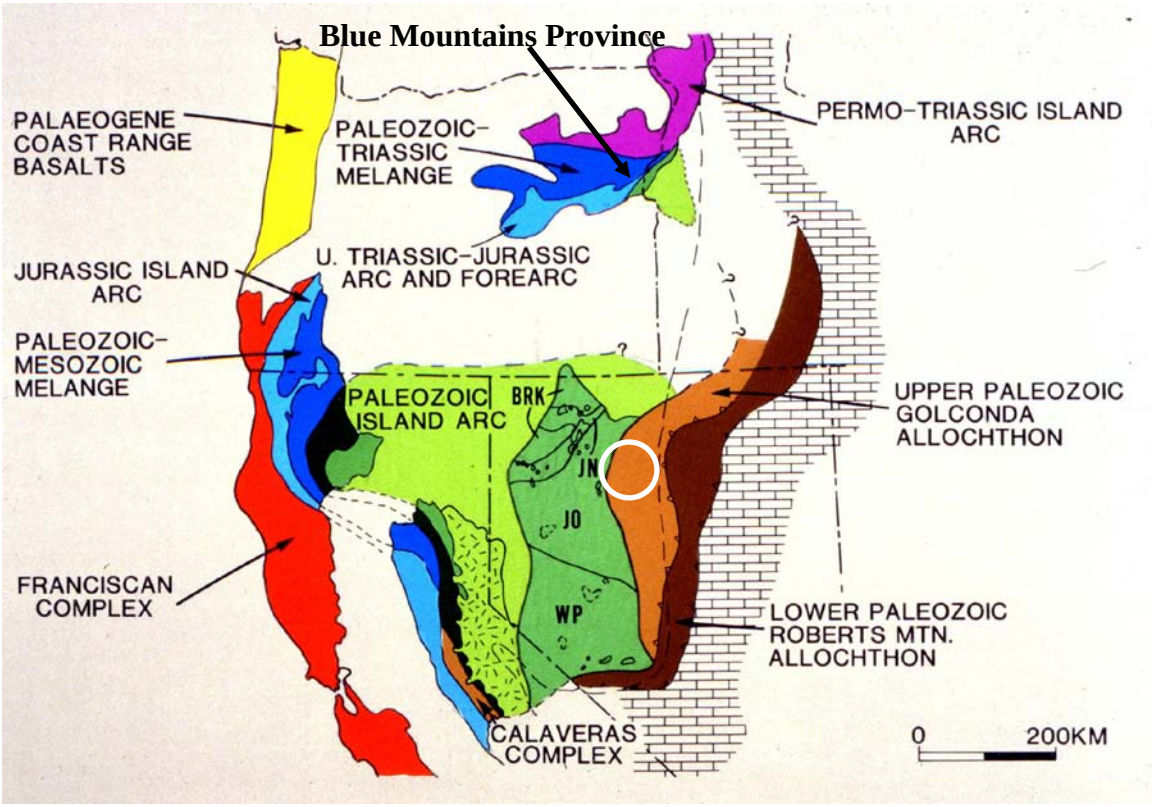

Figure 1.9. Terrane map of the western U.S. showing the major tectonic provinces. White circle denotes approximate position of the Humboldt Range and study area. BRK – Black Rock terrane (Upper Paleozoic island arc); JN – Jackson terrane (Mesozoic); JO – Jungo terrane (Mesozoic); WP – Walker Lake terrane (Mesozoic). From Snyder and Brueckner (1989).

Table 1.1. Major element oxide concentrations for samples from the Koipato Formation.

Sample #:	RSK-13	Lim-76-13C	Lim-2			79119	79120	RD79-3	RD79-4	RD79-9
Description:				Flow	Tuff	Flow	Flow	Flow	Flow	Flow
Classification:	Greenstone	Greenstone	Greenstone	Rhyolite	Rhyolite	Rhyolite	Rhyolite	Rhyolite	Rhyolite	Rhyolite
Unit/Location:	Limerick	Limerick	Limerick	Rochester	Rochester	Rochester	Rochester	Rochester	Rochester	Rochester
Reference:	Kistler and Speed (2000)	Kistler and Speed (2000)	Kistler and Speed (2000)	Vikre (1977)	Vikre (1977)	Vikre (1981)	Vikre (1981)	Vikre (1981)	Vikre (1981)	Vikre (1981)
Normalized Results (Weight %):										
SiO_2	47.83	58.06	61.6	78.2	72.62	78.00	77.30	78.7	73.6	74.9
TiO_2	-	-	-	0.1	0.23	0.08	0.12	0.33	0.25	0.33
Al_2O_3	-	-	-	11.9	13.84	11.10	11.10	10.6	13.4	12.1
Fe_2O_3	-	-	-	0.66	2.2	0.77	0.77	1.8	1.2	1.4
FeO	-	-	-	0.39	0.52	0.13	0.13	0.01	0.02	0.02
MnO	-	-	-	0.103	0.07	-	-	-	-	-
MgO	-	-	-	0.15	0.98	0.17	0.11	0.1	0.22	0.16
CaO	-	-	-	0.11	0.78	0.13	0.13	0.04	0.05	0.05
Na_2O	4.21	2.16	3.52	1	1.3	0.50	1.30	0.19	0.23	0.2
K_2O	2.83	3.48	3.46	6.12	5.6	8.40	8.20	8	9	9
BaO	-	-	-	-	-	0.08	0.08	0.34	0.34	0.11
H_2O	2.67	1.71	-	0.98	1.36	-	-	-	-	-
S	-	-	-	-	-	0.05	0.05	1.4	0.05	1.1
P_2O_5	-	-	-	0.02	0.06	-	-	-	-	-
CO_2	-	-	-	<0.07	0.35	-	-	-	-	-
$K_2O + Na_2O$	7.04	5.64	6.98	7.12	6.9	8.9	9.5	8.19	9.23	9.2

Table 1.1 continued

Sample #:	RSK-7	K-20	RD79-5	57W387	RD79-2	RD79-1	RSK-2	RSK-5	RSK-6	RSK-1
Description:			Flow	Ash-flow tuff	Ash-flow tuff	Ash-flow tuff				
Classification:	Rhyolite	Rhyolite	Rhyolite	Rhyolite	Rhyolite	Rhyolite	Rhyolite	Rhyolite	Rhyolite	Rhyolite
Unit/Location:	Rochester	Rochester	Weaver	Weaver	Weaver	Weaver	Weaver	Weaver	Weaver	Weaver
Reference:	Kistler and Speed (2000)	Kistler and Speed (2000)	Vikre (1981)	Johnson (1977)	Vikre (1981)	Vikre (1981)	Kistler and Speed (2000)	Kistler and Speed (2000)	Kistler and Speed (2000)	Kistler and Speed (2000)
Normalized Results (Weight %):										
SiO_2	79.42	68.8	72.2	75	83.9	82.5	78.84	77.97	78.33	79.23
TiO_2	-	-	0.25	0.07	0.17	0.17	-	-	-	-
Al_2O_3	-	-	19.1	13.4	8.7	10.2	-	-	-	-
Fe_2O_3	-	-	0.21	0.3	1.2	0.57	-	-	-	-
FeO	-	-	0.02	0.5	0.01	0.08	-	-	-	-
MnO	-	-	-	0.07	-	-	-	-	-	-
MgO	-	-	0.04	0.13	0.34	0.42	-	-	-	-
CaO	-	-	0.06	0.08	0.05	0.06	-	-	-	-
Na_2O	-	4.23	0.67	0.3	0.16	0.15	1.52	-	-	0.9
K_2O	-	4.67	4.9	9.6	5.8	6.3	7.53	-	7.8	8.23
BaO	-	-	-	-	0.22	0.11	-	-	-	-
H_2O	0.16	-	-	0.55	-	-	0.26	-	5.63	0.26
S	-	-	0.01	-	0.86	0.05	-	-	-	-
P_2O_5	-	-	-	0.02	-	-	-	-	-	-
CO_2	-	-	-	0.05	-	-	-	-	-	-
$K_2O + Na_2O$	-	8.9	5.57	9.9	5.96	6.45	9.05	-	7.8	9.13

Table 1.1 continued

Sample #:	RSK-16	T152	W578	W579	W580		RSK-15	W392	T1	W576
Description:		Pluton	Pluton	Pluton	Pluton	Pluton	Pluton	Dikes	Dikes	Dikes
Classification:	Rhyolite	Leucogranite	Leucogranite	Leucogranite	Leucogranite	Leucogranite	Leucogranite	Rhyolite	Rhyolite	Rhyolite
Unit/Location:	Weaver	Lone Mt.	Lone Mt.	Black Ridge	Black Ridge			Lone Mt.	Lone Mt.	Lone Mt.
Reference:	Kistler and Speed (2000)	Johnson (1977)	Johnson (1977)	Johnson (1977)	Johnson (1977)	Vikre (1977)	Kistler and Speed (2000)	Johnson (1977)	Johnson (1977)	Johnson (1977)
Normalized Results (Weight %):										
SiO_2	80	78.5	76.2	77	75.9	76.9	77.35	77	77.1	80
TiO_2	-	0.08	0.11	0.06	0.1	0.09	-	0.08	0.12	0.08
Al_2O_3	-	12.4	13.2	12.9	13.4	12.98	-	13.3	12.6	12.3
Fe_2O_3	-	0.32	0.53	0.43	1	0.57	-	0.4	1	0.49
FeO	-	0.22	0.32	0.18	0.21	0.23	-	1.1	0.18	0.23
MnO	-	0.02	0.02	0.02	0.03	0.02	-	0.06	0.01	0.02
MgO	-	0.12	0.11	0.18	0.23	0.16	-	0.34	0.12	0.26
CaO	-	0.06	0.08	0.15	0.1	0.1	-	0.1	0.06	0.07
Na_2O	-	0.29	2.9	0.12	3.2	0.8	-	1.7	3.7	4.4
K_2O	-	6.8	5.8	7.5	5.4	6.38	4.87	4.4	4.4	1.6
BaO	-	-	-	-	-	-	-	-	-	-
H_2O	-	-	-	-	-	0.97	-	-	-	-
S	-	-	-	-	-	-	-	-	-	-
P_2O_5	-	-	-	-	-	0	-	0.02	0.01	0.01
CO_2	-	-	-	-	-	-0.05	-	0.07	-	-
$K_2O + Na_2O$	-	7.09	8.7	7.62	8.6	7.18	4.87	6.1	8.1	6

Table 1.1 continued

Sample #:	W577	T10		SW-113	SW-105	SW-397	SW-11
Description:	Dikes	Dikes	Dike	Stillwater Range	Stillwater Range	Stillwater Range	Stillwater Range
Classification:	Rhyolite	Rhyolite	Rhyolite				
Unit/Location:	Lone Mt.	Lone Mt.		Koipato Group	Koipato Group	Koipato Group	Koipato Group
Reference:	Johnson (1977)	Johnson (1977)	Vikre (1977)	Kistler and Speed (2000)	Kistler and Speed (2000)	Kistler and Speed (2000)	Kistler and Speed (2000)
Normalized Results (Weight %):							
SiO_2	72.3	77.2	77.49	79.25	80.18	79.49	77.82
TiO_2	0.1	0.1	0.23	-	-	-	-
Al_2O_3	15.2	12.4	12.7	-	-	-	-
Fe_2O_3	1.1	0.7	0.5	-	-	-	-
FeO	0.44	0.32	0.51	-	-	-	-
MnO	0.05	0.02	0.05	-	-	-	-
MgO	0.24	0.19	0.2	-	-	-	-
CaO	0.88	0.06	0.18	-	-	-	-
Na_2O	2.7	0.22	1.35	2.76	0.91	2.36	2.04
K_2O	5.8	8.1	5.79	3.92	5.55	6.26	5.21
BaO	-	-	-	-	-	-	-
H_2O	-	-	0.19	-	-	-	-
S	-	-	-	-	-	-	-
P_2O_5	-	0.01	0.1	-	-	-	-
CO_2	0.69	-	0.05	-	-	-	-
$K_2O + Na_2O$	8.5	8.32	7.14	6.68	6.46	8.62	7.25

References Cited

Brookfield, M.E., 1993, Neoproterozoic Laurentia-Australia fit: Geology, v. 21, p. 683-686.

Brueckner, H.K., and Snyder, W.S., 1985, Structure of the Havallah sequence, Golconda allochthon, Nevada: Evidence for prolonged evolution in an accretionary prism: Geological Society of America Bulletin, v. 96, p. 1113-1130.

Burchfiel, B.C., and Davis, G.A., 1972, Structural framework and evolution of the southern part of the Cordilleran orogen, western United States: American Journal of Science, v. 272, p. 97-118.

—, 1975, Nature and controls of Cordilleran orogenesis, western United States: Extensions of an earlier synthesis: American Journal of Science, v. 275-A, p. 363-396.

—, 1981, Triassic and Jurassic tectonic evolution of the Klamath Mountains-Sierra Nevada geologic terrane, in Ernst, W.G., ed., The geotectonic development of California; Rubey Volume 1: Englewood Cliffs, New Jersey, p. 50-70.

Burchfiel, B.C., and Royden, L.H., 1991, Antler orogeny: A Mediterranean-type orogeny: Geology, v. 19, p. 66-69.

Burchfiel, B.C., Cowan, D.S., and Davis, G.A., 1992, Tectonic overview of the Cordilleran orogen in the western United States, in Burchfiel, B.C., Lipman, P.W., and Zoback, M.L., eds., The Cordilleran Orogen: Conterminous U.S., Volume G-3: The Geology of North America: Boulder, Colorado, Geological Society of America, p. 407-479.

Burke, D.B., 1973, Reinterpretation of the Tobin thrust – Pre-Tertiary geology of the southern Tobin Range, Pershing County, Nevada: Ph.D. thesis, Stanford University, Stanford, California, 82 p.

Burke, D.B., and Silberling, N.J., 1973, The Auld Lang Syne Group, of Late Triassic and Jurassic (?) age, north-central Nevada: U.S. Geological Survey Bulletin 1394-E, 14 p.

Churkin, M., Jr., 1974, Paleozoic marginal ocean basin-volcanic arc systems in the Cordilleran foldbelt, in Dott, R.H., Jr., and Shaver, R.H., eds., Modern and Ancient Geosynclinal Sedimentation: Society of Economic Paleontologists and Mineralogists, Special Publication, no. 19, p. 174-192.

Coats, R.R., and Gordon, M., Jr., 1972, Tectonic Implications of the presence of the Edna Mountain Formation in northern Elko, County: U.S. Geological Survey Professional Paper 800C, p. C85-C94.

Colpron, M., Logan, J.M., and Mortensen, J.K., 2002, U-Pb zircon age constraint for late Neoproterozoic rifting and initiation of the lower Paleozoic passive margin of western Laurentia: Canadian Journal of Earth Science, v. 39, p. 133-143.

Crafford, A.E.J., 2007, Geologic Map of Nevada: U.S. Geological Survey Data Series 249.

Dalziel, I.W.D., 1991, Pacific margins of Laurentia and East Antarctica-Australia as a conjugate rift pair: Evidence and implications for an Eocambrian supercontinent: Geology, v. 19, p. 598-601.

Dickinson, W.R., 1977, Paleozoic plate tectonics and the evolution of the Cordilleran continental margin, in Stewart, J.H., Stevens, C.H., and Fritsche, A.E., eds., Paleozoic paleogeography of the western United States: Pacific Coast Paleogeography Symposium 1: Los Angeles, Society of Economic Paleontologists and Mineralogists, Pacific Section, p. 137-155.

—, 2000, Geodynamic interpretation of Paleozoic tectonic trends oriented oblique to the Mesozoic Klamath-Sierran continental margin in California, in Soreghan, M.J., and Gehrels, G.E., eds., Paleozoic and Triassic paleogeography and tectonics of western Nevada and northern California: Boulder, Colorado, Geological Society of America Special Paper 347, p. 209-245.

—, 2004, Evolution of the North American Cordillera: Annual Review of Earth and Planetary Sciences, v. 32, p. 13-45.

—, 2006, Geotectonic evolution of the Great Basin: Geosphere, v. 2, p. 353–368.

Dickinson, W.R., and Lawton, T.F., 2001, Tectonic setting and sandstone petrofacies of the Bisbee basin (USA-Mexico): Journal of South American earth Sciences, v. 14, p. 475-501.

Dickinson, W.R., Harbaugh, D.W., Saller, A.H., Heller, P.L., and Snyder, W.S., 1983, Detrital modes of upper Paleozoic sandstones derived from Antler orogen in Nevada: Implications for nature of Antler orogeny: American Journal of Science, v. 283, p. 481-509.

Dunston, J.R., Northrup, C.J., and Snyder, W.S., 2001, Post-Latest Triassic thrust emplacement of the Golconda Allochthon, Sonoma Range, Nevada [abs.]: GSA Annual Meeting.

Elison, M.W., Speed, R.C., and Kistler, R.W., 1990, Geologic and isotopic constraints on the crustal structure of the northern Great Basin: Geological Society of America Bulletin, v. 102, p. 1077-1092.

Erickson, R.L., and Marsh, S.P., 1974, Paleozoic tectonics in the Edna Mountain Quadrangle, Nevada: U.S. Geological Survey Journal of Research, v. 2, p. 331-337.

Ferguson, H.G., Roberts, R.J., and Muller, S.W., 1952, Geology of the Golconda quadrangle, Nevada: U.S. Geological Survey Geologic Quadrangle Map GQ-15.

Hansen, V.L., 1988, A model for terrane accretion, Yukon-Tanana and Slide Mountain terranes, northwest, North America: Tectonics, v. 6, p. 1167-1177.

Harwood, D.S., 1983, Stratigraphy of upper Paleozoic volcanic rocks and regional unconformities in part of the northern Sierra terrane, California: Geological Society of America Bulletin, v. 94, p. 413-422.

—, 1988, Tectonism and metamorphism in the Northern Sierra Terrane, northern California, in Ernst, W.G., ed., Metamorphism and crustal evolution of the western United States: Englewood Cliffs, New Jersey, p. 764-788.

Hoffman, P.F., 1991, Did the breakout of Laurentia turn Gondwanaland inside-out?: Science, v. 252, p. 1409-1412.

Jenney, C.P., 1935, Geology of the central Humboldt Range, Nevada: University of Nevada Bulletin, v. 29, no. 6, 73 p.

Johnson, M.G., 1977, Geology and Mineral Deposits of Pershing County, Nevada: Nevada Bureau of Mines and Geology, Bulletin 89, 115 p.

Johnson, J.G., and Pendergast, A., 1981, Timing and mode of emplacement of the Roberts Mountains allochthon, Antler orogeny: Geological Society of America Bulletin, v. 92, p. 648-658.

Karlstrom K.E., Harlan, S.S., Williams, H.L., McClelland, J., Geissman, J.W., et al., 1999, Refining Rodinia: geologic evidence for the Australia-western U.S. connection in the Proterozoic: GSA Today, v. 9, no. 10, p. 1-7.

Ketner, K.B., 1977, Late Paleozoic orogeny and sedimentation, southern California, Nevada, Idaho, and Montana, in Stewart, J.H., Stevens, C.H., and Fritsche, A.E., eds., Paleozoic paleogeography of the western United States: Pacific Section, Society of Economic Paleontologists and Mineralogists, Pacific Coast Paleogeography Symposium 1, p. 363–369.

—, 1984, Recent studies indicate that major structures in northwestern Nevada and the Golconda thrust in north-central Nevada are of Jurassic or Cretaceous age: Geology, v. 12, p. 483-486.

King, C., 1878, Systematic geology: U.S. Geological Explorations of the 40th Parallel: Government Printing Office, v. 1, 803 p.

Kistler, R.W., and Speed, R.C., 2000, $^{40}Ar/^{39}Ar$, K-Ar, Rb-Sr Whole-Rock and Mineral Ages, Chemical Composition, Strontium, Oxygen and Hydrogen Isotopic Systematics of Jurassic Humboldt Lopolith and Permian(?) and Triassic Koipato Group rocks, Pershing and Churchill Counties, Nevada: U.S. Geological Survey Open-File Report 00-217, 14p.

Knopf, A., 1924, Geology and ore deposits of the Rochester District, Nevada, U.S. Geological Survey Bulletin 762.

Le Bas, M.J., Le Maitre, R.W., Streckeisen, A., and Zanettin, B., 1986, A chemical classification of volcanic rocks based on the total alkali-silica diagram: Journal of Petrology, v. 27, p. 745-750.

Lupe, R., and Silberling, N. J., 1985, Genetic relationship between lower Mesozoic continental strata of the Colorado Plateau and marine strata of the western Great Basin: significance for accretionary history of Cordilleran lithotectonic terranes: in Howell, D.G., ed., Tectonostratigraphic terranes of the Circum-Pacific region: Circum-Pacific Council for Energy and Mineral Resources, Earth Science Series, no. 1, p. 263–271.

MacMillan, J.R., 1972, Late Paleozoic and Mesozoic Tectonic events in west central Nevada: Ph.D. thesis, Northwestern University, Evanston, Illinois, 146 p.

McKee, E.H., and Burke, D.B., 1972, Fission-track age bearing on the Permian-Triassic boundary and time of the Sonoma orogeny in north-central Nevada: Geological Society of America Bulletin, v. 83, no. 7, p. 1949-1952.

Miller, E.L., Holdsworth, B.K., Whiteford, W.B., and Rodgers, D., 1984, Stratigraphy and structure of the Schoonover sequence, northeastern Nevada: Implications for

Paleozoic plate-margin tectonics: Geological Society of America Bulletin, v. 95, p. 1063-1076.

Miller, E.L., Miller, M.M., Stevens, C.H., Wright, J.E., and Madrid, R., 1992, Late Paleozoic paleogeographic and tectonic evolution of the western U.S. Cordillera, in Burchfiel, B.C., Lipman, P.W., and Zoback, M.L., eds., The Cordilleran Orogen: Conterminous U.S., Volume G-3: The Geology of North America: Boulder, Colorado, Geological Society of America.

Miller, M.M., 1987, Dispersed remnants of a northeast Pacific fringing arc: Upper Paleozoic terranes of Permian McCloud faunal affinity, western U.S.: Tectonics, v. 6, p. 807-830.

Moores, E.M., 1991, Southwest U.S.-East Antartica (SWEAT) connection: A hypothesis: Geology, v. 19, p. 425-428.

Mortimer, N., 1987, The Nicola Group: Late Triassic and Early Jurassic subduction-related volcanism in British Columbia: Canadian Journal of Earth Science, v. 24, p. 2521–2536.

Nichols, K.M., and Silberling, N.J., 1977, Stratigraphy and depositional history of the Star Peak Group (Triassic), northwestern Nevada: Geological Society of America Special Paper 178, 142 p.

Nilsen, T.H., and Stewart, J.H., 1980, The Antler orogeny-Mid-Paleozoic tectonism in western North America: Geology, v. 8, p. 298-302.

Northrup, C.J., and Snyder, W.S., 2000, Significance of the Sonoma Orogeny, Western U.S.: What, Where, and When? Geological Society of Nevada Symposium 2000, Program with Abstracts, p. 66-67.

Oldow, J.S., 1984, Evolution of a late Mesozoic back-arc fold and thrust belt, northwestern Great Basin, U.S.A.: Tectonophysics, v. 102, p. 245–274.

Oldow, J.S., Bally, A.W., Avé Lallement, H.G., and Leeman, W.P., 1989, Phanerozoic evolution of the North American Cordillera, in Bally, A.W., and Palmer, A.R., eds., The geology of North America—an overview (The Geology of North America, v. A): Boulder, Colo., Geological Society of America, p. 139–232.

Prave, A.R., 1999, Two diamictites, two cap carbonates, two δ^{13} excursions, two rifts: Geology, v. 27, p. 339-342.

Ransome, F.L., 1909, Notes on some mining districts in Humboldt County, Nevada: U.S. Geological Survey Belletin 414, 75 p.

Riggs, N.R., Lehman, T., Gehrels, G.E., and Dickinson, W.R., 1996, Detrital zircon link between headwaters and terminus of the Chinle-Dockum paleoriver system: Science, v. 273, p. 97-100.

Roberts, R.J., 1951, Geology of the Antler Peak quadrangle, Nevada: U.S. Geological Survey Geologic Quadrangle Map GQ-10.

—, 1964, Stratigraphy and structure of the Antler Peak quadrangle, Humboldt and Lander Counties, Nevada: U.S. Geological Survey, Professional Paper 459-A, 93 p.

Roberts, R.J., Hotz, P E., Gilluly, J., and Ferguson, H.G., 1958, Paleozoic rocks of north-central Nevada: American Association of Petroleum Geologists Bulletin, v. 42, p. 2813-2857.

Ross, G.M., 1991, Tectonic setting of the Windermere Supergroup revisited: Geology, v. 19, p. 1125-1128.

Royden, L., and Burchfiel, B.C., 1989, Are systematic variations in thrust belt style related to plate boundary processes? (The western Alps versus the Carpathians): Tectonics, v. 8, p. 51-61.

Saleeby, J.B., and Busby-Spera, C., 1992, Early Mesozoic tectonic evolution of the western U.S. Cordillera, in Burchfiel, B.C., Lipman, P.W., and Zoback, M.L., eds., The Cordilleran Orogen: Conterminous U.S., Volume G-3: The Geology of North America: Boulder, Colorado, Geological Society of America, p. 107-168.

Saleeby, J.B., Hannah, J.L., and Varga, R.J., 1987, Isotopic age constraints on middle Paleozoic deformation in the northern Sierra Nevada, California: Geology, v. 15, p. 757-760.

Schweickert, R.A., and Lahren, M.M., 1987, Continuation of the Antler and Sonoma orogenic belts to the eastern Sierra Nevada, California, and Late Triassic thrusting in a compressional arc: Geology, v. 15, p. 270-273.

—, 1993, Triassic-Jurassic magmatic arc in eastern California and western Nevada: arc evolution, cryptic tectonic breaks, and significance of the Mojave–Snow Lake fault, in Dunne, G., and McDougall, K., eds., Mesozoic Paleogeography of the western United States-II: Los Angeles, California, Society of Economic Paleontologists and Mineralogists, Pacific Section, Book 71, p. 227-246.

Schweickert, R.A., and Snyder, W.S., 1981, Paleozoic plate tectonics of the Sierra Nevada and adjacent regions, in Ernst, W.G., ed., The Geotectonic Development of California, Rubey Volume I: Englewood Cliffs, New Jersey, Prentice-Hall, p. 182-201.

Sears, J.W., and Price, R.A., 2003, Tightening the Siberian connection to western Laurentia: Geological Society of America Bulletin, v. 115, p. 943-953.

Sears, J.W., Khudoley, A.K., Prokopiev, A.V., Chamberlain, K., and MacLean, J.S., 2005, Lithostratigraphic matches of Meso- and Neoproterozoic strata between Siberia and SW Laurentia: Geological Society of America Abstracts with Programs, v. 37, no. 7, p. 41-42.

Silberling, N.J., 1973, Geologic events during the Permian-Triassic time along the Pacific margin of the United States, in Logan, A., and Hills, L.V., eds., The Permian and Triassic systems and their mutual boundary: Canada Society of Petroleum Geologists Memoir 2, p. 345-362.

Silberling, N.J. and Roberts, R.J., 1962, Pre-Tertiary stratigraphy and structure of north-western Nevada: Geological Society of America, Special Paper 72, 58 p.

Skalbeck, J.D., 1985, Paleomagnetism of the Early Triassic Koipato Group, western Nevada, and its tectonic implications: M.S. Thesis, Western Washington University, 206 p.

Smith, M.T., and Gehrels, G.E., 1991, Detrital zircon geochronology of upper Proterozoic to lower Paleozoic continental margin strata of the Kootenay arc: implications for the early Paleozoic tectonic development of the eastern Canadian Cordillera: Canadian Journal of Earth Science, v. 28, p. 1271-1284.

—, 1992, Structural geology of the Lardeau Group near Trout Lake, British Columbia: implications for the structural evolution of the Kootenay arc: Canadian Journal of Earth Science, v. 29, p. 1305-1319.

Snyder, W.S., and Brueckner, H.K., 1983, Tectonic evolution of the Golconda allochthon, Nevada: Problems and perspectives, in Stevens, C.H., ed., Pre-Jurassic rocks in western North American suspect terranes: Society of Economic Paleontologists and Mineralogists, Pacific Section, p. 103-123.

—, 1989, Permian-Carboniferous tectonics of the Golconda Allochthon; an accreted terrane in the Western United States: Compte Rendu 4 – XI Congres International de Stratigraphie et de Geologie du Carbonifere, p. 294-312.

Snyder, W.S., Trexler, J.H., Jr., Davydov, V.I., Cashman, P., Schiappa, T.A., and Sweet, D., 2002, Upper Paleozoic Tectonostratigraphic Framework for the Western Margin of North America: AAPG Hedberg Conference, 4 p.

Speed, R.C., 1977, Island-arc and other paleogeographic terranes of late Paleozoic age in the western Great Basin, in Stewart, J.H., Stevens, C.H., and Fritsche, A.E., eds., Paleozoic paleogeography of the western United States: Pacific Coast Paleogeography Symposium 1: Los Angeles, Society of Economic Paleontologists and Mineralogists, Pacific Section, p. 349-362.

—, 1979, Collided Paleozoic microplate in the western United States: Journal of Geology, v. 87, p. 279-292.

Speed, R.C., and Sleep, N.H., 1982, Antler orogeny and foreland basin: A model: Geological Society of America Bulletin, v. 93, p. 815-828.

Speed, R.C., Elison, M.W., and Heck, R.R., 1988, Phanerozoic tectonic evolution of the Great Basin, in Ernst, W.G., ed., Metamorphism and crustal evolution of the western United States, Rubey Volume 7: Englewood Cliffs, New Jersey, p. 572–605.

Stone, P., and Stevens, C.H., 1988, Pennsylvanian and Early Permian paleogeography of east-central California: Implications for the shape of the continental margin and timing of continental truncation: Geology, v. 16, p. 330-333.

Timmons, J.M., Karlstrom, K.E., Dehler, C.M., Geissman, J.W., and Heizler, M.T., 2001, Proterozoic multistage (ca. 1.1 and 0.8 Ga) extension recorded in the Grand Canyon Supergroup and establishment of northwest- and north-trending tectonic grains in the southwestern United States: Geological Society of America Bulletin, v. 113, p. 163-180.

Trexler, J.H., Jr., Cashman, P.H., Snyder, W.S., and Davydov, V.I., 2004, Late Paleozoic tectonism in Nevada: Timing, kinematics, and tectonic significance: Geological Society of America Bulletin, v. 116, no. 5/6, p. 525–538.

Turner, R.J.W., Madrid, R., and Miller, E.L., 1989, Roberts Mountains allochthon: Stratigraphic comparison with lower Paleozoic outer continental margin strata of the northern Canadian Cordillera: Geology, v. 17, p. 341-344.

Vikre, P.G., 1977, Geology and Silver Mineralization of the Rochester District, Pershing County, Nevada: Ph.D. thesis, Stanford University, Stanford, California, 404 p.

—, 1981, Silver mineralization in the Rochester District, Pershing County, Nevada: Economic Geology, v. 76, p. 580-609.

Walker, J.D., 1988, Permian and Triassic rocks of the Mojave Desert and their implications for the timing and mechanisms of continental truncation: Tectonics, v. 7, p. 685-709.

Wallace, R.E., Tatlock, D.B., and Silberling, N.J., 1960, Intrusive rocks of Permian and Triassic age in the Humboldt Range, Nevada: U.S. Geological Survey Professional Paper 400B, p. B291-B293.

Wallace, R.E., Tatlock, D.B., Silberling, N.J., and Irwin, W.P., 1969a, Geologic map of the Unionville Quadrangle, Pershing County, NV: U.S. Geological Survey Geologic Quadrangle Map GQ-820.

Wallace, R.E., Silberling, N.J., Irwin, W.P., and Tatlock, D.B., 1969b, Geologic map of the Buffalo Mountain Quadrangle, Pershing and Churchill Counties, NV: U.S. Geological Survey Geologic Quadrangle Map GQ-821.

Wardlaw, B.R., Snyder, W.S., Spinosa, C., and Gallegos, D.M., 1995, Permian of the Western United States, in Scholle, P.A., Peryt, T.M., and Ulmer-Scholle, D.S., eds., Permian Stratigraphy of the World, Volume 2: Sedimentary Basins and Economic Resources: Springer-Verlag, New York, p. 23-40.

Watkins, R., 1985, Volcaniclastic and carbonate sedimentation in late Paleozoic island-arc deposits, eastern Klamath Mountains: Geology, v. 13, no. 10, p. 709-713.

Wheeler, H.E., 1939, Helicoprion in the Anthracolithic (Late Paleozoic) of Nevada and California, and its stratigraphic significance, Journal of Paleontology, v. 13, n. 1, p. 103–114.

Wilkins, J., 2010, Structural and Stratigraphic Age Constraints of the Inskip Formation, East Range, Nevada: Implications for Mesozoic Tectonics of Western North America: M.S. thesis, Boise State University, Boise, Idaho, 117 p.

Wyld, S.J., 1991, Permo-Triassic tectonism in volcanic arc sequences of the western U.S. Cordillera and implications for the Sonoma Orogeny: Tectonics, v. 10, no. 5, p. 1007-1017.

CHAPTER TWO: STRATIGRAPHY AND GEOCHRONOLOGY OF THE KOIPATO FORMATION, CENTRAL NEVADA

Abstract

The Koipato Formation unconformably overlies the Golconda Allochthon, and this relationship has been used to define the timing of the Sonoma Orogeny. New lithologic and high-precision CA-TIMS U-Pb zircon geochronology from the Koipato Formation in the Humboldt, East, and Tobin Ranges allows for a more detailed understanding of the Koipato Formation's stratigraphic architecture and its importance for the Early Mesozoic tectonic setting of the U.S. Cordillera.

New U-Pb geochronology reveals that Koipato Formation units were deposited predominately in the Early Triassic (Olenekian) and that the majority of Koipato-type volcanism lasted only ~1.2 Ma. The existence of ~254 Ma inherited zircons within the leucogranite of the Humboldt Range has been inferred to represent the earliest stages of Limerick Greenstone-type Koipato volcanism, which extends the age of Koipato Formation volcanism to the latest Permian. The Koipato Formation also records the transition from intermediate to felsic volcanism and a short-term hiatus in volcanism. Volcanism within the Koipato Formation most likely lasted until just after deposition of the youngest Weaver Rhyolite sample from this study (248.32 Ma). U-Pb geochronology was performed on the felsic units (volcanic and intrusive) and shows that the volcanic Rochester and lower Weaver Rhyolites are coeval with the intrusive units. Two phases of

silicic volcanism are now identified within the Koipato Formation, separated by a previously unidentified unconformity. The older phase is composed of the Rochester and lower Weaver Rhyolites of Troy Canyon and the Rochester Rhyolite in the East and Tobin Ranges, whereas the younger phase is documented within the Rochester and lower Weaver Rhyolites of Limerick Canyon and the sedimentary and upper Weaver Rhyolites of Troy Canyon. This unconformity lasted for <350,000 years in Troy Canyon, but continued for another 100,000 years in Limerick Canyon. Finally, the transition in volcanic composition and the volcanic hiatus between the Limerick Greenstone and Rochester Rhyolite is constrained by the youngest intermediate (249.37 Ma) and oldest felsic (249.18 Ma) samples analyzed from the Koipato Formation, which demonstrate that the unconformity between the Limerick Greenstone and the Rochester and Weaver Rhyolites lasted for no more than 200,000 years. However, in Limerick Canyon, the unconformity appears to have lasted for ~1 Ma and resulted in the erosion of the older phase of silicic volcanism from the Limerick Canyon area.

Unconformities also bound the Koipato Formation, with new U-Pb geochronology helping to constrain their duration. The lower bounding unconformity separating the Golconda Allochthon from the Koipato Formation has been constrained to a time span of ~15 to 6 Ma based on the occurrence of ~254 Ma inherited zircons within the leucogranite exposed in the Humboldt Range. During this time, the later stages of deformation observed within the Golconda Allochthon must have occurred, but this age does not constrain the emplacement of the Golconda Allochthon due to the Koipato Formation not overlapping the Golconda thrust and overlying the autochthon. The upper

bounding unconformity separates the Koipato Formation from the overlying Prida Formation and an age of 248.32 Ma from the upper Weaver Rhyolite constrains the unconformity to a time span of 3 to 7 Ma. During this time, volcanism ceased and the western margin of the U.S. Cordillera transformed to a carbonate platform, which facilitated the deposition of thick carbonate sequences of the Star Peak Group that overlie the Koipato Formation in the Humboldt Range and elsewhere throughout central Nevada.

Introduction

The Early Triassic Koipato Formation is an intermediate to felsic volcanic sequence confined to central Nevada (Fig. 2.1). King (1878) and Ransome (1909) were the first to name and describe the Koipato Formation and recognize its volcanic nature, but Knopf (1924) was the first to subdivide it into individual members: the Rochester Trachyte, Nenzel Rhyolite Breccia, and the Weaver Rhyolite. This terminology was revised by Jenney (1935) into the Limerick Keratophyre, Rochester Rhyolite, and Weaver Rhyolite. Subsequent work (e.g., Wallace et al., 1969a; MacMillan, 1972; Silberling, 1973; Burke, 1973) devised the current usage, dividing the Koipato Formation into the Limerick Greenstone, Rochester Rhyolite, and Weaver Rhyolite (Fig. 2.2). Since the work of Vikre (1977), the Koipato Formation has been relatively unstudied as a unit, although it has been the focus of local studies related to mineralization (e.g., Vikre, 1981; Vikre and McKee, 1985; Cheong, 1999, 2002). The current study calls into question the simple tripartite division of the Koipato and suggests a more complex stratigraphy that reflects the Early Triassic tectonomagmatic environment.

Since its description by the U.S. Geological Survey 40th parallel survey by King (1878), the Koipato Formation has been recognized as an Early Triassic formation, although the exact age has been debated. Wheeler (1939) was the first to examine fossil specimens from the Rochester Rhyolite, which he assigned a Late Permian age, leaving open the possibility that the overlying Weaver Rhyolite could still be Early Triassic. Subsequent authors continued to use Wheeler's interpretation of a Late Permian-Early Triassic age for the Koipato Formation, but it wasn't until the work of Silberling and Roberts (1962) that Early Triassic fauna were found in the Weaver Rhyolite (Fig. 2.2). Silberling (1973) expanded on this discovery, suggesting that Wheeler's Rochester Rhyolite fossil (a helicoprion) did not originate within the Koipato Formation. Instead, Silberling (1973) described Early Triassic ammonite impressions and an isolated fish tooth from the Rochester Rhyolite, which restricted the Koipato Formation to the Early Triassic. An Early Triassic age is supported by Pb-α analyses (230 ± 40 and 290 ± 45 Ma) (Wallace et al., 1960) and a fission-track zircon age (225 ± 30 Ma) (McKee and Burke, 1972) from the Rochester Rhyolite and related intrusive units (Fig. 2.2). Subsequent research has continued to support an Early Triassic age for deposition of the Koipato Formation's felsic units (Vikre, 1977). A definitive age for the Limerick Greenstone has, until the work reported here, never been established, and this has left open the possibility that the Koipato Formation extended into the Late Permian. A maximum age for the Koipato Formation is established using the youngest unit in the Golconda Allochthon, which includes siliceous bedded cherts assigned Middle Permian (Guadalupian) ages (Roberts, 1951, 1964; Laule et al., 1981; Murchey, 1990; Murchey and Jones, 1992).

The age of the intrusive units within the Koipato Formation has also been a matter of debate. Leucogranite intrusive complexes and rhyolite porphyry dikes are widespread throughout the southern Humboldt Range (Fig. 2.3) and elsewhere in central Nevada, in particular in the East Range where they intrude the Golconda Allochthon (Stewart and Carlson, 1978). Within the Humboldt Range, these intrusive units cut the Limerick Greenstone and Rochester Rhyolite and have been interpreted as feeders for the Weaver Rhyolite (Fig. 2.3) (Wallace et al., 1969a; Silberling, 1973; Vikre, 1977). The intrusive units were dated by McKee and Burke (1972) using two Pb-α analyses that returned ages of 230 ± 40 and 290 ± 45 Ma, but the large uncertainty precludes definitive interpretation of the age relationship between these intrusive and the subunits of the Koipato Formation (Fig. 2.2). Vikre (1977) did note that the intrusive units are similar in composition and texture to the Rochester Rhyolite, which leaves open the possibility that the intrusive units could have acted as feeders for both the Rochester and Weaver Rhyolites.

The tectonic history of the Koipato Formation has long been a matter of discussion. It wasn't until the work of Ferguson et al. (1952), in the Tobin Range, that the Koipato Formation was recognized as unconformably overlying the faulted and folded Pumpernickel and Havallah Formations of what is now recognized as of the Golconda Allochthon (Fig. 2.4). This stratigraphic relationship was utilized by Silberling and Roberts (1962) to define the Sonoma Orogeny and to assign an age of Late Permian to Early Triassic to this event. The Sonoma Orogeny has been described as the event that emplaced the Golconda Allochthon onto the continental margin along the Golconda thrust, with Koipato Formation deposition occurring after final emplacement (e.g.,

Silberling and Roberts, 1962; Burchfiel and Davis, 1972, 1981; Schweickert and Snyder, 1981; Speed and Sleep, 1982; Snyder and Brueckner, 1983; Burchfiel et al., 1992; Dickinson, 2004, 2006). Vikre (1977) postulated that the Koipato Formation represents the first vestiges of a newly developing, post-Sonoma Orogeny continental arc, with the Limerick Greenstone representing the final stages of melting of oceanic crust beneath the accreted Sonoma Orogeny island-arc system and the overlying Rochester and Weaver Rhyolites representing the initial products of continental arc volcanism. The idea of the Koipato Formation as entirely post-tectonic supports the idea of Williams (1939) and amplified by Burke (1973) who believe that it was deposited in a tectonic depression. This tectonic depression resulted from the down warping of the continental crust due to the emplacement of the Golconda Allochthon and associated island arc. However, recent research has called this theory into question by suggesting that either part or all of the Koipato Formation could have been deposited pre- to syn-tectonically and then was carried piggyback on the Golconda Allochthon (e.g., Dickinson, 1977; Speed, 1977; Snyder and Brueckner, 1983; Burchfiel et al., 1992; Dunston et al., 2001; Wilkins, 2010). This theory would imply that the Sonoma Orogeny was a longer-lived event. This view of the Koipato Formation carried piggyback on the Golconda Allochthon is supported by the fact that nowhere has it been documented that Koipato Formation units overlap the Golconda thrust (Dickinson, 1977; Burchfiel et al., 1992) and that the Rochester Rhyolite in the East Range is interpreted to have been cut by the Golconda thrust and so must have been deposited pre- or syn-tectonically (Wilkins, 2010). If the Koipato Formation was carried piggyback, then thrusting associated with the Sonoma Orogeny didn’t end until post-Early Triassic time, and could have lasted into the Jurassic as some authors have put

forth (Ketner, 1984; Snyder and Brueckner, 1989; Northrup and Snyder, 2000; Dunston et al., 2001).

This chapter provides new data about the nature and timing of Triassic volcanism and intrusive units of the Koipato Formation of central Nevada. U-Pb geochronology was used to determine that the majority of Koipato volcanism in the Humboldt Range lasted for ~1.2 Ma in the Early Triassic and probably extended into at least the latest Permian (~254 Ma). All these data, combined with previous research, are used to redefine the tectonostratigraphic setting of the Koipato Formation volcanism along the western U.S. Cordilleran margin.

Geologic Background

The most extensive exposures of volcanic and sedimentary units of the Koipato Formation occur at the southern end of the Humboldt Range, northeast of Lovelock, Nevada, where the main part of field work was conducted for this study (Fig. 2.3). The Limerick Greenstone, Rochester Rhyolite, and Weaver Rhyolite of the Koipato Formation are exposed along with intrusive units and the overlying carbonate Middle Triassic Prida and Natchez Pass Formations of the Star Peak Group (Fig. 2.3) (e.g., Wallace et al., 1969a, b; Vikre, 1977).

The Koipato Formation is composed of intermediate to felsic volcanic and volcaniclastic units, with minor amounts of metasedimentary strata. The composition of the Koipato Formation volcanic subunits becomes more silicic stratigraphically upwards, with andesite as the primary volcanic component of the Limerick Greenstone and rhyolite

constituting the majority of the Rochester and Weaver Rhyolites. Metamorphism and hydrothermal alteration of the Koipato Formation units vary, but all units have experienced some degree of alteration and greenschist facies metamorphism in part, if not mostly, due to widespread hydrothermal activity (e.g., Vikre, 1977; Cheong, 1999, 2002). The thickness of the Koipato Formation is difficult to quantify due to faulting, but a maximum estimated thickness of approximately 5000 m has been suggested in the Humboldt Range (Knopf, 1924; Wheeler, 1939; Johnson, 1977). Outside of the Humboldt Range, the Koipato Formation thins to <500 m in the Tobin and Sonoma Ranges (Ferguson et al., 1952; Roberts et al., 1958).

The current stratigraphic usage for the Koipato Formation separates it into three distinct lithostratigraphic units based on differences in volcanic composition and percentage of sedimentary units (Fig. 2.2) (Wallace et al., 1969a; Burke, 1973; Silberling, 1973; Vikre, 1977). The lowermost unit of the Koipato Formation, the Limerick Greenstone, is primarily exposed in Limerick and American Canyons of the southern Humboldt Range (Figs. 2.2 and 2.3). The Limerick Greenstone is predominately composed of rhyodacite flows, a biotite–hornblende andesite intrusive complex, and schistose metasediments (Vikre, 1977). Extensive contact and hydrothermal alteration has completely altered the original mineral assemblages of most of the units to greenschist grade (Burke, 1973; Vikre, 1977). The contact between the Limerick Greenstone and the overlying Rochester Rhyolite has been interpreted to be conformable and gradational, where no faulting has occurred (Wallace et al., 1969a; Vikre, 1977), but

recent research has identified a possible angular unconformity between the Limerick Greenstone and Rochester Rhyolite in the East Range (Fig. 2.5) (Wilkins, 2010).

Overlying the Limerick Greenstone is the Rochester Rhyolite, which is identified throughout central Nevada and the most extensive exposures are located in the southern Humboldt Range (Figs. 2.2 and 2.3). The Rochester Rhyolite is primarily composed of banded rhyolite flows and rhyolite tuffs with minor amounts of tuff breccias and sedimentary deposits (Vikre, 1977). The units have experienced sericite alteration along with mineral replacement, but the degree of metamorphism is considerably less than that observed within the Limerick Greenstone (Burke, 1973; Vikre, 1977).

The Weaver Rhyolite overlies the Rochester Rhyolite, but the contact is often difficult to discern due to the similar compositions and textures of these two units (Fig. 2.2) (e.g., Burke, 1973). Outcrops of the Weaver Rhyolite have been described at several locations in central Nevada, but the main exposures are found in the southern Humboldt Range (Fig. 2.3). The Weaver Rhyolite is composed of rhyolite flows and ignimbrites that make up the majority of the lower part of the section, with sedimentary units (siltstones and sandstones) becoming increasingly abundant upward (Vikre, 1977). The Weaver Rhyolite volcanic units have compositions very similar to the Rochester Rhyolite, but the two units have been separated based primarily on the presence of ignimbrites in the lower sections of the Weaver Rhyolite and more common sedimentary units within the upper portions of the Weaver Rhyolite (Vikre, 1977). Vikre (1977) does note that parts of the lower Weaver Rhyolite intertongue with tuffs of the upper Rochester Rhyolite, which may indicate a more complex stratigraphy to the Koipato

Formation than has previously been described. An almost complete lack of alteration within the Weaver Rhyolite has led researchers to postulate that the intrusive units observed in the southern Humboldt Range acted as the magma source for the Weaver Rhyolite (Wallace et al., 1969a; Silberling, 1973). The lower Weaver Rhyolite likely reflects the continuation of magmatism recorded in the Rochester Rhyolite, but the upper sections of the Weaver Rhyolite, with their increased amount of sandstones and siltstones and decreased volcanic components, suggest a waning of magmatic activity (Burke, 1973; Vikre, 1977). The Weaver Rhyolite in the Humboldt Range is unconformably overlain by the limestones of the Middle Triassic Prida Formation. This angular unconformity marks the end of Early Triassic silicic volcanism in central Nevada and the establishment of a carbonate platform (Vikre, 1977; Nichols and Silberling, 1977).

The intrusive units present throughout the southern Humboldt Range are related to the Koipato Formation and are likely related to the same episode of magmatism as the silicic volcanic subunits (Fig. 2.3) (Wallace et al., 1969a; Silberling, 1973; Vikre, 1977). The leucogranite is composed primarily of coarse-grained feldspar and quartz, whereas the rhyolite porphyry dikes closely mirror the composition of the Rochester and Weaver Rhyolite flow units (Vikre, 1977). Burke (1973) and Vikre (1977) reported that it is difficult to differentiate the intrusive units in the field, which they attribute to a shared magmatic source. Vikre (1977) also concluded that the intrusive units were feeders for the Weaver Rhyolite, which he used to explain the lack of alteration observed within the Weaver Rhyolite compared to the pervasive alteration described within the Limerick Greenstone and to a lesser degree in the Rochester Rhyolite.

Geology

Fieldwork conducted during the summer and fall of 2009-2010 resulted in modifications to the Wallace et al. (1969a, b) maps for the southern Humboldt Range (Fig. 2.3). The locations of samples collected during fieldwork and discussed in this section can be found on this modified map, Figures 2.4 and 2.5, and in Table 2.1. Rocks that are interpreted to be lava flows will be described as such, whereas pyroclastic rocks will be described using standard terminology such as tuff, ash-flow tuff, and tuff breccia (following White and Houghton, 2006). Sedimentary and metasedimentary units are described using sedimentary terminology such as sandstone, shale, siltstone, etc. Sedimentary units composed of a large percentage of volcanic clasts will be described using terms such as volcanic sandstone and volcanic conglomerate. The term volcaniclastic will be used to describe volcanic rocks that have an unclear pyroclastic or epiclastic origin.

Limerick Canyon

Limerick Canyon, within the core of the Humboldt Range, was one of the main study sites (Fig. 2.3). The type locality for the Limerick Greenstone is within Limerick Canyon as well as exposures of the leucogranite, Rochester Rhyolite, and Weaver Rhyolite (Fig. 2.3). The main leucogranite body is termed the Lone Mountain Pluton by Johnson (1977) (Fig. 2.3). In addition to the Lone Mountain Pluton, numerous felsic dikes cut the Limerick Greenstone throughout its exposure in Limerick Canyon (Fig. 2.3). Whether the dikes in Limerick Canyon cut the Lone Mountain Pluton or represent feeders off of the main leucogranite body is difficult to ascertain due to the similar

composition of both the leucogranite and felsic dikes. However, the Wallace et al. (1969a) geologic map shows some dikes cross-cutting the leucogranite (Fig. 2.3).

In the western part of Limerick Canyon, the Rochester Rhyolite overlies the Limerick Greenstone, with a few degrees difference in the angle of dip between the two units, suggesting the existence of a slight angular unconformity (Figs. 2.3). The Weaver Rhyolite outcrops in the westernmost portion of Limerick Canyon, and overlies the Rochester Rhyolite. Although bedding/foliation measurements are few, the similarity of strike and dip of these two units suggests a conformable contact (Fig. 2.3). Further to the west, the Middle Triassic Prida Formation unconformably overlies the Weaver Rhyolite. The Prida Formation is not discussed in this report (see Nichols and Silberling (1977) for more information). The westernmost edge of Limerick Canyon is bounded by a large normal fault related to Cenozoic Basin and Range extension.

The Limerick Greenstone in Limerick Canyon consists of sedimentary units that range from breccias to siltstones. Some volcanic lithic sandstones and siltstones are identified along with a few exposures of volcaniclastic rocks. Quartz, feldspar, and micas appear to be the major constituents of the sedimentary units and within coarse sandstones and conglomerates these grains float in a fine-grained matrix. Slightly angular and broken feldspar grains are observed in some samples and sericite alteration of the feldspar is common. Also, most sedimentary units exhibit pervasive secondary chlorite and calcite replacement/overprinting combined with a small amount of mineral alignment that defines the poorly developed foliation.

One sample from the Limerick Greenstone in Limerick Canyon was dated for this study. Sample LC 09-42 was acquired from an ash-flow tuff exposed along Gold Ridge, immediately to the south of Limerick Canyon, just northeast of Golden Gate Hill (Figs. 2.3). This sample is close to the contact with the overlying Rochester Rhyolite. The sample contains a few large, broken grains of feldspar and quartz in a very fine-grained matrix (Fig. 2.6).

The Rochester Rhyolite in Limerick Canyon is primarily composed of rhyolite flows and tuffs with minor amounts of tuff breccia. Flows and tuffs from the Rochester Rhyolite are mainly composed of quartz-phyric rhyolite with minor amounts of phenocrystic feldspar and sparsely distributed mica. Burke (1973) has observed Limerick Greenstone clasts within the Rochester Rhyolite tuff breccias in the Tobin Range, but this could not be confirmed during the fieldwork for this report. In thin section, samples of the Rochester Rhyolite (LC 10-01; RHC 10-03) exhibit sericite alteration and calcite replacement, but lack the greenschist facies metamorphism observed within the Limerick Greenstone (AC 09-22; AC 09-13; LC 09-42) (Fig. 2.6).

Sample LC 10-01 of the mapped Rochester Rhyolite was acquired from a rhyolitic flow on the north side of Limerick Canyon just west of the Limerick Greenstone-Rochester Rhyolite contact on the Lovelock-Unionville road (Fig. 2.3). This sample was collected from a 1 m thick rhyolitic flow within a thicker succession (~15 m) of flows and a few tuffs. LC 10-01 is composed of sparsely distributed quartz phenocrysts in a mainly fine-grained quartz matrix (Fig. 2.6). Quartz phenocrysts exhibit slight rounding and a few are broken, but for the most part the grains appear to be

relatively unaltered (Fig. 2.6). Veins filled with calcite are present in the sample and are probably the result of younger (Jurassic and/or Cretaceous) hydrothermal activity (Fig. 2.6).

Sample LC 10-03 of the Weaver Rhyolite was collected from a rhyolitic ash unit interbedded with porphyritic rhyolite flows, with the felsic flow units constituting the majority of the lower member of the Weaver Rhyolite. The sample location is on the north side of Limerick Canyon just to the west of where the Rochester Rhyolite-Weaver Rhyolite contact crosses the Lovelock-Unionville road (Fig. 2.3). Based on the map relationships, this sample is from the stratigraphically lowest portion of the Weaver Rhyolite (Fig. 2.3). The sample is composed of quartz and feldspar phenocrysts that are contained within a fine-grained matrix (Fig. 2.6).

As mentioned, the leucogranite of the Lone Mountain Pluton intrudes the Limerick Greenstone at this locality (Fig. 2.3). The Lone Mountain Pluton consists mainly of quartz (~70%) and equal amounts of potassium feldspar (~15%) and albite (~15%). No mafic minerals were identified in the leucogranite. Grains within the leucogranite range in size from 0.5 mm up to 2-3 mm. Minor sericite alteration has occurred to some feldspar grains, but overall the leucogranite is relatively unmetamorphosed. A large number of quartz and quartz-tourmaline veins cut the leucogranite and range in widths of a few mm to over a meter. Associated with the Lone Mountain Pluton, in Limerick Canyon, are numerous rhyolite porphyry dikes, which cut through the Limerick Greenstone and are quite difficult to distinguish from the leucogranite in the field. Sample 09NV41 was collected from the Lone Mountain Pluton

just north of the Lovelock-Unionville road (Fig. 2.3). This sample is composed of 0.5 to 1 mm feldspar (albite and potassium feldspar) and quartz grains, with the feldspar grains exhibiting slight sericite alteration (Fig. 2.6). No other metamorphism or alteration is evident in the sample.

American Canyon

Fieldwork conducted in American Canyon focused on a section of the Limerick Greenstone and a rhyolite porphyry dike intrusive units that cut through it. The Limerick Greenstone forms a massive complex that occupies the area from the base of American Canyon to the top of the first ridgeline to the south where it is cut out by a larger leucogranite intrusive (Fig. 2.3). Less extensive exposures of the Limerick Greenstone occur on the north side of American Canyon (Fig. 2.3). The dikes in this area are fewer in number and smaller in size than those observed in Limerick Canyon, but they stand out from the Limerick Greenstone making them fairly simple to identify in the field.

The Limerick Greenstone exposed in American Canyon is composed of porphyritic igneous rocks that have an intermediate composition and appear to represent a hypabyssal intrusive complex. Evidence for an intermediate composition includes the prevalence of hydrous ferromagnesian minerals and feldspar with little to no quartz. Feldspar and hornblende phenocrysts range from <1 mm to 6-7 mm in size. Outcrops in the field are massive and exhibit no bedding planes, but a pervasive foliation is present. All outcrops exhibit metamorphism to greenschist facies. The Limerick Greenstone clearly underlies what is mapped as the Rochester Rhyolite in this area, but the relation of the hypabyssal intrusives here to the Limerick Greenstone metasediments in Limerick

Canyon is harder to define due to the lack of stratigraphic continuity. Because of the uncertain relation between the Limerick Greenstone subunits in these two areas, and the fact that the Limerick Greenstone-Rochester Rhyolite contact is an unconformity, the age of the Limerick Greenstone could be highly variable.

Two samples were collected from the Limerick Greenstone in American Canyon and dated for this study. The first sample (AC 09-13) is from a massive outcrop of the Limerick Greenstone intrusion exposed on the north side of American Canyon (Fig. 2.3). This is a sample of the intermediate hypabyssal intrusion and contains plagioclase, potassium feldspar, and biotite phenocrysts in a fine-grained matrix (Fig. 2.6). Phenocrysts in the sample range in size from 0.5 to 3 mm, with the plagioclase grains representing the largest fraction (Fig. 2.6). A small amount of sericite alteration of feldspar is evident along with minor amounts of calcite, quartz, and chlorite replacement (Fig. 2.6).

The second sample (AC 09-22) was obtained from a massive exposure of the Limerick Greenstone intrusion along the south side of American Canyon (Fig. 2.3). The composition and texture of sample AC 09-22 is very similar to that described for AC 09-13, but alteration of this unit is much more pervasive (Fig. 2.6). Plagioclase grains have been completely altered to sericite and the sample exhibits extensive chlorite and calcite replacement (Fig. 2.6).

Cutting through the Limerick Greenstone in American Canyon are several rhyolite porphyry dikes that stand out from the dark colored Limerick Greenstone. Based upon their similar composition and texture, it is interpreted that these dikes are related to

the leucogranite intrusive observed in Limerick Canyon (09NV41) and that they probably represent feeders off the large plutonic body. Sample AC 09-09 was collected from one of these dikes close to the top of the first ridgeline to the south of American Canyon (Fig. 2.3). It is composed of plagioclase, potassium feldspar, and quartz phenocrysts ranging in size from 0.5 to 6 mm in a microcrystalline groundmass (Fig. 2.6). Feldspar grains exhibit a minor amount of sericite alteration, but the sample is generally unmetamorphosed (Fig. 2.6).

Troy Canyon

The Weaver Rhyolite, in Troy Canyon, is composed of silicic volcanic sequences with volcanic conglomerates, sandstones, and siltstones becoming more numerous higher in the stratigraphic sequence. The lowermost stratigraphic unit of the Weaver Rhyolite (TRwp) is composed of porphyritic felsic flow units, the middle Weaver Rhyolite (TRwc) is composed of tuffaceous sandstone and siltstone, and the upper Weaver Rhyolite (TRwf) is composed of equal amounts of silicic flows and tuffs with less abundant phenocrysts along with minor amounts of sedimentary units. The entire stratigraphic sequence of the Weaver Rhyolite can be observed by walking along the first ridgeline to the south of Troy Canyon (Fig. 2.3).

Two samples were obtained from the Weaver Rhyolite in Troy Canyon for analysis. The first sample (TC 10-06) was collected from a felsic flow unit within the lower sections of the Weaver Rhyolite, based on map relationships, close to Rochester Rhyolite-Weaver Rhyolite contact (Fig. 2.3) (Wallace et al., 1969a; mapped as a fault

contact). This sample is composed of quartz and feldspar phenocrysts in a fine-grained quartz matrix (Fig. 2.6). Feldspar grains exhibit variable sericite alteration (Fig. 2.6).

The second sample (TC 10-01) was obtained from a silicic ash-flow unit from the upper sections of the Weaver Rhyolite at the far eastern point of the first ridgeline to the south of Troy Canyon (Fig. 2.3). This sample is composed of 3-4 mm quartz phenocrysts in a microcrystalline, quartz matrix (Fig. 2.6). Relict glass shards have been identified in this sample, which lead to the interpretation that the sample was collected from an ash-flow unit (Fig. 2.6).

Rockhill Canyon, East Range

The Limerick Greenstone and Rochester Rhyolite have both been documented in the East Range, but this study will focus on the exposed Rochester Rhyolite on the north side of Rockhill Canyon (Figs. 2.1 and 2.5) (Whitebread, 1994; Wilkins, 2010). Within the East Range, the Rochester Rhyolite is primarily composed of tuffs, flows, and volcanic breccias with minor amounts of siltstone, quartzite, and conglomerate (Whitebread, 1994). This is very similar to the Rochester Rhyolite observed in the Humboldt Range, except for the occurrence of more numerous sedimentary units. One sample of the Rochester Rhyolite was collected from this canyon and analyzed for this study. Sample RHC 10-03 was collected from a felsic flow unit along the north side of the canyon fairly close to what has been mapped by Whitebread (1994) and Wilkins (2010) as the contact between the Rochester Rhyolite and the Havallah sequence of the Golconda Allochthon (Fig. 2.5). The sample is composed of plagioclase and quartz phenocrysts in a fine-grained groundmass, with the phenocrysts ranging in size from 1 to

5 mm (Fig. 2.6). The largest phenocrysts are plagioclase grains, which exhibit twinning and minor amounts of sericite alteration (Fig. 2.6). Veins cut through the sample and are likely the product of later hydrothermal activity as suggested by the veins deflecting around the large phenocrysts (Fig. 2.6).

Hoffman Canyon, Tobin Range

No fieldwork was conducted in the Tobin Range during this study, but sample 00NV-17 was procured from a previous expedition and analyzed for this report (C.J. Northrup, personal communication). This sample originates from an outcrop of the Koipato Formation approximately 1 m above the unconformity with the Havallah Formation of the Golconda Allochthon in Hoffman Canyon, which is the type location for the Sonoma Orogeny (Fig. 2.1 and 2.4) (Silberling and Roberts, 1962). The sample is classified as a rhyolite tuff breccia that is not welded and contains grains that range in size from 1 to 10 mm in an ashy matrix (C.J. Northrup, per. comm.). The presence of slightly rounded, non-volcanic lithic clasts does suggest that the sample was reworked prior to final deposition, but the degree of reworking is inferred not to have affected the overall sample composition and the zircons ages are effectively synchronous with the age of deposition (C.J. Northrup, per. comm.). Based on the unit description and mineral composition, this sample would most likely have been procured from an exposure of the Rochester Rhyolite.

Geochronology

Zircon was separated from samples using standard density and magnetic mineral separation methods. After separation, zircon grains were picked and mounted into epoxy pucks, which were polished and carbon coated in preparation for cathodoluminescence imaging. Using the images, individual zircon gains were plucked for further analysis based on the lack of inherited cores (Fig. 2.7). The selected zircon grains were then subjected to a modified version of the chemical abrasion method of Mattinson (2005), reflecting a preference to analyze single grains. Zircon was placed in a muffle furnace at 900°C for 60 hours in quartz beakers. Details of chemical separation and mass spectrometry are described in Davydov et al. (2010).

U-Pb dates and uncertainties were calculated using the algorithms of Schmitz and Schoene (2007), $^{235}U/^{205}Pb$ of 77.93 and $^{233}U/^{235}U$ of 1.007066 for the Boise State University tracer solution, and U decay constants recommended by Jaffey et al. (1971). $^{206}Pb/^{238}U$ ratios and dates were corrected for initial ^{230}Th disequilibrium using a Th/U[magma] = 3. All common Pb in analyses was attributed to laboratory blank and subtracted based on the measured laboratory Pb isotopic composition and associated uncertainty. U blanks are difficult to precisely measure, but are estimated at 0.07 pg.

Sample ages are interpreted from the weighted means of the $^{206}Pb/^{238}U$ dates from single zircon grain analyses (Table 2.2). The weighted mean ages are based on 5 to 8 equivalent single grain analyses per sample. Grains that are older than those used in the weighted mean age calculations are interpreted as inherited antecrysts, whereas younger grains are considered to have experienced Pb-loss not completely alleviated by chemical

abrasion. Individual analysis errors are based upon non-systematic analytical uncertainties, which include counting statistics, spike subtraction, and blank Pb subtraction. Errors on weighted mean ages are reported as internal 2σ for all samples. Period, epoch, and age assignments are based on the timescales of Walker and Geissman (2009) and Mundil et al. (2010).

Limerick Greenstone

Three samples from the Limerick Greenstone in the Humboldt Range were dated for this study. Six zircon grains were analyzed from sample AC 09-13, an intermediate intrusive unit located in American Canyon (Fig. 2.3). All six grains have overlapping errors and give a weighted mean $^{206}Pb/^{238}U$ age of 249.59 ± 0.08 Ma, which places this intrusion in the Olenekian stage of the Early Triassic (Fig. 2.8). This is the oldest sample dated for this study and provides a minimum age for Limerick Greenstone, but the precise age of initial Limerick Greenstone magmatic activity cannot be definitely determined because the base of the Limerick Greenstone is not exposed in the Humboldt Range.

Nine zircon grains were analyzed from sample LC 09-42, an ash-flow tuff unit that was collected from the sedimentary sequences of the Limerick Greenstone exposed in Limerick Canyon (Fig. 2.3). Eight grains have overlapping errors and give a weighted mean $^{206}Pb/^{238}U$ age of 249.56 ± 0.09 Ma, which places this unit in the Olenekian stage of the Early Triassic (Fig. 2.8). The grain that is discarded from the weighted mean is younger than almost all other zircons and is interpreted to have been affected by Pb-loss, which was only partially mitigated by chemical abrasion of these very U-rich zircons.

This sample is within error of AC 09-13 and suggests that sedimentary and volcanic deposition was occurring coevally with the production of the Limerick Greenstone intrusive complex.

Seven zircon grains were dated from sample AC 09-22, an intermediate intrusive unit petrographically similar to AC 09-13. All seven grains have overlapping errors and give a weighted mean $^{206}Pb/^{238}U$ age of 249.37 ± 0.1 Ma, which places this intrusion in the Olenekian stage of the Early Triassic (Fig. 2.8). This is the youngest sample of the Limerick Greenstone dated during this study and indicates that Limerick Greenstone magmatism occurred until ~249.3 Ma, but could be slightly younger depending on the ages of the leucogranite and rhyolite dike intrusives and the overlapping Rochester Rhyolite in the southern Humboldt Range.

Rochester Rhyolite

Sample RHC 10-03 was the only dated sample from the East Range and it was obtained from an outcrop of the Rochester Rhyolite in Rockhill Canyon (Figs. 2.1 and 2.5). Nine zircon grains from this sample were dated for this study, of which, six have overlapping errors and provide a weighted mean $^{206}Pb/^{238}U$ age of 249.18 ± 0.07 Ma (Fig. 2.8). The three older grains dated from this sample are interpreted to represent antecrysts from an earlier phase of magmatism. The age of this sample places it within the Olenekian stage of the Early Triassic. This is the oldest dated felsic volcanic sample from this study, which indicates that silicic volcanism was occurring in this area by ~249.18 Ma.

Sample 00NV-17 was obtained from Hoffman Canyon, Tobin Range and

provides a credible age constraint on the Koipato Formation that directly overlies the Golconda Allochthon (Fig. 2.4). This is the locality that has been employed to define the Sonoma Orogeny. From this sample, 12 grains were dated, with 7 having overlapping errors and providing a weighted mean $^{206}Pb/^{238}U$ age of 249.14 ± 0.14 Ma (Fig. 2.8). This sample does exhibit scatter in the individual grain analyses, with four older grains interpreted to represent antecrysts from an older phase of magmatism and one younger grain interpreted to be a product of Pb-loss that was only partially mitigated by chemical abrasion. Three older grains provide overlapping errors around 250 Ma, which could indicate that undocumented volcanism or plutonism was occurring in the area at that time (Table 2.2). The composition and age of this sample supports the interpretation that it was obtained from an exposure of the Rochester Rhyolite. Also, the age of this sample indicates that the Rochester Rhyolite was deposited over a wide swath of central Nevada during the early stages of the felsic Koipato Formation. This may indicate that these units were not deposited in a localized tectonic basin as previously thought (Williams, 1939; Burke, 1973), but they still could represent a discrete basin.

Sample LC 10-01 is from a rhyolite flow unit of the Rochester Rhyolite in Limerick Canyon from which seven grains were dated (Fig. 2.3). Of these seven grains, six of them have overlapping errors and give a weighted mean $^{206}Pb/^{238}U$ age of 248.53 ± 0.07 Ma, with the one older grain interpreted to represent an antecryst from an earlier episode of magmatism (Fig. 2.8). This sample is within the Olenekian stage of the Early Triassic. This sample indicates that Rochester-type volcanism lasted for >600,000 years.

Leucogranite and Dike Units

Eleven zircon grains were dated from sample 09NV41, a leucogranite intrusive unit in Limerick Canyon that cuts through the sedimentary and volcanic deposits of the Limerick Greenstone (Fig. 2.3). Five grains have overlapping errors and give a weighted mean $^{206}Pb/^{238}U$ age of 249.09 ± 0.08 Ma, which places this intrusion in the Olenekian stage of the Early Triassic (Fig. 2.8). Five older grains are interpreted to represent antecrysts, which record an earlier period of magmatism in the area. The youngest grain that is discarded from the weighted mean is interpreted to have been affected by Pb-loss, which was only partially mitigated by chemical abrasion. Three older grains that were discarded from the mean age of the sample range in age from 249.6 – 249.4 Ma, which are interpreted to represent inherited grains from the previous magmatic episode that produced the Limerick Greenstone (Table 2.2). Along with these slightly older grains, two grains returned ages close to ~254 Ma, and are interpreted to be grains derived from an older phase of Koipato Formation volcanism (Table 2.2).

Sample AC 09-09 is from a rhyolite porphyry dike in American Canyon, which intrudes the intrusive section of the Limerick Greenstone (Fig. 2.3). Nine zircon grains were analyzed, with six grains yielding a weighted mean $^{206}Pb/^{238}U$ age of 249.07 ± 0.14 Ma, which places this intrusion in the Olenekian stage of the Early Triassic (Fig. 2.8). The three older grains are interpreted to represent antecrysts, which record an earlier period of magmatism in the area. Both samples from the intrusive units within the southern Humboldt Range have overlapping weighted means and confirm the hypothesis

that the rhyolite porphyry dikes are related to the leucogranite intrusive and possibly acted as feeders off the larger plutonic body.

Weaver Rhyolite

Three samples of the Weaver Rhyolite in the Humboldt Range were dated for this study. Sample TC 10-06 is from a felsic flow unit in the lowermost section of the Weaver Rhyolite in Troy Canyon (Fig. 2.3). Seven grains were dated from this sample, with all seven grains having overlapping errors and producing a weighted mean $^{206}Pb/^{238}U$ age of 248.97 ± 0.07 Ma, which places this unit in the Olenekian stage of the Early Triassic (Fig. 2.8). The weighted mean age of this sample overlaps with that of the samples from the silicic intrusive units in the southern Humboldt Range, which is interpreted to mean that the intrusive units and the lower Weaver Rhyolite were part of the same magmatic episode and that these intrusive units possibly served as feeders for parts of the Weaver Rhyolite.

Eight zircon grains were analyzed from sample TC 10-01, a felsic ash-flow unit from the upper parts of the Weaver Rhyolite in Troy Canyon (Fig. 2.3). Six grains have overlapping errors and give a weighted mean $^{206}Pb/^{238}U$ age of 248.62 ± 0.08 Ma, which places this unit in the Olenekian stage of the Early Triassic (Fig. 2.8). The two older grains are interpreted to represent antecrysts, which record an earlier period of magmatism in the area. The age of this sample indicates that part of what is mapped as upper Weaver Rhyolite volcanism was occurring coevally with that of Rochester Rhyolite sample LC 10-01 (Fig. 2.8).

Ten zircon grains were dated from sample LC 10-03, an ash unit from the lowermost Weaver Rhyolite in Limerick Canyon (Fig. 2.3). Ten grains were analyzed, with five of them giving a weighted mean $^{206}Pb/^{238}U$ age of 248.32 ± 0.08 Ma, which places this unit in the Olenekian stage of the Early Triassic (Fig. 2.8). The five younger grains that are not included in the weighted mean are interpreted to have been affected by Pb-loss, which was mitigated to varying degrees by chemical abrasion.

Discussion

Timing of Volcanism and Deposition of the Koipato Formation

The Koipato Formation has routinely been defined as a Late Permian to Early Triassic volcanic and sedimentary assemblage based on limited fossil and imprecise radiometric data (Wheeler, 1939; Wallace et al., 1960; Silberling and Roberts, 1962; McKee and Burke, 1972; Silberling, 1973; Vikre, 1977). The new U-Pb zircon geochronology data presented in this study demonstrates that the Koipato Formation is a predominately late Early Triassic (Olenekian) sequence that documents a relatively punctuated period of magmatic activity in central Nevada that lasted for ~1.2 Ma based on the results of the studies presented here.

Previously, the Limerick Greenstone has been described as a possibly Late Permian to Early Triassic volcanic unit due to the lack of reliable age constraints and that it underlies the Rochester Rhyolite, but this study demonstrates that the main magmatic phase of the Limerick Greenstone, at least within the Humboldt Range, initiated around 249.59 Ma (AC 09-13) with the intrusion of a large intermediate plutonic body. Based on

the lithologic characteristics of this sample and AC 09-22, it has been determined that the intrusive body was emplaced hypabyssally. Because of this, the plutonic body had to intrude something at least older than itself; therefore, the Limerick Greenstone must be older than 249.6 Ma. It is possible that Limerick Greenstone volcanism initiated in the latest Permian based on ~254 Ma inherited grains observed within 09NV41 (Fig. 2.8). The Limerick Greenstone plutonic body is associated with active volcanism and sedimentation that was occurring coevally within the Koipato Formation system based on the age of sample LC 09-42. This sample is taken from an ash-flow tuff unit within the sedimentary component of the Limerick Greenstone in Limerick Canyon and provides an age of deposition of 249.56 Ma. This sample was not taken from the lowermost part of the Limerick Greenstone and so this magmatic activity could have started at an earlier time. Sample AC 09-22 (249.37 Ma) provides the youngest observed age for the Limerick Greenstone in this study, which is consistent with a minimum age for the Limerick Greenstone, in the Humboldt Range, from the cross-cutting 249.09 Ma leucogranite intrusive (09NV41) in Limerick Canyon. Ages from the Rochester Rhyolite in the East Range and Hoffman Canyon indicate that rhyolitic volcanism was occurring by 249.18 Ma (RHC 10-03), which further constrains the end of Limerick Greenstone magmatism. All dated samples from the Limerick Greenstone indicate that Limerick-type volcanic and plutonic activity in the Humboldt Range occurred for at least 300,000 years and possibly longer. Evidence from this study demonstrates that Limerick Greenstone magmatism and deposition was definitively occurring from 249.59 to 249.37 Ma with a possible maximum age of ~254 Ma and minimum of 249.18 Ma.

Just as new age constraints have redefined the timing of the Limerick Greenstone magmatism, so to have they altered the understanding of the Rochester and Weaver Rhyolite magmatism. Within the Humboldt Range, the maximum age constraint obtained from this study on the Rochester and Weaver Rhyolites is provided by the youngest sample from the Limerick Greenstone with an age of 249.37 Ma (AC 09-22). The stratigraphic relationships indicate that felsic volcanism was not occurring before this time. The leucogranite and felsic dikes are the oldest silicic units, from the Humboldt Range, based on samples 09NV41 and AC 09-09, providing ages of 249.09 and 249.07 Ma, respectively. A second younger set of felsic dikes are observed to cut the leucogranite in Limerick Canyon, but these were not dated for this study (Fig. 2.3). These intrusive units are inferred to be related to the Rochester and lower Weaver Rhyolites, acting as a possible feeder system. Additional evidence for these silicic intrusive units feeding the Rochester and lower Weaver Rhyolites is provided by previous geochemical investigations of these units, which demonstrate that their major oxide compositions are equivalent (Johnson, 1977; Vikre, 1977, 1981; Kistler and Speed, 2000). Most likely, initiation of rhyolitic volcanism happened between 249.37 and 249.09 Ma, with field relationships in the Humboldt Range suggesting that it is closer to the latter due to an observed unconformity between the Limerick Greenstone and Rochester Rhyolite. This relationship has been observed outside of the Humboldt Range as a slight angular unconformity between the Limerick Greenstone and Rochester Rhyolite in the East Range (Wilkins, 2010), which will be discussed in more detail later in this report.

The oldest felsic samples are RHC 10-03 (249.18 Ma) and 00NV-17 (249.14 Ma), which both come from outside the Humboldt Range. Both of these samples overlap in

error with the age of samples 09NV41 (249.09 Ma) and AC 09-09 (249.07 Ma) from a leucogranite and a rhyolite dike in the Humboldt Range, which suggests that the intrusive units observed in the southern Humboldt Range were probably feeders for the older felsic units within the Koipato Formation (Fig. 2.9). In the Humboldt Range, the first definitive age of rhyolitic volcanism comes from sample TC 10-06 (248.97 Ma), from the lower Weaver Rhyolite, which overlaps within error of Rochester Rhyolite sample 00NV-17. This relationship is evidence that units mapped as the Rochester Rhyolite and Weaver Rhyolite volcanism were occurring coevally for a period of time (Fig. 2.9). Sample TC 10-01, from the upper Weaver Rhyolite has an age of 248.62 Ma, which combined with sample TC 10-06 brackets the age of the Weaver Rhyolite in the Troy Canyon area. Map relations to the southwest of Troy Canyon indicate a large dike complex that is similar to AC 09-09, which provided an age of 249.07 Ma (Fig. 2.3). This dike complex cuts the lower and middle Weaver Rhyolite (Fig. 2.3). Based on this evidence, Weaver Rhyolite volcanism, on the eastern side of the Humboldt Range, lasted from ~249.07 to <248.62 Ma. The Prida Formation provides the minimum age constraint on the Weaver Rhyolite where early Middle Triassic (Anisian) ammonites have been uncovered (Nichols and Silberling, 1977). This is a minimum age constraint on the Koipato Formation, but the existence of an angular unconformity between the Weaver Rhyolite and Prida Formation and the fact that sample TC 10-01 was taken from the upper sections of the Weaver Rhyolite indicate that there is most likely a 3 Ma or more lacuna between the two units.

On the west side of the Humboldt Range in Limerick Canyon, the oldest dated felsic sample is LC 10-01, which based on map relationships reflects the lower portion of

the Rochester Rhyolite and gives an age of 248.53 Ma. This sample was collected from very close to the contact with the Limerick Greenstone in Limerick Canyon and demonstrates that there is likely an unconformity between the two units that spans ~1 Ma. The age constraints for this lacuna are based on the age of this sample and the age of the youngest sample dated from the Limerick Greenstone in Limerick Canyon (LC 09-42; 249.56 Ma).The youngest dated sample from the Koipato Formation is LC 10-03, from the mapped lower Weaver Rhyolite, which provides an age of 248.32 Ma. These ages are younger than those determined for the Weaver Rhyolite in Troy Canyon and may indicate that either the mapped relationships are incorrect or the currently accepted stratigraphic relationships within the Koipato Formation need redefining based on the newly presented geochronology. The first hypothesis is based on the fact that the Wallace et al. (1969a, b) maps, used during this study, were compiled from fieldwork conducted by several researchers who may have each had their own views of what classified the map units as either Rochester and Weaver Rhyolites. Therefore, samples LC 10-01 and LC 10-03 are possibly from a sliver of the upper Weaver Rhyolite in Limerick Canyon instead of what is mapped as Rochester and lower Weaver Rhyolites (Fig. 2.3).

An alternative hypothesis is that the stratigraphic relationships within the Koipato Formation are more complex than previously thought, with multiple phases of volcanism and “Rochester-type” and “Weaver-type” magmatism occurring coevally (Fig. 2.9). This complexity is observed mainly within the felsic sections of the Koipato Formation, where the new data presented here demonstrates that the Rochester and Weaver Rhyolites are coeval units that can be separated into at least two separate phases of volcanism (Fig.

2.9). The older phase is observed in Troy Canyon and the East and Tobin Ranges and is composed of an older section of the Rochester Rhyolite (TRr1; 249.18 to ~249.07 Ma) and lower Weaver Rhyolite (TRwp1; 248.97 Ma), which pinches out to the west (Fig. 2.9). This older package is bounded by unconformities, with the Limerick Greenstone underneath and a second younger felsic package above (Fig. 2.9). This younger felsic section is considered to be composed of a basal sedimentary section (TRwc), containing clasts from the older silicic section, and the dated upper Weaver Rhyolite (TRwc; 248.62 Ma) on the eastern side of the Humboldt Range, which transitions into a second younger Rochester Rhyolite (TRr2; 248.53 Ma) and lower Weaver Rhyolite (TRwp2; 248.32 Ma) section in Limerick Canyon (Fig. 2.9). As with the older section, the young felsic section is bounded by unconformities with the older felsic section and the Limerick Greenstone to the bottom and the Middle Triassic Prida Formation on top.

These samples demonstrate that the majority of the Koipato Formation represents ~1.2 Ma period of mixed intermediate and felsic volcanic activity. Koipato Formation volcanism, and specifically Limerick Greenstone activity, possibly dates back to ~254 Ma, but the bulk of volcanism occurred within a relatively short time period in the Olenekian. Within this punctuated period of volcanism, the volcanic composition of the units transitioned from intermediate to felsic within <200,000 years, which is demonstrated by the change from Limerick Greenstone to Rochester Rhyolite deposition. Lastly, data presented here documents the probable occurrence of previously unrecognized unconformities, which separate various periods of volcanism within the Koipato Formation. Understanding the changes that occurred within the Koipato

Formation and their causes will lead to a better comprehension of the Early Triassic continental margin and may be helpful in correlating the units exposed in the Humboldt Range with terranes elsewhere along the Cordillera margin.

Unconformities within the Koipato Formation

Previous research into the age and stratigraphic nature of the Koipato Formation has been based on sparse fossil evidence and imprecise radiometric data with the understanding that this formation represents a Late Permian to Early Triassic conformable volcanic sequence that is bounded by unconformities (Wheeler, 1939; Wallace et al., 1960; McKee and Burke, 1972; Silberling, 1973; Vikre, 1977). Since the work of Ferguson et al. (1952), it has been interpreted that the Koipato Formation unconformably overlies the allochthonous units of the Golconda Allochthon. This relationship has been used to describe the Sonoma Orogeny as a Late Permian to Early Triassic event with the Koipato Formation representing the initial stages of continental arc magmatism (Ferguson et al., 1952; Silberling and Roberts, 1962; Silberling, 1973; Vikre, 1977). The duration of the unconformity between the Golconda Allochthon and the basal units of the Koipato Formation is not well constrained. The youngest unit (Edna Mountain Formation) within the Antler Overlap sequence is dated to be Middle Permian (~270 to 260 Ma) based on fossil assemblages identified within the unit (Roberts, 1951, 1964; Coats and Gordon, 1972; Erickson and Marsh, 1974; Wardlaw et al., 1995). The youngest documented age of rocks within the Golconda Allochthon is similarly Middle Permian (Guadalupian) (Laule et al., 1981; Murchey, 1990). This provides a maximum age constraint on the unconformity, but constraining the minimum age using the Koipato

Formation has proved problematic, as no age constraints existed for the Limerick Greenstone prior to the studies presented here. This lack of age constraints on the Limerick Greenstone has prevented the definitive determination of the duration of the unconformity, with estimates ranging from a few million years to tens of millions of years. New U-Pb geochronology performed, during this study, on the Limerick Greenstone has identified the oldest age definitively analyzed from this unit as 249.59 Ma (AC 09-13), with the possibility it dates back to ~254 Ma based on inherited grains within the leucogranite (09NV41). The age of the inherited zircons can be interpreted as the minimum age for the pre-Koipato Formation deformation observed within the Golconda Allochthon. This new minimum age constraint has better defined the unconformity between the Golconda Allochthon and Koipato Formation to a time gap of ~15 to 6 Ma. This age constraint does not absolutely constrain the final emplacement of the Golconda Allochthon (e.g., Dunston et al., 2001), but does constrain the age the Sonoma Orogeny as classically defined.

New field evidence and U-Pb geochronology presented in this study demonstrates that the Koipato Formation is predominately a late Early Triassic volcanic sequence that is not as stratigraphically simple as previously thought. The Koipato Formation volcanics erupted within a complex volcanotectonic setting, which allowed the intermixing of volcanic units and the development of intra-formational unconformities. An unconformity between the Limerick Greenstone and Rochester Rhyolite was observed by Wilkins (2010) in the East Range, but he did not provide any estimate for the duration of this unconformity. Fieldwork performed in the Humboldt Range during this study has

identified the same unconformity and U-Pb geochronology has provided the first reliable age constraints. New radiometric data for the youngest mafic intrusive in the Limerick Greenstone provides a maximum age constraint on this unconformity at 249.37 Ma. Using the age (249.09 Ma) determined for the leucogranite intrusive, the unconformity can be constrained to a time gap of <350,000 years (Fig. 2.9). If the ages determined for the Rochester Rhyolite from outside of the Humboldt Range are used, the unconformity can be constrained to a time gap of about ~200,000 years based on the age of sample RHC 10-03 (249.18 Ma). In light of the new stratigraphic understanding of the Koipato Formation, this unconformity between the Limerick Greenstone and felsic sections has various durations throughout the Humboldt Range. The previously discussed duration explains the data collected in Troy Canyon, but the geochronology from Limerick Canyon documents that the unconformity lasted for ~1 Ma (Fig. 2.9). This extended duration is due to the erosion of the older felsic units in the Limerick Canyon area before the deposition of the presently exposed younger silicic section and the older age (254.56 Ma) of the Limerick Greenstone in the area. This unconformity also documents the transition within the volcanic system from intermediate to felsic volcanism due to changing conditions within the magma system feeding the Koipato Formation volcanics. Vikre (1977) attributed this compositional change to a magma source switch from oceanic crustal melting for the Limerick Greenstone to that for the felsic units, which reflect the initial stages of continental arc magmatism and consequent partial melting of continental crust. This interpretation can neither be confirmed nor denied by the data collected for this report. Wilkins (2010) does mention that the unconformity between the Limerick Greenstone and Rochester Rhyolite has a slight angular component, but this

could not be confirmed by the field work conducted in the Humboldt Range. If this is in fact an angular unconformity, then a minimal amount of syn-eruptive normal faulting was likely occurring during the deposition of the Koipato Formation volcanics. This view is supported by Speed (1979), who interpreted that the Koipato Formation was deposited in a block-faulted terrane following the Sonoma Orogeny.

A second unconformity within the Koipato Formation of the Humboldt Range is interpreted to exist between the observed outcrops of older Rochester (TRr1) and lower Weaver Rhyolites (TRwp1) in Troy Canyon and the younger sequence of felsic volcanics observed both in Troy (TRwc and TRwf) and Limerick (TRr2 and TRwp2) Canyons (Figs. 2.3 and 2.9). This unconformity is primarily observed on the east side of the Humboldt Range due to the erosion of the older felsic sequence from the west side. This unconformity separates the two identified periods of silicic volcanism within the Koipato Formation. The duration of this unconformity is constrained to a time span of <350,000 years based on the ages of the older lower Weaver Rhyolite (TC 10-06; 248.97 Ma) and upper Weaver Rhyolite (TC 10-01; 248.62 Ma) in Troy Canyon (Figs. 2.3 and 2.9). In Troy Canyon, immediately above the unconformity is a sedimentary sequence (TRwc), which is not observed in Limerick Canyon (Fig. 2.3 and 2.9). This may be due erosion still going on during the initial stages of the second phase of volcanism in Limerick Canyon.

The contact between the overlying Middle Triassic Prida Formation and the Koipato Formation has also been identified as an unconformity. The age and duration of this unconformity has long been debated with most of the interpretations having been

based on fossil evidence. A maximum age for the unconformity has been provided by the discovery of Late Olenekian ammonites from the upper Weaver Rhyolite (Vikre, 1977), where as a minimum age is provided by the occurrence of Anisian ammonites in the lower Prida Formation (Nichols and Silberling, 1977). These fossil assemblages confine the unconformity to a wide age range depending on the fossil positions within their time periods. New U-Pb geochronology presented in this study provides a more definitive constraint on the maximum age of this unconformity. Sample LC 10-03 is the youngest dated sample from the Weaver Rhyolite and provides an age of 248.32 Ma. This age is slightly older than the Late Olenekian assignment of Vikre (1977), but it does provide a definitive age that can be used to complement the fossil data. This sample was taken from close to the faulted Weaver Rhyolite-Prida Formation contact in Limerick Canyon, but movement along that fault is interpreted to not be substantial (Fig. 2.3). This means that the maximum age of the unconformity is just slightly younger than the age determined for the sample. Using this new evidence, the time gap of the unconformity is interpreted to represent ~3 to7 Ma. An unconformity of this duration is long enough to allow for erosion to occur within the younger sections of the Koipato Formation and for the depositional environment of the area to transition to a carbonate platform.

Conclusions

New field evidence and geochronology presented in this study demonstrates that the Koipato Formation represents an intermediate to felsic volcanic sequence that documents a short-lived latest Permian to Early Triassic series of magmatic events. Geochronologic data identifies previously unrecognized unconformities within the

Koipato Formation and helps to constrain these unconformities and the ones bounding the Koipato Formation.

Field evidence and U-Pb geochronology support the interpretation that the Rochester and lower Weaver Rhyolites are partly coeval units. Also, U-Pb geochronology has proven that the silicic intrusive units observed throughout the Humboldt Range are coeval to the older sequence of the Rochester and the lower Weaver Rhyolites and acted as feeders for these felsic volcanics. Finally, two phases of silicic volcanism are identified within the Koipato Formation, which are separated by a previously unidentified unconformity. This unconformity is documented to have a time span of <350,000 years, separate the older Rochester and Weaver Rhyolites in Troy Canyon and the East and Tobin Ranges from the young Rochester and lower Weaver Rhyolites of Limerick Canyon and the sedimentary and upper Weaver Rhyolites in Troy Canyon, and record the erosion of the older phase of silicic volcanism from the west side of the Humboldt Range.

U-Pb geochronology shows that the Koipato Formation is predominately late Early Triassic, with the majority of volcanism lasting for ~1.2 Ma and the initial magmatism extending into the latest Permian (~254 Ma). Field and geochronology data obtained during this study constrained the timing of an unconformity between the Limerick Greenstone and Rochester Rhyolite identified by Wilkins (2010) in the East Range. This unconformity spans a time gap of ~200,000 years in Troy Canyon and ~1 Ma in Limerick Canyon. Also, this unconformity may have a slight angular component, but this could not be confirmed in the Humboldt Range. This unconformity documents

that the transition from intermediate to felsic volcanism was associated with a pause in magmatism and perhaps tectonism. The lower unconformity between the Golconda Allochthon and the Koipato Formation has been constrained in this study to represent a time gap of ~15 to 6 Ma based on the age of Middle Permian for the youngest unit within the Golconda Allochthon and ~254 Ma from the inherited grains of the leucogranite intrusive. The unconformity between the overlying Prida Formation and the Koipato Formation represents a time gap of ~3 to7 Ma based on an Anisian age of the Prida Formation and the 248.32 Ma obtained from the youngest sample of the Koipato Formation. This time gap would be long enough to allow for a major change from the volcanic setting of the Koipato Formation to a carbonate platform, which is required for deposition of the Prida Formation.

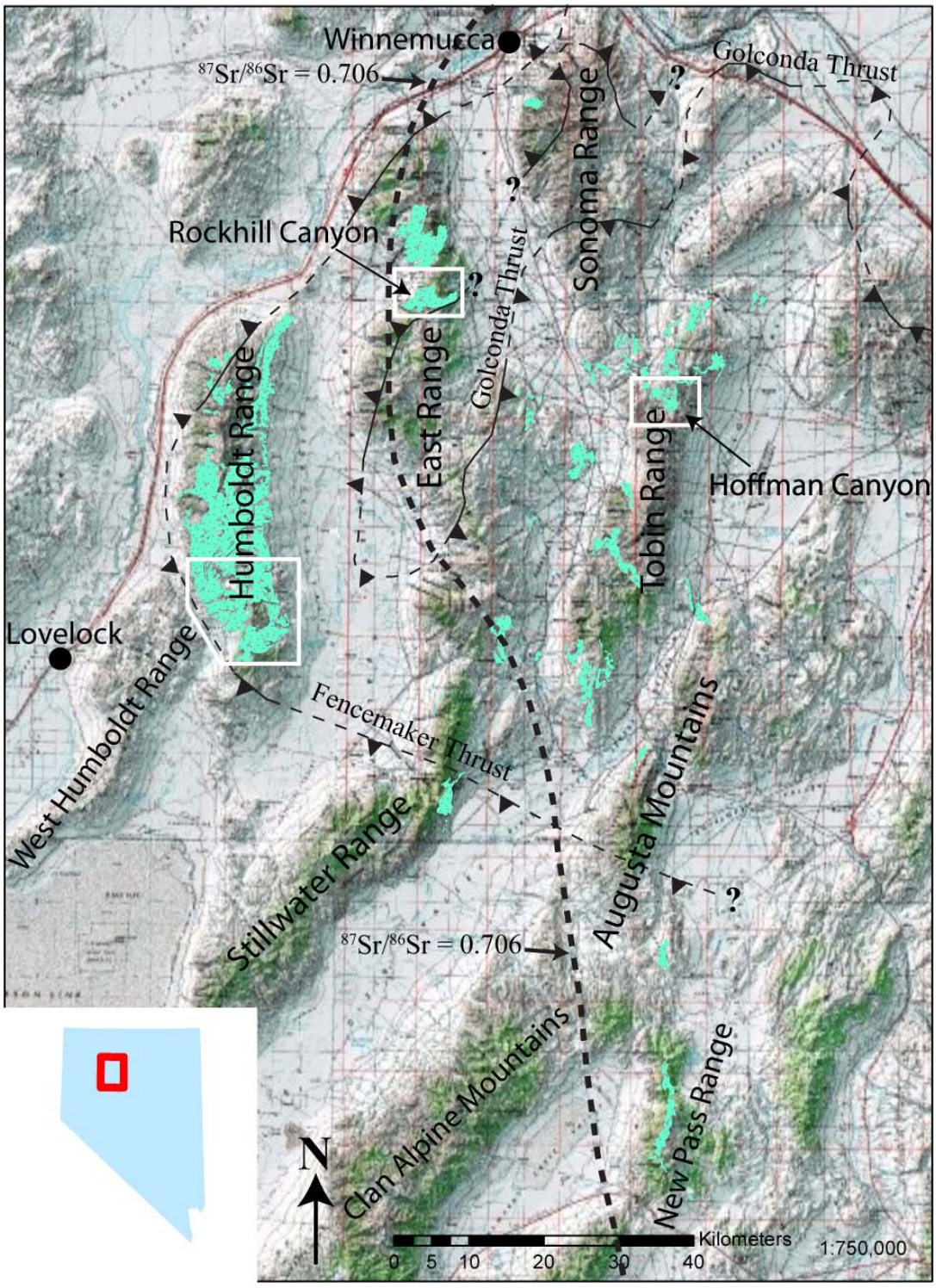

Figure 2.1. Topographic map of central Nevada showing the location of outcrops of the Koipato Formation and related units (bright green). Important mountain ranges and canyons are noted. White boxes outline the main field areas discussed in this report. Golconda and Fencemaker Thrust trends from Wilkins (2010). The $^{87}Sr/^{86}Sr = 0.706$ line is from Elison et al. (1990). Modified from Crafford (2007).

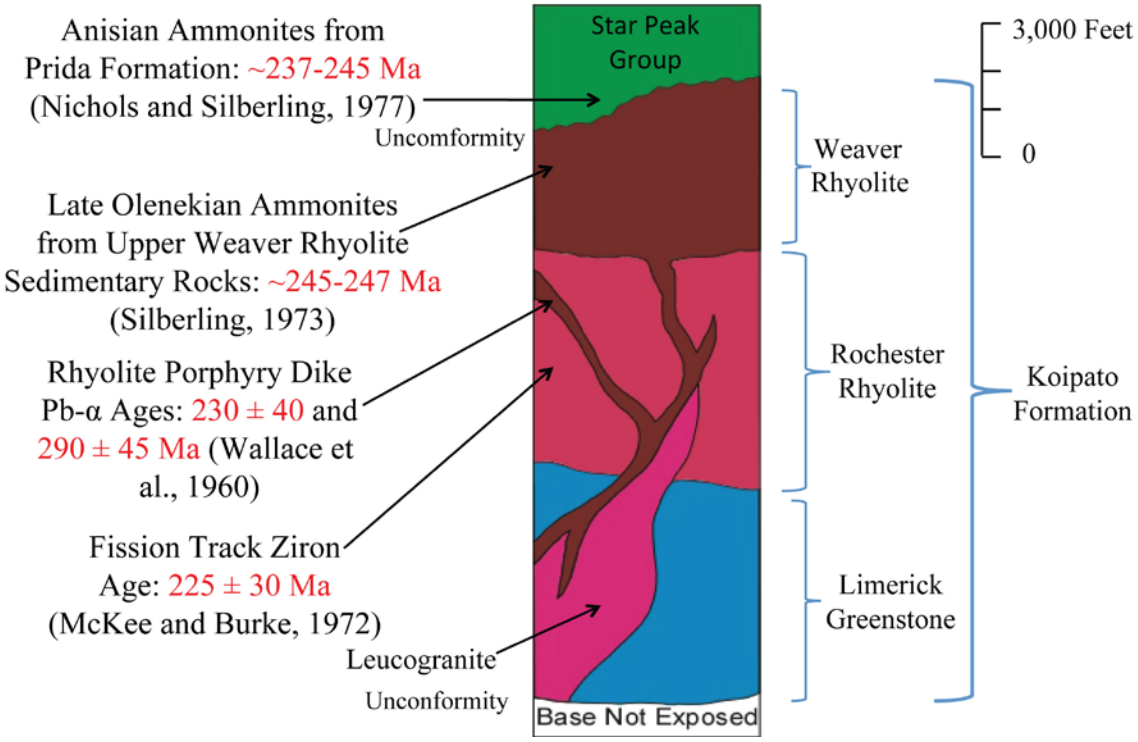

Figure 2.2. Generalized stratigraphic column for the Koipato Formation, in the Humboldt Range, showing previously interpreted stratigraphic relationships and age constraints (paleontological and radiometric). It is important to note that the base of the Koipato Formation in the Humboldt Range is not exposed. Modified from Silberling (1973).

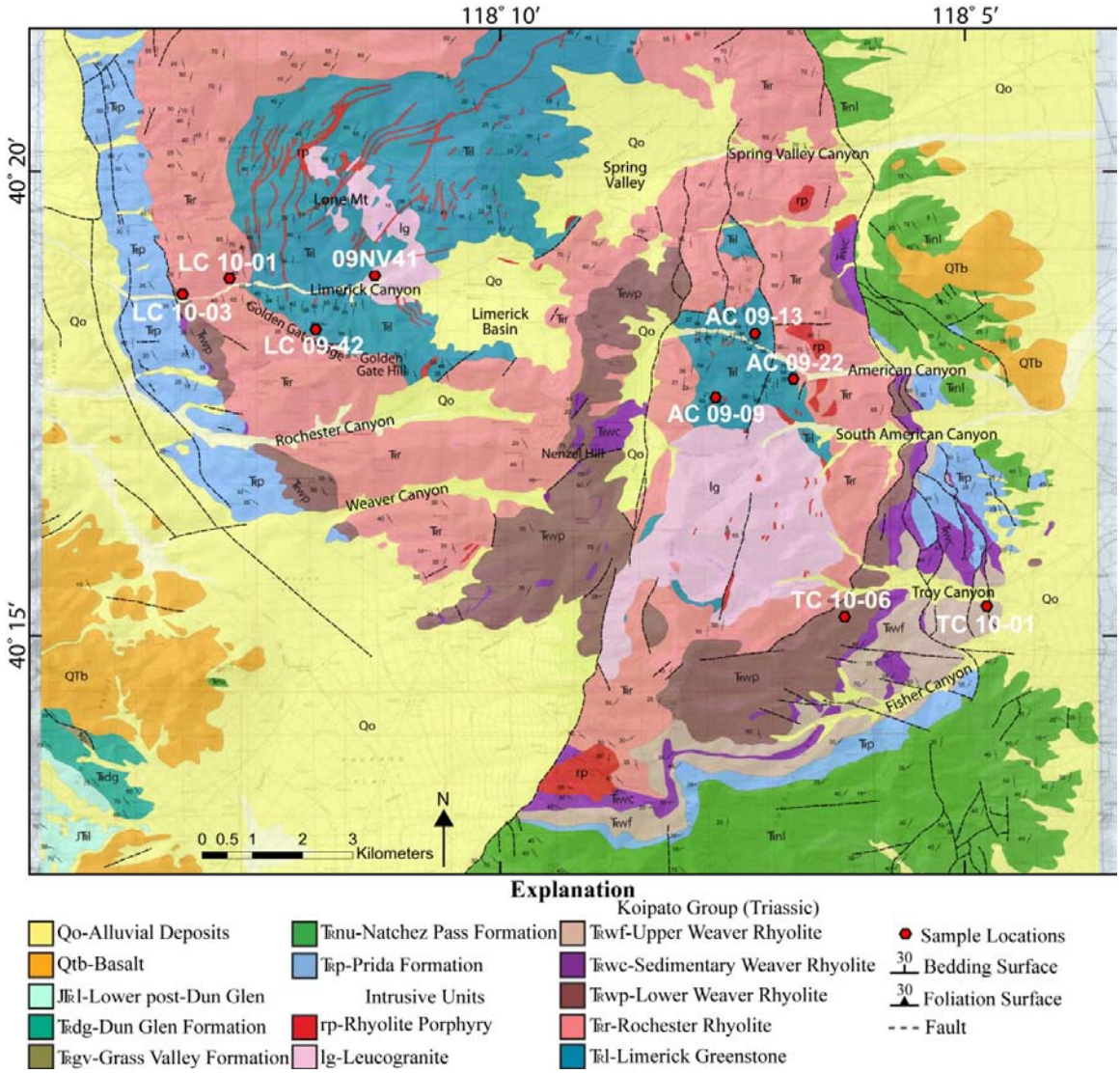

Figure 2.3. Geologic map of the southern Humboldt Range slightly modified from Wallace et al. (1969a, b). Map depicts sample locations analyzed in this study and geologic units discussed in the text.

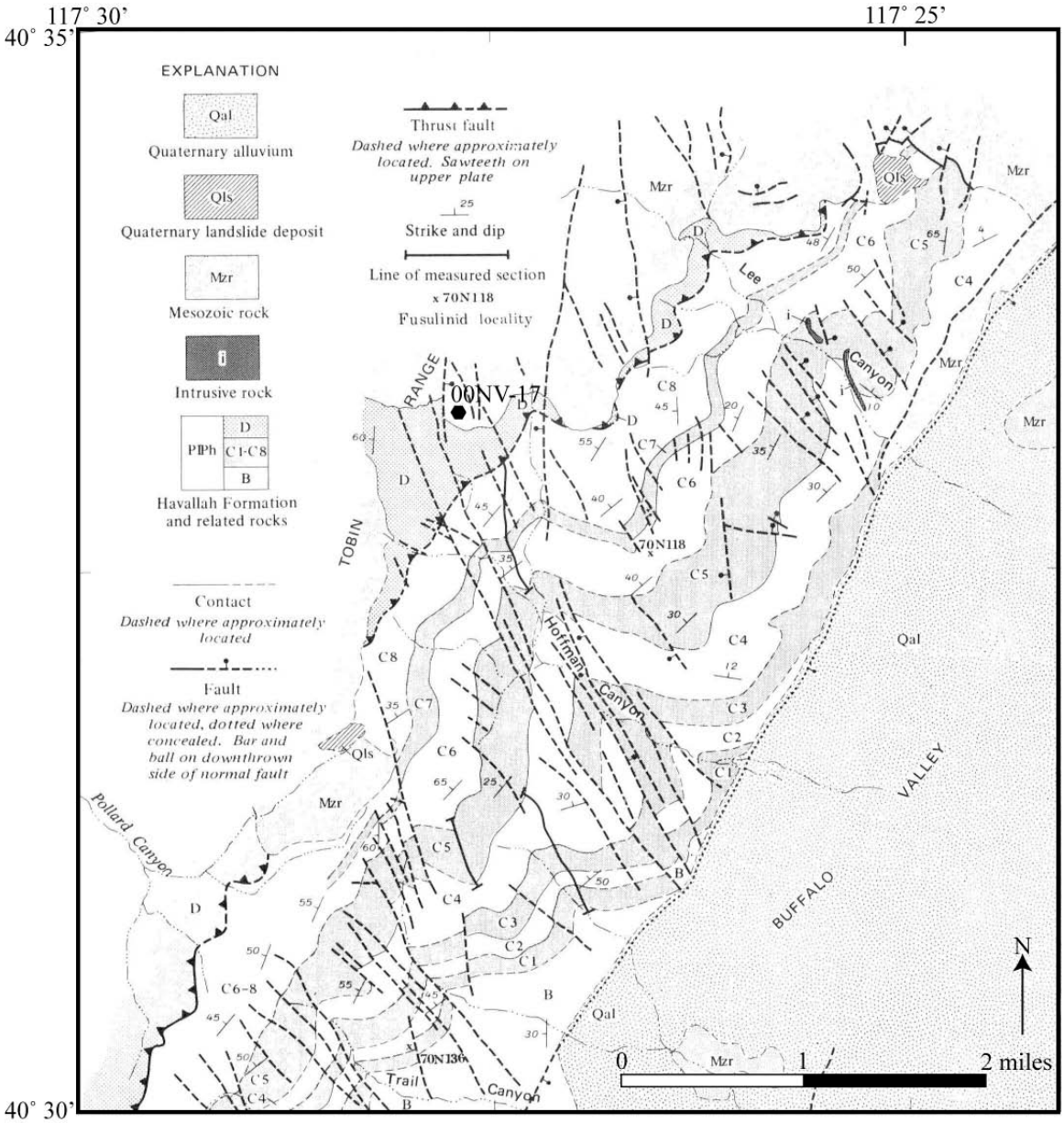

Figure 2.4. Geologic map of Hoffman Canyon in the Tobin Range from Stewart et al. (1977). Location of sample 00NV-17 is approximated on the map.

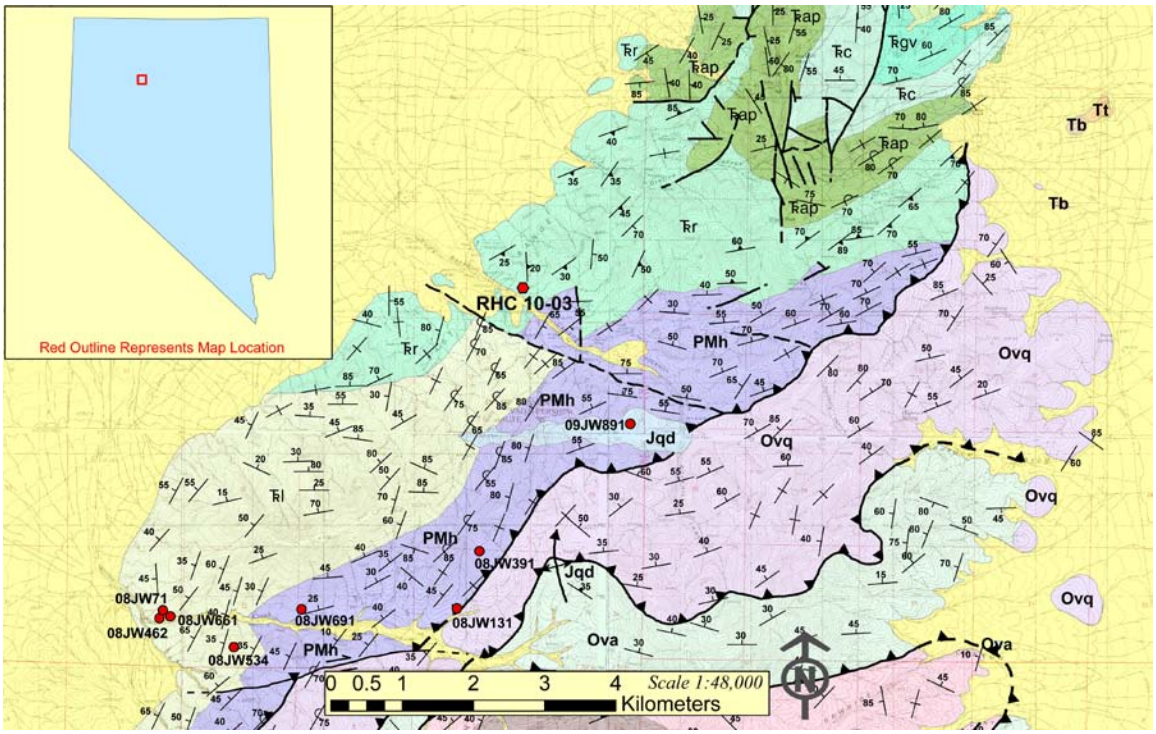

Figure 2.5. Geologic map of the East Range from Wilkins (2010). Light green and tan units are the Rochester Rhyolite and Limerick Greenstone discussed in this report. Sample location RHC 10-03, analyzed in this study, is positioned on the map alongside samples analyzed by Wilkins (2010).

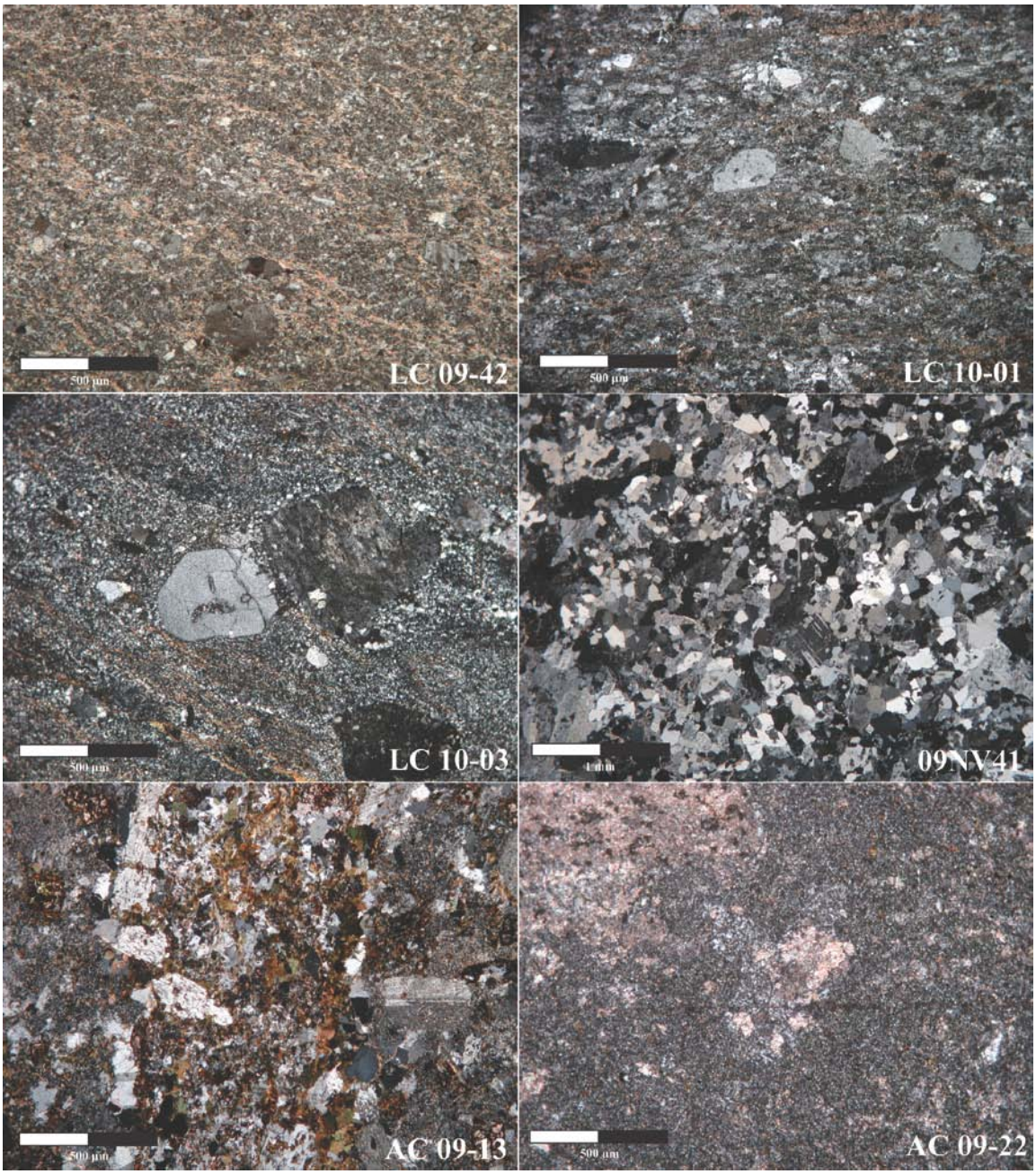

Figure 2.6. Pictomicrographs of thin sections from samples analyzed during this study. Consult the text for description of each sample and refer to Figures 2.3 and 2.4 for sample localities.

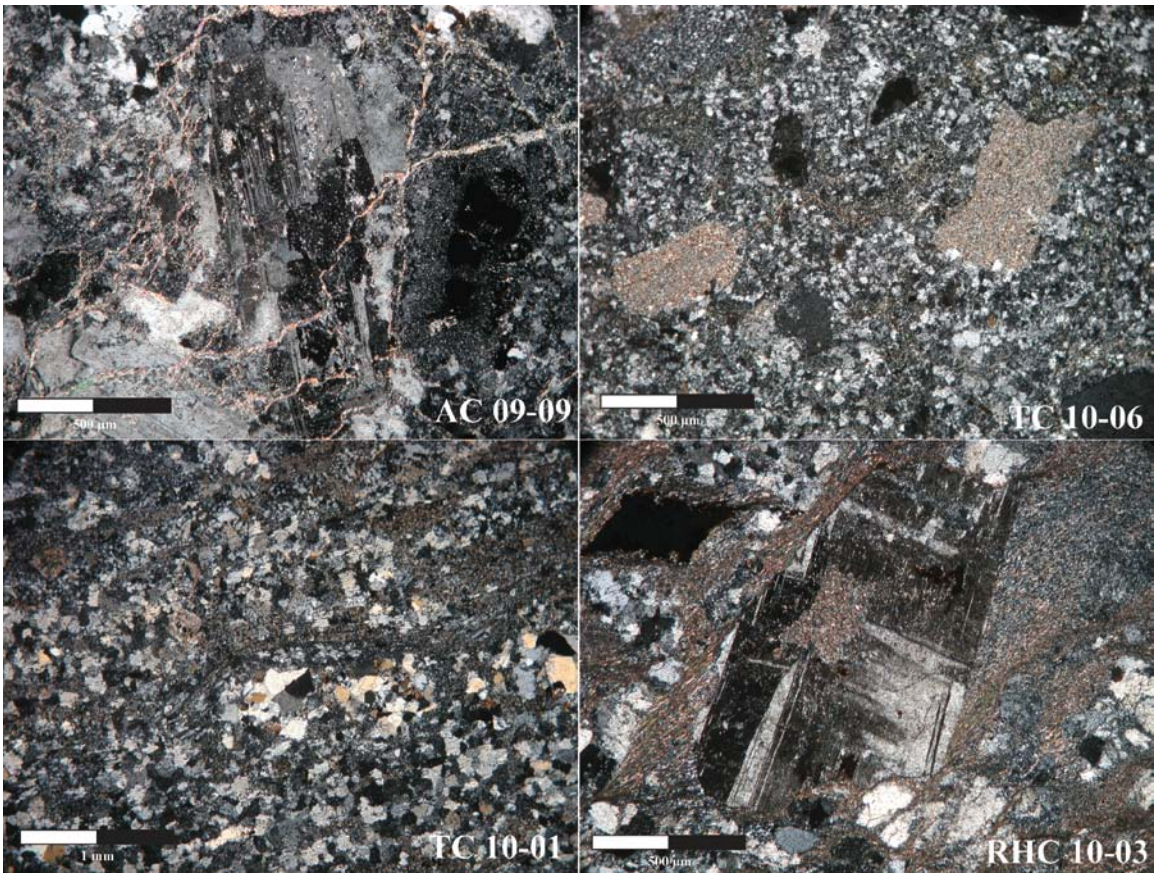

Figure 2.6 continued

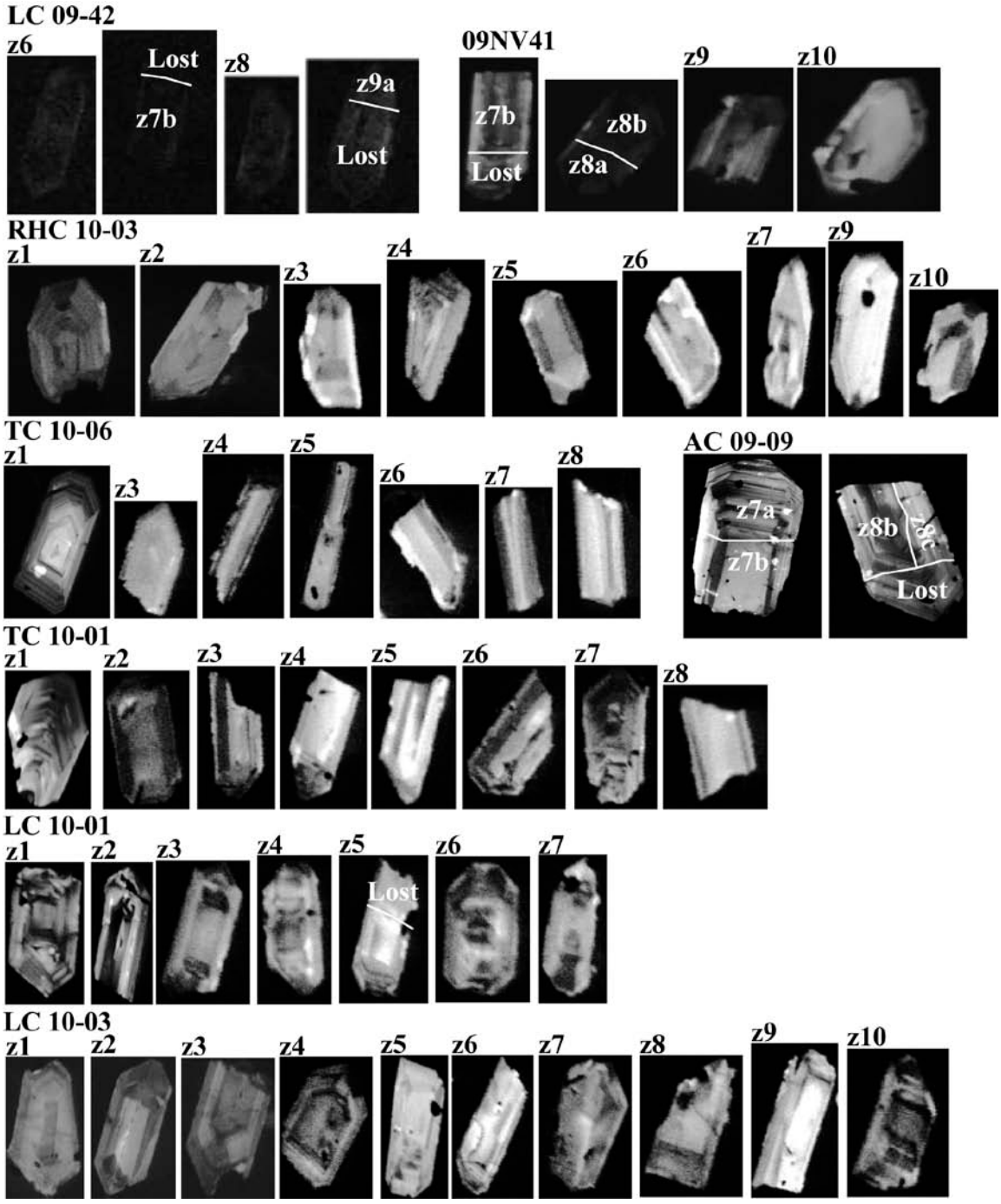

Figure 2.7. Cathodoluminescence images of zircons selected for U-Pb geochronology from certain samples. Consult the text for description of each sample and refer to Figures 2.3 and 2.5 for sample localities. Consult Figure 2.6 for thin section images of samples.

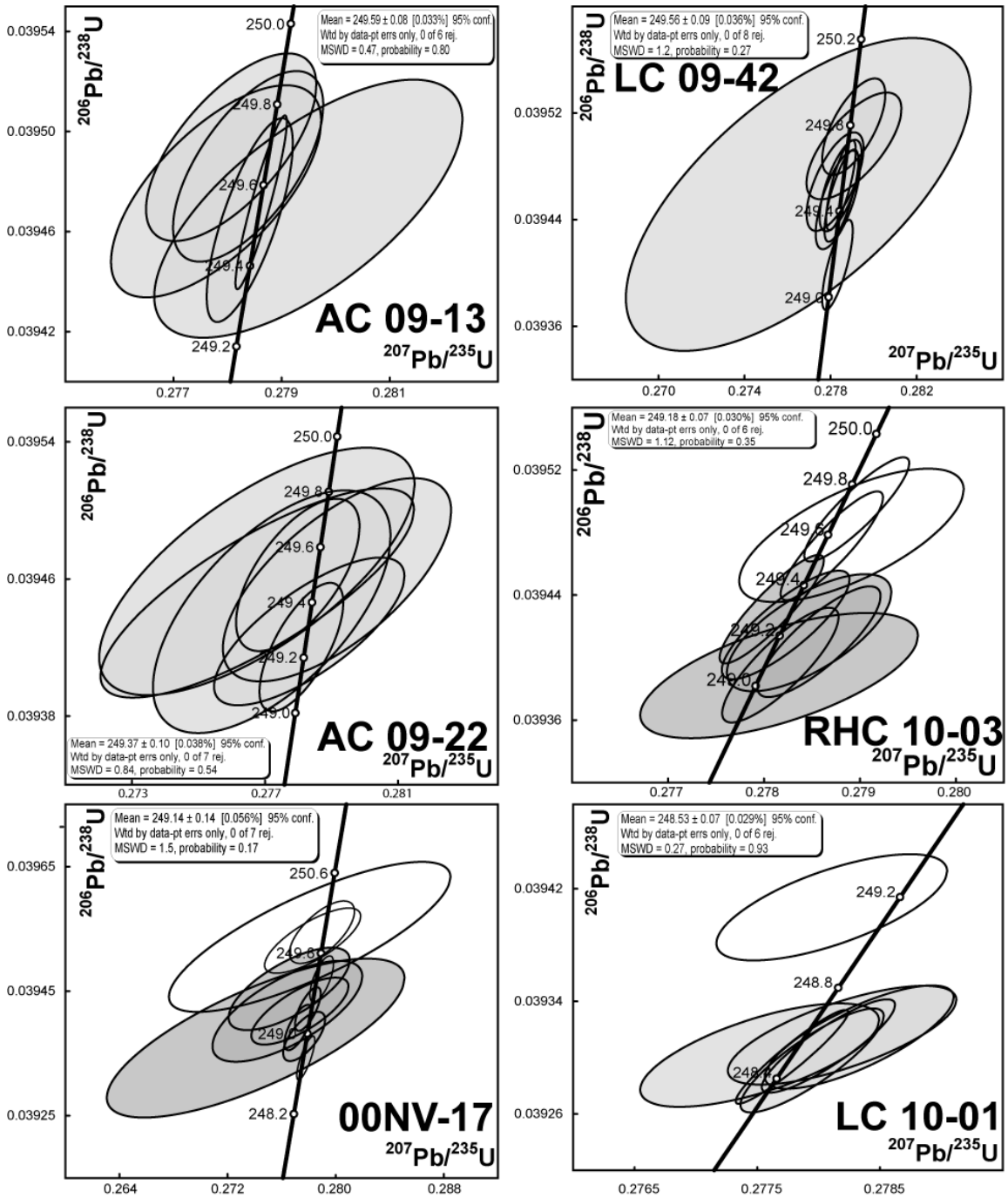

Figure 2.8. Concordia diagrams for all samples displaying the results of chemically abraded single grain analyses. Shaded ellipses denote analyses used in weighted mean age calculations. Consult text for reasons unshaded ellipses were excluded. Data point error ellipses are 2σ.

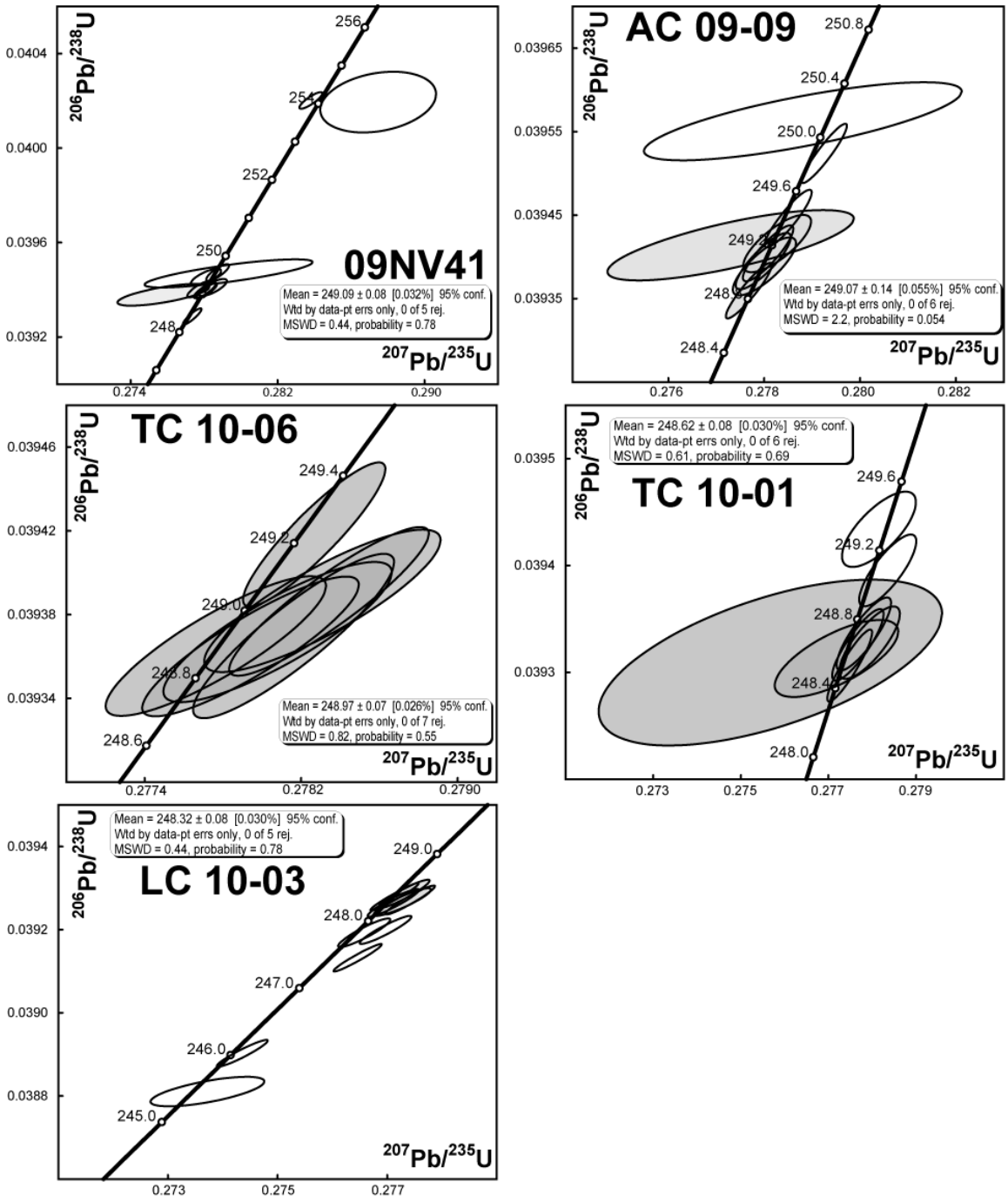

Figure 2.8 continued

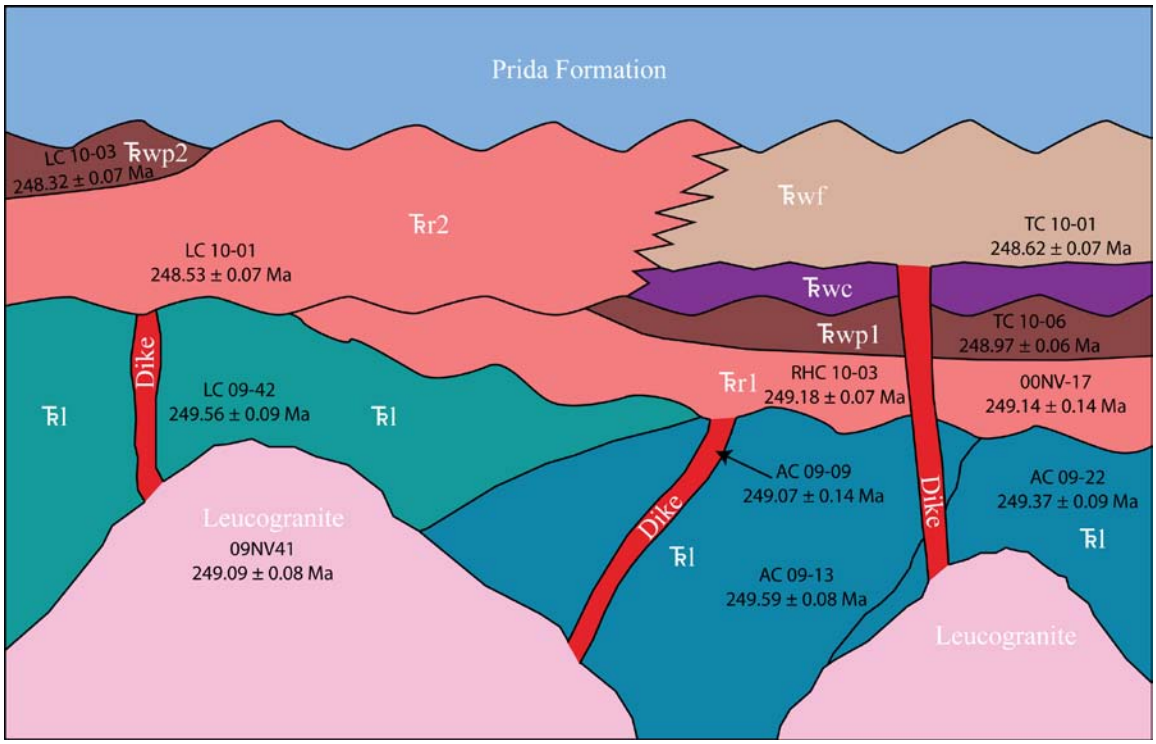

Figure 2.9. Interpretive cross-section for the Koipato Formation in the Humboldt Range based on field evidence and geochronology conducted during this study. Sample ages reported in this study are placed as close as possible to their inferred stratigraphic position. Consult text for unit and sample descriptions along with reasons for relationships depicted in this figure.

Table 2.1. Summary of Sample Ages and Locations

Sample Name	Sample Type	Formation	Location	Latitude	Longitude	$^{206}Pb/^{238}U$ Age (Ma)	MSWD	Prob. of fit	n
LC 10-03	Rhyolite tuff	Young Lower Weaver Rhyolite	Humboldt Range, NV	40.310	-118.224	248.32 ± 0.08	0.44	0.78	5 of 10
LC 10-01	Rhyolite flow	Young Rochester Rhyolite	Humboldt Range, NV	40.312	-118.216	248.53 ± 0.07	0.27	0.93	6 of 7
TC 10-01	Rhyolite tuff	Young Upper Weaver Rhyolite	Humboldt Range, NV	40.255	-118.079	248.62 ± 0.08	0.61	0.69	6 of 8
TC 10-06	Rhyolite flow	Old Lower Weaver Rhyolite	Humboldt Range, NV	40.252	-118.104	248.97 ± 0.07	0.82	0.55	7 of 7
AC 09-09	Rhyolite porphyry	Dike	Humboldt Range, NV	40.292	-118.128	249.07 ± 0.14	2.2	0.054	6 of 9
09NV41	Felsic intrusive	Lone Mountain Pluton	Humboldt Range, NV	40.313	-118.189	249.09 ± 0.08	0.44	0.78	5 of 11
00NV-17	Rhyolite tuff breccia	Old Rochester Rhyolite	Tobin Range, NV	40.553	-117.460	249.14 ± 0.14	1.5	0.17	7 of 12
RHC 10-03	Rhyolite flow	Old Rochester Rhyolite	East Range, NV	40.643	-117.892	249.18 ± 0.07	1.1	0.35	6 of 9
AC 09-22	Intermediate intrusive	Limerick Greenstone	Humboldt Range, NV	40.295	-118.114	249.37 ± 0.10	0.84	0.54	7 of 7
LC 09-42	Ash-flow tuff	Limerick Greenstone	Humboldt Range, NV	40.304	-118.200	249.56 ± 0.09	1.2	0.27	8 of 9
AC 09-13	Intermediate intrusive	Limerick Greenstone	Humboldt Range, NV	40.302	-118.121	249.59 ± 0.08	0.47	0.8	6 of 6

Notes: Lat/Long coordinates are in WGS 1984 datum.

Table 2.2. U-Pb Isotopic Data

Grain (a)	Th/U (b)	$^{206}Pb^*$ x10^{-13} mol (c)	mol % $^{206}Pb^*$ (c)	Pb^*/Pbc (c)	Pbc (pg) (c)	$^{206}Pb/^{204}Pb$ (d)	Radiogenic Isotopic Ratios: $^{208}Pb/^{206}Pb$ (e)	$^{207}Pb/^{206}Pb$ (e)	% err (f)	$^{207}Pb/^{235}U$ (e)	% err (f)	$^{206}Pb/^{238}U$ (e)	% err (f)	corr. coef.	Radiogenic Isotopic Dates: $^{207}Pb/^{206}Pb$ (g)	± (f)	$^{207}Pb/^{235}U$ (g)	± (f)	$^{206}Pb/^{238}U$ (g)	± (f)
AC 09-13																				
z4	**0.500**	**1.0373**	**98.56%**	**21**	**1.25**	**1290**	**0.158**	**0.051066**	**0.411**	**0.278075**	**0.458**	**0.039494**	**0.078**	**0.663**	**243.82**	**9.46**	**249.13**	**1.01**	**249.69**	**0.19**
z2	**0.488**	**1.4782**	**98.71%**	**23**	**1.59**	**1439**	**0.155**	**0.051134**	**0.358**	**0.278389**	**0.404**	**0.039486**	**0.079**	**0.644**	**246.87**	**8.24**	**249.38**	**0.89**	**249.65**	**0.19**
z5	**0.464**	**0.4607**	**98.44%**	**19**	**0.60**	**1193**	**0.147**	**0.051039**	**0.512**	**0.277802**	**0.566**	**0.039476**	**0.088**	**0.663**	**242.59**	**11.80**	**248.91**	**1.25**	**249.58**	**0.22**
z1	**0.678**	**9.2752**	**99.86%**	**235**	**1.03**	**13747**	**0.215**	**0.051197**	**0.077**	**0.278629**	**0.139**	**0.039471**	**0.072**	**0.926**	**249.70**	**1.77**	**249.57**	**0.31**	**249.56**	**0.18**
z6	**0.428**	**0.1985**	**97.45%**	**11**	**0.43**	**729**	**0.136**	**0.051359**	**0.756**	**0.279495**	**0.825**	**0.039469**	**0.107**	**0.681**	**256.98**	**17.37**	**250.26**	**1.83**	**249.54**	**0.26**
z7	**0.454**	**1.1780**	**99.49%**	**58**	**0.50**	**3623**	**0.144**	**0.051167**	**0.177**	**0.278417**	**0.232**	**0.039464**	**0.085**	**0.752**	**248.36**	**4.09**	**249.40**	**0.51**	**249.51**	**0.21**
LC 09-42																				
z4	**0.624**	**3.0052**	**98.58%**	**22**	**3.57**	**1307**	**0.198**	**0.051235**	**0.377**	**0.279044**	**0.423**	**0.039501**	**0.075**	**0.665**	**251.40**	**8.68**	**249.90**	**0.94**	**249.74**	**0.18**
z5	**0.509**	**4.0556**	**97.77%**	**13**	**7.60**	**835**	**0.161**	**0.051254**	**0.584**	**0.279107**	**0.639**	**0.039495**	**0.083**	**0.691**	**252.26**	**13.44**	**249.95**	**1.41**	**249.70**	**0.20**
z8	**0.835**	**1.0022**	**98.81%**	**27**	**0.99**	**1560**	**0.264**	**0.051130**	**0.336**	**0.278242**	**0.382**	**0.039468**	**0.077**	**0.670**	**246.69**	**7.73**	**249.26**	**0.84**	**249.54**	**0.19**
z2	**0.544**	**4.6665**	**99.10%**	**34**	**3.49**	**2065**	**0.172**	**0.051181**	**0.244**	**0.278499**	**0.287**	**0.039465**	**0.071**	**0.686**	**248.98**	**5.61**	**249.47**	**0.63**	**249.52**	**0.17**
z3	**0.553**	**3.4841**	**99.50%**	**61**	**1.45**	**3696**	**0.175**	**0.051184**	**0.154**	**0.278518**	**0.201**	**0.039465**	**0.070**	**0.773**	**249.13**	**3.53**	**249.48**	**0.44**	**249.52**	**0.17**
z9a	**0.542**	**0.1092**	**92.89%**	**4**	**0.69**	**262**	**0.171**	**0.050831**	**2.193**	**0.276547**	**2.346**	**0.039459**	**0.244**	**0.661**	**233.16**	**50.61**	**247.91**	**5.16**	**249.48**	**0.60**
z7b	**0.753**	**1.1477**	**99.43%**	**56**	**0.54**	**3250**	**0.239**	**0.051197**	**0.181**	**0.278535**	**0.229**	**0.039458**	**0.072**	**0.749**	**249.73**	**4.17**	**249.49**	**0.51**	**249.47**	**0.18**
z6	**0.442**	**0.8147**	**99.24%**	**39**	**0.51**	**2442**	**0.140**	**0.051172**	**0.252**	**0.278374**	**0.298**	**0.039454**	**0.077**	**0.682**	**248.58**	**5.80**	**249.37**	**0.66**	**249.45**	**0.19**
z1	0.516	5.9161	99.45%	55	2.67	3401	0.164	0.051230	0.160	0.278344	0.206	0.039406	0.070	0.762	251.19	3.67	249.34	0.46	249.15	0.17
AC 09-22																				
z4	**0.572**	**0.2891**	**95.42%**	**6**	**1.14**	**407**	**0.180**	**0.050864**	**1.285**	**0.276768**	**1.385**	**0.039464**	**0.150**	**0.696**	**234.68**	**29.64**	**248.09**	**3.05**	**249.51**	**0.37**
z1	**0.727**	**3.2211**	**98.18%**	**17**	**4.90**	**1025**	**0.230**	**0.051090**	**0.487**	**0.277984**	**0.540**	**0.039462**	**0.092**	**0.630**	**244.90**	**11.22**	**249.06**	**1.19**	**249.50**	**0.23**
z7	**0.578**	**0.2097**	**96.92%**	**10**	**0.55**	**604**	**0.184**	**0.051308**	**0.917**	**0.279151**	**0.996**	**0.039459**	**0.123**	**0.674**	**254.71**	**21.09**	**249.98**	**2.21**	**249.48**	**0.30**
z6	**0.627**	**0.1653**	**95.85%**	**7**	**0.59**	**448**	**0.198**	**0.050883**	**1.280**	**0.276782**	**1.379**	**0.039452**	**0.127**	**0.794**	**235.53**	**29.53**	**248.10**	**3.03**	**249.43**	**0.31**
z8	**0.597**	**0.2266**	**96.86%**	**10**	**0.60**	**592**	**0.189**	**0.050977**	**0.959**	**0.277215**	**1.043**	**0.039441**	**0.147**	**0.618**	**239.77**	**22.10**	**248.45**	**2.30**	**249.36**	**0.36**
z5	**0.973**	**2.6772**	**97.08%**	**11**	**6.62**	**637**	**0.309**	**0.051197**	**0.767**	**0.278330**	**0.831**	**0.039429**	**0.089**	**0.747**	**249.69**	**17.64**	**249.33**	**1.84**	**249.29**	**0.22**
z2	**0.578**	**0.5543**	**98.98%**	**30**	**0.47**	**1830**	**0.183**	**0.051164**	**0.317**	**0.278088**	**0.366**	**0.039420**	**0.078**	**0.689**	**248.23**	**7.30**	**249.14**	**0.81**	**249.24**	**0.19**
RHC 10-03																				
z4	0.528	2.1918	99.75%	120	0.46	7322	0.167	0.051230	0.103	0.278975	0.159	0.039495	0.069	0.886	251.19	2.37	249.84	0.35	249.70	0.17
z6	0.412	0.7857	99.20%	37	0.52	2319	0.131	0.051241	0.286	0.278919	0.339	0.039478	0.089	0.686	251.70	6.57	249.80	0.75	249.60	0.22

Table 2.2 continued

Grain (a)	Th/U (b)	$^{206}Pb^*$ x10^{-13} mol (c)	mol % $^{206}Pb^*$ (c)	Pb^*/Pbc (c)	Pbc (pg) (c)	$^{206}Pb/^{204}Pb$ (d)	Radiogenic Isotopic Ratios: $^{208}Pb/^{206}Pb$ (e)	$^{207}Pb/^{206}Pb$ (e)	% err (f)	$^{207}Pb/^{235}U$ (e)	% err (f)	$^{206}Pb/^{238}U$ (e)	% err (f)	corr. coef.	Radiogenic Isotopic Dates: $^{207}Pb/^{206}Pb$ (g)	± (f)	$^{207}Pb/^{235}U$ (g)	± (f)	$^{206}Pb/^{238}U$ (g)	± (f)
z1	0.433	2.4573	99.80%	148	0.41	9250	0.137	0.051213	0.097	0.278718	0.155	0.039472	0.072	0.887	250.43	2.23	249.64	0.34	249.56	0.18
z7	**0.413**	**1.4953**	**99.81%**	**155**	**0.24**	**9747**	**0.131**	**0.051151**	**0.099**	**0.278096**	**0.158**	**0.039431**	**0.072**	**0.894**	**247.66**	**2.28**	**249.15**	**0.35**	**249.30**	**0.18**
z3	**0.611**	**1.3175**	**99.65%**	**90**	**0.38**	**5369**	**0.194**	**0.051192**	**0.139**	**0.278243**	**0.194**	**0.039421**	**0.072**	**0.833**	**249.47**	**3.20**	**249.26**	**0.43**	**249.24**	**0.18**
z9	**0.449**	**1.7245**	**99.37%**	**48**	**0.89**	**2970**	**0.143**	**0.051243**	**0.204**	**0.278485**	**0.249**	**0.039416**	**0.078**	**0.684**	**251.76**	**4.69**	**249.46**	**0.55**	**249.21**	**0.19**
z10	**0.494**	**1.3029**	**99.65%**	**86**	**0.38**	**5313**	**0.157**	**0.051269**	**0.132**	**0.278585**	**0.186**	**0.039410**	**0.074**	**0.824**	**252.93**	**3.03**	**249.53**	**0.41**	**249.17**	**0.18**
z5	**0.520**	**1.6978**	**99.70%**	**103**	**0.41**	**6276**	**0.165**	**0.051215**	**0.120**	**0.278189**	**0.177**	**0.039395**	**0.076**	**0.837**	**250.53**	**2.77**	**249.22**	**0.39**	**249.08**	**0.19**
z2	**0.399**	**1.8186**	**98.75%**	**23**	**1.89**	**1493**	**0.127**	**0.051221**	**0.374**	**0.278176**	**0.421**	**0.039388**	**0.083**	**0.632**	**250.81**	**8.60**	**249.21**	**0.93**	**249.04**	**0.20**
00NV-17																				
z10	0.470	0.2429	97.94%	14	0.42	903	0.149	0.051179	0.634	0.279041	0.698	0.039544	0.104	0.668	248.88	14.58	249.90	1.55	250.00	0.25
z8	0.438	0.0754	90.46%	3	0.65	195	0.139	0.051025	2.838	0.278154	3.032	0.039536	0.250	0.796	241.98	65.38	249.19	6.70	249.96	0.61
z2	0.429	0.2622	96.55%	8	0.77	538	0.136	0.051070	0.958	0.278355	1.036	0.039530	0.108	0.750	243.99	22.06	249.35	2.29	249.92	0.26
z1	0.435	1.1505	99.52%	62	0.46	3879	0.138	0.051273	0.210	0.279028	0.255	0.039469	0.077	0.677	253.14	4.83	249.89	0.56	249.54	0.19
z11	**0.408**	**0.1220**	**96.47%**	**8**	**0.37**	**526**	**0.129**	**0.050856**	**1.218**	**0.276650**	**1.311**	**0.039454**	**0.138**	**0.700**	**234.31**	**28.10**	**248.00**	**2.88**	**249.45**	**0.34**
z4	**0.404**	**0.9813**	**99.21%**	**37**	**0.64**	**2368**	**0.128**	**0.051151**	**0.232**	**0.278026**	**0.278**	**0.039421**	**0.073**	**0.714**	**247.66**	**5.33**	**249.09**	**0.61**	**249.24**	**0.18**
z12	**0.402**	**0.1251**	**95.02%**	**6**	**0.54**	**374**	**0.127**	**0.050877**	**1.506**	**0.276511**	**1.617**	**0.039417**	**0.168**	**0.691**	**235.28**	**34.74**	**247.89**	**3.56**	**249.22**	**0.41**
z13	**0.407**	**0.2531**	**96.74%**	**9**	**0.70**	**571**	**0.129**	**0.051048**	**0.966**	**0.277443**	**1.045**	**0.039418**	**0.112**	**0.735**	**243.00**	**22.25**	**248.63**	**2.30**	**249.22**	**0.27**
z9	**0.404**	**0.6115**	**99.25%**	**39**	**0.38**	**2485**	**0.128**	**0.051060**	**0.249**	**0.277323**	**0.297**	**0.039391**	**0.076**	**0.711**	**243.56**	**5.73**	**248.53**	**0.65**	**249.06**	**0.19**
z3	**0.425**	**0.6045**	**98.61%**	**21**	**0.70**	**1337**	**0.135**	**0.051159**	**0.400**	**0.277758**	**0.451**	**0.039377**	**0.082**	**0.675**	**248.02**	**9.22**	**248.88**	**1.00**	**248.97**	**0.20**
z7	**0.455**	**0.0666**	**90.64%**	**3**	**0.57**	**199**	**0.143**	**0.050507**	**3.056**	**0.274198**	**3.250**	**0.039374**	**0.265**	**0.752**	**218.38**	**70.72**	**246.04**	**7.10**	**248.95**	**0.65**
z5	0.405	1.0821	99.63%	80	0.33	5028	0.128	0.051226	0.140	0.277869	0.192	0.039342	0.073	0.807	250.99	3.22	248.97	0.42	248.75	0.18
09NV41																				
z2	0.585	1.8001	99.59%	76	0.61	4562	0.185	0.051210	0.126	0.283853	0.181	0.040201	0.071	0.856	250.28	2.89	253.71	0.41	254.08	0.18
z10	0.570	1.0161	85.79%	2	13.94	128	0.183	0.051877	0.862	0.287497	0.892	0.040194	0.262	0.262	279.97	19.72	256.59	2.02	254.03	0.65
z3	0.526	1.7432	99.63%	83	0.53	5041	0.167	0.051232	0.126	0.278820	0.180	0.039472	0.073	0.828	251.27	2.91	249.72	0.40	249.56	0.18
z7b	0.601	0.2577	95.39%	6	1.02	404	0.191	0.051345	1.233	0.279411	1.330	0.039468	0.124	0.798	256.33	28.33	250.19	2.95	249.54	0.30
z4	0.464	1.4584	99.40%	50	0.72	3125	0.147	0.051140	0.189	0.278185	0.237	0.039452	0.074	0.739	247.16	4.36	249.22	0.52	249.43	0.18
z9	**0.590**	**2.2682**	**99.32%**	**45**	**1.28**	**2723**	**0.187**	**0.051266**	**0.171**	**0.278558**	**0.221**	**0.039408**	**0.075**	**0.757**	**252.80**	**3.94**	**249.51**	**0.49**	**249.16**	**0.18**
z8b	**0.734**	**1.5514**	**99.65%**	**91**	**0.45**	**5251**	**0.233**	**0.051138**	**0.135**	**0.277813**	**0.186**	**0.039401**	**0.071**	**0.812**	**247.07**	**3.11**	**248.92**	**0.41**	**249.12**	**0.17**
z6	**0.608**	**2.1487**	**99.66%**	**92**	**0.60**	**5484**	**0.193**	**0.051203**	**0.122**	**0.278136**	**0.174**	**0.039397**	**0.069**	**0.843**	**249.96**	**2.80**	**249.18**	**0.39**	**249.09**	**0.17**

Table 2.2 continued

Grain (a)	Th/U (b)	$^{206}Pb^*$ x10^{-13} mol (c)	mol % $^{206}Pb^*$ (c)	Pb^*/Pbc (c)	Pbc (pg) (c)	$^{206}Pb/^{204}Pb$ (d)	Radiogenic Isotopic Ratios: $^{208}Pb/^{206}Pb$ (e)	$^{207}Pb/^{206}Pb$ (e)	% err (f)	$^{207}Pb/^{235}U$ (e)	% err (f)	$^{206}Pb/^{238}U$ (e)	% err (f)	corr. coef.	Radiogenic Isotopic Dates: $^{207}Pb/^{206}Pb$ (g)	± (f)	$^{207}Pb/^{235}U$ (g)	± (f)	$^{206}Pb/^{238}U$ (g)	± (f)
z5	**0.431**	**2.1677**	**99.72%**	**108**	**0.49**	**6761**	**0.137**	**0.051222**	**0.108**	**0.278221**	**0.163**	**0.039394**	**0.070**	**0.865**	**250.85**	**2.48**	**249.25**	**0.36**	**249.07**	**0.17**
z8a	**0.759**	**0.2842**	**97.76%**	**14**	**0.54**	**829**	**0.239**	**0.050812**	**0.668**	**0.275879**	**0.730**	**0.039378**	**0.095**	**0.699**	**232.32**	**15.41**	**247.38**	**1.60**	**248.97**	**0.23**
z1	0.614	4.3314	99.80%	152	0.73	9086	0.195	0.051219	0.090	0.277438	0.148	0.039286	0.070	0.898	250.70	2.07	248.62	0.33	248.40	0.17
AC 09-09																				
z2	0.591	15.0213	96.61%	9	43.33	549	0.187	0.051117	0.890	0.278832	0.962	0.039562	0.097	0.761	246.09	20.50	249.73	2.13	250.12	0.24
z3	0.553	13.0441	99.87%	236	1.40	14279	0.176	0.051247	0.074	0.279271	0.137	0.039523	0.073	0.932	251.96	1.69	250.08	0.30	249.88	0.18
z6	0.532	7.0023	99.82%	171	1.03	10403	0.169	0.051212	0.084	0.278523	0.143	0.039445	0.071	0.908	250.37	1.93	249.49	0.32	249.39	0.17
z8b	**0.635**	**1.7110**	**99.49%**	**61**	**0.72**	**3635**	**0.201**	**0.051209**	**0.157**	**0.278299**	**0.205**	**0.039415**	**0.072**	**0.767**	**250.25**	**3.62**	**249.31**	**0.45**	**249.21**	**0.18**
z8c	**0.476**	**0.5103**	**97.43%**	**11**	**1.11**	**722**	**0.150**	**0.051035**	**0.687**	**0.277337**	**0.750**	**0.039413**	**0.088**	**0.751**	**242.40**	**15.82**	**248.54**	**1.65**	**249.19**	**0.21**
z1	**0.571**	**16.8919**	**99.73%**	**113**	**3.78**	**6845**	**0.181**	**0.051189**	**0.098**	**0.278107**	**0.153**	**0.039403**	**0.070**	**0.875**	**249.36**	**2.25**	**249.15**	**0.34**	**249.13**	**0.17**
z7a	**0.463**	**3.5839**	**99.67%**	**90**	**0.98**	**5583**	**0.147**	**0.051183**	**0.113**	**0.278007**	**0.166**	**0.039394**	**0.070**	**0.847**	**249.08**	**2.61**	**249.08**	**0.37**	**249.08**	**0.17**
z7b	**0.440**	**2.1817**	**99.57%**	**70**	**0.77**	**4361**	**0.139**	**0.051196**	**0.140**	**0.278034**	**0.191**	**0.039388**	**0.072**	**0.798**	**249.66**	**3.22**	**249.10**	**0.42**	**249.04**	**0.18**
z5	**0.584**	**6.8315**	**99.84%**	**195**	**0.89**	**11713**	**0.185**	**0.051175**	**0.081**	**0.277713**	**0.140**	**0.039359**	**0.069**	**0.922**	**248.71**	**1.86**	**248.84**	**0.31**	**248.86**	**0.17**
TC 10-06																				
z1	**0.367**	**16.0666**	**99.90%**	**304**	**1.27**	**19311**	**0.116**	**0.051200**	**0.051**	**0.278132**	**0.108**	**0.039398**	**0.074**	**0.908**	**249.86**	**1.16**	**249.17**	**0.24**	**249.10**	**0.18**
z7	**0.494**	**2.2533**	**99.82%**	**166**	**0.34**	**10232**	**0.157**	**0.051256**	**0.087**	**0.278349**	**0.148**	**0.039386**	**0.074**	**0.911**	**252.35**	**1.99**	**249.35**	**0.33**	**249.03**	**0.18**
z8	**0.524**	**1.6420**	**99.70%**	**103**	**0.40**	**6295**	**0.166**	**0.051249**	**0.121**	**0.278315**	**0.176**	**0.039387**	**0.071**	**0.850**	**252.05**	**2.79**	**249.32**	**0.39**	**249.03**	**0.17**
z3	**0.421**	**1.8595**	**99.66%**	**88**	**0.52**	**5526**	**0.134**	**0.051227**	**0.117**	**0.278089**	**0.170**	**0.039372**	**0.070**	**0.849**	**251.06**	**2.69**	**249.14**	**0.38**	**248.94**	**0.17**
z5	**0.419**	**4.6663**	**99.81%**	**158**	**0.72**	**9903**	**0.133**	**0.051244**	**0.084**	**0.278169**	**0.150**	**0.039370**	**0.082**	**0.897**	**251.83**	**1.94**	**249.20**	**0.33**	**248.93**	**0.20**
z4	**0.419**	**2.4111**	**99.73%**	**111**	**0.53**	**6941**	**0.133**	**0.051211**	**0.106**	**0.277952**	**0.161**	**0.039365**	**0.069**	**0.880**	**250.33**	**2.43**	**249.03**	**0.36**	**248.89**	**0.17**
z6	**0.523**	**2.1510**	**99.73%**	**113**	**0.48**	**6882**	**0.166**	**0.051178**	**0.111**	**0.277776**	**0.164**	**0.039365**	**0.069**	**0.858**	**248.87**	**2.55**	**248.89**	**0.36**	**248.89**	**0.17**
TC 10-01																				
z1	0.474	2.5256	99.31%	43	1.44	2702	0.150	0.051159	0.199	0.278157	0.245	0.039434	0.073	0.718	248.00	4.59	249.19	0.54	249.32	0.18
z2	0.495	3.3572	99.57%	70	1.19	4342	0.157	0.051245	0.138	0.278353	0.188	0.039395	0.070	0.811	251.88	3.17	249.35	0.42	249.08	0.17
z6	**0.524**	**1.1284**	**99.70%**	**103**	**0.27**	**6299**	**0.166**	**0.051224**	**0.126**	**0.277812**	**0.180**	**0.039335**	**0.071**	**0.849**	**250.90**	**2.89**	**248.92**	**0.40**	**248.71**	**0.17**
z4	**0.529**	**1.2071**	**99.54%**	**66**	**0.46**	**4015**	**0.168**	**0.051258**	**0.152**	**0.277945**	**0.202**	**0.039327**	**0.070**	**0.794**	**252.47**	**3.49**	**249.03**	**0.45**	**248.66**	**0.17**
z3	**0.475**	**1.4600**	**99.70%**	**100**	**0.36**	**6159**	**0.151**	**0.051212**	**0.116**	**0.277677**	**0.170**	**0.039325**	**0.070**	**0.859**	**250.37**	**2.66**	**248.81**	**0.37**	**248.65**	**0.17**
z5	**0.547**	**0.5274**	**99.15%**	**36**	**0.37**	**2183**	**0.173**	**0.051139**	**0.364**	**0.277195**	**0.412**	**0.039312**	**0.075**	**0.698**	**247.11**	**8.37**	**248.43**	**0.91**	**248.57**	**0.18**

Table 2.2 continued

Grain (a)	Th/U (b)	$^{206}Pb^*$ x10^{-13} mol (c)	mol % $^{206}Pb^*$ (c)	Pb*/Pbc (c)	Pbc (pg) (c)	$^{206}Pb/^{204}Pb$ (d)	Radiogenic Isotopic Ratios: $^{208}Pb/^{206}Pb$ (e)	$^{207}Pb/^{206}Pb$ (e)	% err (f)	$^{207}Pb/^{235}U$ (e)	% err (f)	$^{206}Pb/^{238}U$ (e)	% err (f)	corr. coef.	Radiogenic Isotopic Dates: $^{207}Pb/^{206}Pb$ (g)	± (f)	$^{207}Pb/^{235}U$ (g)	± (f)	$^{206}Pb/^{238}U$ (g)	± (f)
z8	**0.569**	**0.8295**	**96.49%**	**8**	**2.48**	**530**	**0.179**	**0.050868**	**1.062**	**0.275696**	**1.149**	**0.039308**	**0.162**	**0.588**	**234.85**	**24.51**	**247.24**	**2.52**	**248.54**	**0.39**
z7	**0.446**	**2.5718**	**99.81%**	**159**	**0.40**	**9894**	**0.141**	**0.051203**	**0.089**	**0.277490**	**0.148**	**0.039306**	**0.070**	**0.914**	**249.96**	**2.05**	**248.66**	**0.33**	**248.53**	**0.17**
LC 10-01																				
z1	0.803	2.8898	99.19%	40	1.94	2301	0.254	0.051095	0.228	0.277617	0.274	0.039407	0.079	0.677	245.11	5.26	248.77	0.60	249.15	0.19
z6	**0.494**	**0.9640**	**99.27%**	**41**	**0.58**	**2544**	**0.157**	**0.051228**	**0.224**	**0.277700**	**0.271**	**0.039316**	**0.073**	**0.714**	**251.12**	**5.16**	**248.83**	**0.60**	**248.59**	**0.18**
z5	**0.516**	**1.1923**	**99.54%**	**66**	**0.45**	**4056**	**0.164**	**0.051256**	**0.172**	**0.277840**	**0.224**	**0.039314**	**0.077**	**0.770**	**252.35**	**3.96**	**248.94**	**0.49**	**248.58**	**0.19**
z3	**0.612**	**2.4860**	**99.73%**	**116**	**0.55**	**6903**	**0.194**	**0.051218**	**0.103**	**0.277589**	**0.158**	**0.039308**	**0.069**	**0.879**	**250.64**	**2.37**	**248.74**	**0.35**	**248.54**	**0.17**
z7	**0.612**	**1.0016**	**99.34%**	**47**	**0.55**	**2814**	**0.194**	**0.051124**	**0.240**	**0.277035**	**0.284**	**0.039302**	**0.077**	**0.670**	**246.42**	**5.52**	**248.30**	**0.63**	**248.50**	**0.19**
z2	**0.606**	**6.0597**	**99.89%**	**284**	**0.55**	**16974**	**0.192**	**0.051174**	**0.072**	**0.277296**	**0.134**	**0.039300**	**0.069**	**0.948**	**248.66**	**1.65**	**248.51**	**0.30**	**248.49**	**0.17**
z4	**0.696**	**1.8940**	**99.72%**	**116**	**0.43**	**6755**	**0.221**	**0.051207**	**0.112**	**0.277458**	**0.171**	**0.039298**	**0.077**	**0.854**	**250.16**	**2.58**	**248.64**	**0.38**	**248.48**	**0.19**
LC 10-03																				
z3	**0.564**	**4.1305**	**99.89%**	**290**	**0.36**	**17500**	**0.179**	**0.051192**	**0.075**	**0.277294**	**0.137**	**0.039286**	**0.071**	**0.933**	**249.50**	**1.74**	**248.51**	**0.30**	**248.40**	**0.17**
z1	**0.428**	**12.8160**	**99.94%**	**500**	**0.63**	**31247**	**0.136**	**0.051171**	**0.064**	**0.277126**	**0.129**	**0.039279**	**0.070**	**0.967**	**248.53**	**1.47**	**248.38**	**0.28**	**248.36**	**0.17**
z5	**0.486**	**6.1021**	**99.94%**	**490**	**0.31**	**30143**	**0.154**	**0.051233**	**0.067**	**0.277408**	**0.131**	**0.039270**	**0.072**	**0.954**	**251.34**	**1.53**	**248.60**	**0.29**	**248.31**	**0.17**
z10	**0.848**	**2.7571**	**99.78%**	**153**	**0.49**	**8596**	**0.269**	**0.051213**	**0.094**	**0.277265**	**0.152**	**0.039266**	**0.070**	**0.902**	**250.44**	**2.16**	**248.49**	**0.33**	**248.28**	**0.17**
z8	**0.451**	**4.3001**	**99.89%**	**278**	**0.38**	**17306**	**0.143**	**0.051185**	**0.076**	**0.277102**	**0.137**	**0.039264**	**0.069**	**0.935**	**249.17**	**1.76**	**248.36**	**0.30**	**248.27**	**0.17**
z7	0.454	5.7779	99.88%	240	0.59	14921	0.144	0.051246	0.076	0.276970	0.138	0.039198	0.071	0.935	251.92	1.75	248.25	0.30	247.86	0.17
z6	0.614	3.8041	99.89%	292	0.33	17383	0.195	0.051183	0.079	0.276582	0.140	0.039192	0.072	0.918	249.10	1.82	247.94	0.31	247.82	0.17
z2	0.509	5.5400	99.95%	573	0.24	35024	0.162	0.051241	0.065	0.276465	0.130	0.039131	0.070	0.966	251.67	1.50	247.85	0.29	247.45	0.17
z9	0.625	3.7483	99.89%	287	0.34	17032	0.198	0.051156	0.075	0.274381	0.137	0.038901	0.069	0.945	247.85	1.74	246.19	0.30	246.02	0.17
z4	0.485	1.0683	99.10%	33	0.80	2059	0.154	0.051159	0.261	0.273748	0.307	0.038808	0.075	0.684	248.02	6.00	245.69	0.67	245.44	0.18

Notes:

(a) z1, z2, etc. are labels for analyses composed of single zircon grains or fragments. Labels in bold denote analyses used in the weighted mean date calculations. Zircon was annealed and chemically abraded (Mattinson, 2005).

(b) Model Th/U ratio calculated from radiogenic $^{208}Pb/^{206}Pb$ ratio and $^{207}Pb/^{235}U$ date.

(c) Pb* and Pbc are radiogenic and common Pb, respectively. mol % $^{206}Pb^*$ is with respect to radiogenic and blank Pb.

(d) Measured ratio corrected for spike and fractionation only. Fractionation correction is 0.18 ± 0.02 (1σ) %/amu (atomic mass unit) for single-collector Daly analyses, based on analysis of NBS-981 and NBS-982.

(e) Corrected for fractionation, spike, common Pb, and initial disequilibrium in $^{230}Th/^{238}U$. Common Pb is assigned to procedural blank with composition of $^{206}Pb/^{204}Pb = 18.60 \pm 0.80\%$; $^{207}Pb/^{204}Pb = 15.69 \pm 0.32\%$; $^{208}Pb/^{204}Pb = 38.51 \pm 0.74\%$ (1-sigma). $^{206}Pb/^{238}U$ and $^{207}Pb/^{206}Pb$ ratios corrected for initial disequilibrium in $^{230}Th/^{238}U$ using Th/U [magma] = 3.
(f) Errors are 2σ, propagated using algorithms of Schmitz and Schoene (2007).
(g) Calculations based on the decay constants of Jaffey et al. (1971). $^{206}Pb/^{238}U$ and $^{207}Pb/^{206}Pb$ dates corrected for initial disequilibrium in $^{230}Th/^{238}U$ using Th/U [magma] = 3.

References Cited

Burchfiel, B.C., and Davis, G.A., 1972, Structural framework and evolution of the southern part of the Cordilleran orogen, western United States: American Journal of Science, v. 272, p. 97-118.

—, 1981, Triassic and Jurassic tectonic evolution of the Klamath Mountains-Sierra Nevada geologic terrane, in Ernst, W.G., ed., The geotectonic development of California; Rubey Volume 1: Englewood Cliffs, New Jersey, p. 50-70.

Burchfiel, B.C., Cowan, D.S., and Davis, G.A., 1992, Tectonic overview of the Cordilleran orogen in the western United States, in Burchfiel, B.C., Lipman, P.W., and Zoback, M.L., eds., The Cordilleran Orogen: Conterminous U.S., Volume G-3: The Geology of North America: Boulder, Colorado, Geological Society of America, p. 407-479.

Burke, D.B., 1973, Reinterpretation of the Tobin thrust – Pre-Tertiary geology of the southern Tobin Range, Pershing County, Nevada: Ph.D. thesis, Stanford University, Stanford, California, 82 p.

Cheong, S., 1999, Structural setting and fluid characteristics of metamorphic gold-quartz veins in northwest Nevada: Ph.D. thesis, University of Nevada-Reno, Reno, Nevada, 332 p.

—, 2002, Fluid inclusion study of metamorphic gold-quartz veins in northwestern Nevada, U.S.A.: Characteristics of tectonically induced fluid: Geosciences Journal, v. 6, no. 2, p. 103-115.

Coats, R.R., and Gordon, M., Jr., 1972, Tectonic Implications of the presence of the Edna Mountain Formation in northern Elko, County: U.S. Geological Survey Professional Paper 800C, p. C85-C94.

Crafford, A.E.J., 2007, Geologic Map of Nevada: U.S. Geological Survey Data Series 249.

Davydov, V.I., Crowley, J.L., Schmitz, M.D., and Poletaev, V.I., 2010, High-precision U-Pb zircon age calibration of the global Carboniferous time scale and Milankovitch band cyclicity in the Donets Basin, eastern Ukraine: Geochemistry Geophysics Geosystems, v. 11, 22 p.

Dickinson, W.R., 1977, Paleozoic plate tectonics and the evolution of the Cordilleran continental margin, in Stewart, J.H., Stevens, C.H., and Fritsche, A.E., eds.,

Paleozoic paleogeography of the western United States: Pacific Coast Paleogeography Symposium 1: Los Angeles, Society of Economic Paleontologists and Mineralogists, Pacific Section, p. 137-155.

—, 2004, Evolution of the North American Cordillera: Annual Review of Earth and Planetary Sciences, v. 32, p. 13-45.

—, 2006, Geotectonic evolution of the Great Basin: Geosphere, v. 2, p. 353–368.

Dunston, J.R., Northrup, C.J., and Snyder, W.S., 2001, Post-Latest Triassic thrust emplacement of the Golconda Allochthon, Sonoma Range, Nevada [abs.]: GSA Annual Meeting.

Elison, M.W., Speed, R.C., and Kistler, R.W., 1990, Geologic and isotopic constraints on the crustal structure of the northern Great Basin: Geological Society of America Bulletin, v. 102, p. 1077-1092.

Erickson, R.L., and Marsh, S.P., 1974, Paleozoic tectonics in the Edna Mountain Quadrangle, Nevada: U.S. Geological Survey Journal of Research, v. 2, p. 331-337.

Ferguson, H.G., Roberts, R.J., and Muller, S.W., 1952, Geology of the Golconda quadrangle, Nevada: U.S. Geological Survey Geologic Quadrangle Map GQ-15.

Jaffey, A.H., Flynn, K.F., Glendenin, L.E., Bentley, W.C., and Essling, A.M., 1971, Precision measurement of half-lives and specific activities of ^{235}U and ^{238}U: Physical Review C, v. 4, p. 1889-1906.

Jenney, C.P., 1935, Geology of the central Humboldt Range, Nevada: University of Nevada Bulletin, v. 29, no. 6, 73 p.

Johnson, M.G., 1977, Geology and Mineral Deposits of Pershing County, Nevada: Nevada Bureau of Mines and Geology Bulletin 89, 115 p.

Ketner, K.B., 1984, Recent studies indicate that major structures in northwestern Nevada and the Golconda thrust in north-central Nevada are of Jurassic or Cretaceous age: Geology, v. 12, p. 483-486.

King, C., 1878, Systematic geology: U.S. Geological Explorations of the 40th Parallel: Government Printing Office, v. 1, 803 p.

Kistler, R.W., and Speed, R.C., 2000, $^{40}Ar/^{39}Ar$, K-Ar, Rb-Sr Whole-Rock and Mineral Ages, Chemical Composition, Strontium, Oxygen and Hydrogen Isotopic Systematics of Jurassic Humboldt Lopolith and Permian(?) and Triassic Koipato Group rocks, Pershing and Churchill Counties, Nevada: U.S. Geological Survey Open-File Report 00-217, 14p.

Knopf, A., 1924, Geology and ore deposits of the Rochester District, Nevada, U.S. Geological Survey Bulletin 762.

Laule, S.W., Snyder, W.S., and Ormiston, A.R., 1981, Willow Canyon Formation, Nevada: An extension of the Golconda Allochthon: Geologic Society of America Abstracts with Programs, v. 13, no. 2, p. 66.

MacMillan, J.R., 1972, Late Paleozoic and Mesozoic Tectonic events in west central Nevada: Ph.D. thesis, Northwestern University, Evanston, Illinois, 146 p.

Mattinson, J.M., 2005, Zircon U-Pb chemical abrasion ("CA-TIMS") method: Combined annealing and multi-step partial dissolution analysis for improved precision and accuracy of zircon ages: Chemical Geology, v. 220, p. 47-66.

McKee, E.H., and Burke, D.B., 1972, Fission-track age bearing on the Permian-Triassic boundary and time of the Sonoma orogeny in north-central Nevada: Geological Society of America Bulletin, v. 83, no. 7, p. 1949-1952.

Mundil, R., Palfy, J., Renne, P., and Brack, P., 2010, The Triassic timescale: new constraints and a review of geochronological data: Geological Society of London Special Publications, v. 334, p. 41-60.

Murchey, B.L., 1990, Age and depositional setting of siliceous sediments in the upper Paleozoic Havallah sequence near Battle Mountain, Nevada; Implications for the paleogeography and structural evolution of the western margin of North America: Geological Society of America Special Paper 255, p. 137-155.

Murchey, B.L., and Jones, D.L., 1992, A mid-Permian chert event: widespread deposition of biogenic siliceous sediments in coastal, island arc and oceanic basins: Paleogeography, Paleoclimatology, Paleoecology, v. 96, no. 1-2, p. 161-174.

Nichols, K.M., and Silberling, N.J., 1977, Stratigraphy and depositional history of the Star Peak Group (Triassic), northwestern Nevada: Geological Society of America Special Paper 178, 142 p.

Northrup, C.J., and Snyder, W.S., 2000, Significance of the Sonoma Orogeny, Western U.S.: What, Where, and When? Geological Society of Nevada Symposium 2000, Program with Abstracts, p. 66-67.

Ransome, F.L., 1909, Notes on some mining districts in Humboldt County, Nevada: U.S. Geological Survey Belletin 414, 75 p.

Roberts, R.J., 1951, Geology of the Antler Peak quadrangle, Nevada: U.S. Geological Survey Geologic Quadrangle Map GQ-10.

—, 1964, Stratigraphy and structure of the Antler Peak quadrangle, Humboldt and Lander Counties, Nevada: U.S. Geological Survey, Professional Paper 459-A, 93 p.

Roberts, R.J., Hotz, P E., Gilluly, J., and Ferguson, H.G., 1958, Paleozoic rocks of north-central Nevada: American Association of Petroleum Geologists Bulletin, v. 42, p. 2813-2857.

Schmitz, M.D., and Schoene, B., 2007, Derivation of isotope ratios, errors and error correlations for U-Pb geochronology using ^{205}Pb-^{235}U-(^{233}U)-spiked isotope dilution thermal ionization mass spectrometric data: Geochemistry, Geophysics, Geosystems (G^3), v. 8, p. Q08006.

Schweickert, R.A., and Snyder, W.S., 1981, Paleozoic plate tectonics of the Sierra Nevada and adjacent regions, in Ernst, W.G., ed., The Geotectonic Development of California, Rubey Volume I: Englewood Cliffs, New Jersey, Prentice-Hall, p. 182-201.

Silberling, N.J., 1973, Geologic events during the Permian-Triassic time along the Pacific margin of the United States, in Logan, A., and Hills, L.V., eds., The Permian and Triassic systems and their mutual boundary: Canada Society of Petroleum Geologists Memoir 2, p. 345-362.

Silberling, N.J. and Roberts, R.J., 1962, Pre-Tertiary stratigraphy and structure of north-western Nevada: Geological Society of America, Special Paper 72, 58 p.

Snyder, W.S., and Brueckner, H.K., 1983, Tectonic evolution of the Golconda allochthon, Nevada: Problems and perspectives, in Stevens, C.H., ed., Pre-Jurassic rocks in western North American suspect terranes: Society of Economic Paleontologists and Mineralogists, Pacific Section, p. 103-123.

—, 1989, Permian-Carboniferous tectonics of the Golconda Allochthon; an accreted terrane in the Western United States: Compte Rendu 4 – XI Congres International de Stratigraphie et de Geologie du Carbonifere, p. 294-312.

Speed, R.C., 1977, Island-arc and other paleogeographic terranes of late Paleozoic age in the western Great Basin, in Stewart, J.H., Stevens, C.H., and Fritsche, A.E., eds., Paleozoic paleogeography of the western United States: Pacific Coast Paleogeography Symposium 1: Los Angeles, Society of Economic Paleontologists and Mineralogists, Pacific Section, p. 349-362.

—, 1979, Collided Paleozoic microplate in the western United States: Journal of Geology, v. 87, p. 279-292.

Speed, R.C., and Sleep, N.H., 1982, Antler orogeny and foreland basin: A model: Geological Society of America Bulletin, v. 93, p. 815-828.

Stewart, J.H., and Carlson, J.E., 1978, Geologic map of Nevada: U.S. Geol. Survey, scale 1:500,000.

Stewart, J.H., MacMillan, J.R., Nichols, K.M., and Stevens, C.H., 1977, Deep-water upper Paleozoic rocks in north-central Nevada – A study of the type area of the Havallah Formation, in Stewart, J.H., Stevens, C.H., and Fritsche, A.E., eds., Paleozoic paleogeography of the western United States: Pacific Coast Paleogeography Symposium 1: Los Angeles, Society of Economic Paleontologists and Mineralogists, Pacific Section, p. 337-347.

Vikre, P.G., 1977, Geology and Silver Mineralization of the Rochester District, Pershing County, Nevada: Ph.D. thesis, Stanford University, Stanford, California, 404 p.

—, 1981, Silver mineralization in the Rochester District, Pershing County, Nevada: Economic Geology, v. 76, p. 580-609.

Vikre, P.G., and McKee, E.H., 1985, Zoning and chronology of hydrothermal events in the Humboldt Range, Pershing County, Nevada: Iscochron/West, v. 44, p. 17-24.

Walker, J.D., and Geissman, J.W., 2009, Geologic Time Scale: GSA Today, v. 19, p. 61.

Wallace, R.E., Tatlock, D.B., and Silberling, N.J., 1960, Intrusive rocks of Permian and Triassic age in the Humboldt Range, Nevada: U.S. Geological Survey Professional Paper 400B, p. B291-B293.

Wallace, R.E., Tatlock, D.B., Silberling, N.J., and Irwin, W.P., 1969a, Geologic map of the Unionville Quadrangle, Pershing County, NV: U.S. Geological Survey Geologic Quadrangle Map GQ-820.

Wallace, R.E., Silberling, N.J., Irwin, W.P., and Tatlock, D.B., 1969b, Geologic map of the Buffalo Mountain Quadrangle, Pershing and Churchill Counties, NV: U.S. Geological Survey Geologic Quadrangle Map GQ-821.

Wardlaw, B.R., Snyder, W.S., Spinosa, C., and Gallegos, D.M., 1995, Permian of the Western United States, in Scholle, P.A., Peryt, T.M., and Ulmer-Scholle, D.S., eds., Permian Stratigraphy of the World, Volume 2: Sedimentary Basins and Economic Resources: Springer-Verlag, New York, p. 23-40.

Wheeler, H.E., 1939, Helicoprion in the Anthracolithic (Late Paleozoic) of Nevada and California, and its stratigraphic significance, Journal of Paleontology, v. 13, n. 1, p. 103–114.

White, J.D.L., and Houghton, B.F., 2006, Primary volcaniclastic rocks: Geology, v. 34, n. 8, p. 677-680.

Whitebread, D.H., 1994, Geologic map of the Dun Glen Quadrangle, Pershing County, Nevada: U.S. Geological Survey, Miscellaneous Investigations Series Map I-2409.

Wilkins, J., 2010, Structural and Stratigraphic Age Constraints of the Inskip Formation, East Range, Nevada: Implications for Mesozoic Tectonics of Western North America: M.S. thesis, Boise State University, Boise, Idaho, 117 p.

Williams, H., 1939, The history and character of volcanic domes: University of California Publications, Bulletin of the Department of Geologic Science, v. 21, p. 51-146.

CHAPTER THREE: ISOTOPIC INVESTIGATION OF THE KOIPATO FORMATION, CENTRAL NEVADA: TECTONIC IMPLICATIONS FOR THE EARLY MESOZOIC WESTERN NORTH AMERICAN CORDILLERA

Abstract

The tectonomagmatic framework of the Early Triassic Koipato Formation of west-central Nevada impacts interpretations of the Permo-Triassic tectonics of the western North American Cordilleran continental margin. New field evidence and Rb-Sr and Sm-Nd isotopic ratios from the Koipato Formation provide insights into the provenance of the volcanic units and their relations to other localities located throughout the northern U.S. Cordillera.

An isotopic investigation of the Koipato Formation demonstrates that intermediate to felsic members exhibit uniformly high $^{87}Sr/^{86}Sr$ (0.7089 – 0.7126) and fairly negative εNd values (-9.73 – -12.89). These compositions require that the volcanics of the Koipato Formation were at least partially sourced from Precambrian continental crust material. Nd (T_{DM}) isotopic evolution modeling for these samples yield mantle extraction model ages of the source continental crustal material between 1.7 and 2.4 Ga, and indicate that the Koipato Formation was erupted through Paleoproterozoic crust. Thus, the Koipato Formation was likely erupted within a newly developed back-arc basin and not as part of an offshore island arc as some authors have postulated (e.g., Speed,

1977; Burchfiel et al., 1992). These data also imply that the underlying Golconda Allochthon was, at the time of Koipato Formation magmatism, already overlying the continental margin, thus precluding the interpretation that the Koipato Formation and the Golconda Allochthon were emplaced piggyback onto the continental margin in post-Koipato time. These data, however, still leave open the possibility that final emplacement of the Golconda Allochthon, with the Koipato Formation on top, did not occur until a later time in the Mesozoic.

Relationships with other Late Permian-Early Triassic units in the western U.S. are less clear. To the east of the Humboldt Range, the Koipato Formation, specifically the Rochester Rhyolite and Limerick Greenstone, is temporally linked to the Inskip Formation in the East Range. To the north, the Quinn River Formation of northwestern Nevada and possibly the Cougar Creek Complex of the Wallowa terrane (east-central Oregon) have been shown to preserve Late Permian to Early Triassic units, with the relationship between the Wallowa terrane and the Koipato Formation poorly defined. The units preserved in the Quinn River Formation are basinal and shelfal sedimentary deposits, which may have been deposited into the same back-arc basin that the Koipato Formation was erupted. To the west and south of the Humboldt Range, the eastern Klamath terrane and Yerington District display a marked unconformity during the time of Koipato Formation volcanism, while poorly constrained plutons from the Mojave Desert area may have been emplaced during the Late Permian-Early Triassic.

Introduction

The Early Triassic Koipato Formation of central Nevada is a sequence of intermediate to felsic volcanic and associated sedimentary units whose origins and importance to the understanding of the Permo-Triassic history of the western North American Cordillera have been enigmatic (Williams, 1939; Ferguson et al., 1952; Silberling and Roberts, 1962; MacMillan, 1972; Burke, 1973; Speed, 1977; Vikre, 1977; Burchfiel et al., 1992; Wilkins, 2010). The general view has been that the Koipato Formation volcanic sequence represented continental arc activity that entirely post-dates the Sonoma Orogeny (Ferguson et al., 1952; Silberling and Roberts, 1962; MacMillan, 1972; Burke, 1973; Silberling, 1973; Vikre, 1977). Vikre (1977) attributes the compositional variations from intermediate to felsic magmatism within the Koipato Formation to the transition from island-arc to continental arc volcanism. If the Koipato Formation represents post-Sonoma volcanism, then the age of the units within the Koipato Formation would act as a minimum age constraint on the timing of the orogeny. However, recent research has presented the idea that the Sonoma Orogeny lasted into the Late Triassic or even Jurassic (Ketner, 1984; Snyder and Brueckner, 1989; Northrup and Snyder, 2000; Dunston et al., 2001). This scenario allows for the possibility that the Koipato Formation was deposited pre- to syn-tectonically on the subduction complex (Golconda Allochthon) of an approaching island arc and that both the allochthon and its piggyback load of the Koipato Formation were emplaced post-Koipato deposition during the final stages of a redefined Sonoma Orogeny (e.g., Dickinson, 1977; Speed, 1977; Snyder and Brueckner, 1983; Burchfiel et al., 1992; Dunston et al., 2001; Wilkins, 2010). This view of the Koipato Formation having been carried piggyback on the Golconda

Allochthon is allowed by the fact that nowhere has it been observed that Koipato Formation units rest on the autochthon and that the Rochester Rhyolite in the East Range is cut by the Golconda thrust (Dickinson, 1977; Burchfiel et al., 1992; Wilkins, 2010). Understanding the origins of Koipato Formation volcanism will improve our understanding of the Early Mesozoic tectonic framework of the western North American Cordillera.

Along with understanding the origin of the Koipato Formation, it is necessary to determine the magmatic provenance of the formation, which can be accomplished through an isotopic analysis of its volcanic and intrusive units. By understanding these features, it can be determined how the Koipato Formation correlates to other volcanic sequences and terranes to the north and south along the western Cordillera margin. Kistler and Speed (2000) performed both major oxide analyses and Rb-Sr and Sm-Nd isotopic investigations on whole rock powders, and showed that the samples of the Koipato Formation were homogenized by pervasive alteration caused by a hydrothermal system related to the emplacement of the Humboldt Lopolith around 169 Ma (Kistler and Speed, 2000). Performing analyses on large populations of fairly resilient grains will hopefully mitigate the effects encountered by Kistler and Speed (2000) when performing an isotopic investigation of the Koipato Formation. Constraining the provenance of the Koipato Formation will increase our knowledge both of the Early Mesozoic tectonic picture of the Cordillera and where the Koipato Formation fits within that picture. Also, understanding these relationships will allow for a better comprehension of the Sonoma Orogeny and its role in the development of the western North American margin.

In this chapter, strontium and neodymium isotopic ratios of volcanic and intrusive rocks within the Koipato Formation are employed to determine both the source of the magmas and the tectonic setting (oceanic vs. continental) of their origin. Data collected through field observations, map relationships, and isotopic geochemistry are used to redefine our understanding of the Koipato Formation. Isotopic geochemistry provides evidence that the Early Triassic Koipato Formation was erupted through continental lithosphere. Also, the data are employed to correlate the Koipato Formation with other volcanic sequences along the Cordilleran margin to produce a more detailed picture of the Early Mesozoic continental margin.

Geologic Setting

The Koipato Formation is exposed throughout central Nevada from the Humboldt Range eastward to at least the Tobin Range (Fig. 3.1). The subunits of the Koipato Formation, the Limerick Greenstone, Rochester Rhyolite, and Weaver Rhyolite, outcrop to varying degrees from range to range, with the Rochester Rhyolite the most extensively exposed unit outside of the Humboldt Range.

The Koipato Formation is composed of intermediate to felsic volcanic and volcaniclastic units, with minor amounts of metasedimentary strata. The composition of the Koipato Formation subunits become more silicic upwards through the stratigraphic section, with andesite the primary volcanic component of the Limerick Greenstone and rhyolite constituting the majority of the Rochester and Weaver Rhyolites. Alteration of the Koipato Formation units vary, but all units have experienced some degree of mineral alteration and greenschist facies metamorphism in part, if not mostly due to widespread

hydrothermal activity (e.g., Vikre, 1977). The thickness of the Koipato Formation is difficult to quantify due to later faulting, but the maximum estimated thickness of approximately 5000 m has been suggested in the Humboldt Range (Knopf, 1924; Wheeler, 1939). Outside of the Humboldt Range, work has shown that the Koipato Formation thins to <500 m thick in the Tobin and Sonoma Ranges, with it pinching out further east (Ferguson et al., 1952; Roberts et al., 1958).

Based on research presented in Chapter 2 (Fig. 2.9), the Koipato Formation is separated into the Limerick Greenstone and two silicic volcanic packages: an older Rochester and lower Weaver Rhyolite section (present in Troy Canyon, Humboldt Range and in the East Range and Tobin Range) and a younger Rochester and lower Weaver Rhyolite section in Limerick Canyon along with the middle and upper Weaver Rhyolites in Troy Canyon of the Humboldt Range (Fig. 3.1 and 3.2). The lowermost unit of the Koipato Formation, the Limerick Greenstone, is primarily exposed in Limerick and American Canyons of the southern Humboldt Range (Fig. 3.2) and the Tobin Range (Burke, 1973). A recent discovery by Wilkins (2010) has indicated the Limerick Greenstone (formerly the upper Inskip Formation) is also exposed near Willow Creek Canyon in the East Range (Fig. 3.1). The Limerick Greenstone is mainly composed of intermediate flows, greenstones, hypabyssal intrusive complexes, and schistose metasediments (Vikre, 1977; See “Geology” in Chapter Two). Extensive contact and hydrothermal alteration has completely altered the original mineral assemblages of most of the units (Burke, 1973; Vikre, 1977). The Limerick Greenstone was most likely deposited in the distal portions of a volcanic arc that was either already sutured to the

continent or some distance offshore (Burke, 1973; Vikre, 1977). The contact between the Limerick Greenstone and the overlying Rochester Rhyolite has been interpreted to be conformable and gradational, where no faulting has occurred (Wallace et al., 1969a; Vikre, 1977), but recent research has documented that an unconformity separates the Limerick Greenstone and Rochester Rhyolite in the East and Humboldt Ranges (Wilkins, 2010; See "Geologic Background" in Chapter Two).

Overlying the Limerick Greenstone is the Rochester Rhyolite, which is widely exposed in central Nevada. The most abundant exposures are located in the southern Humboldt Range, but outcrops in the East and Tobin Ranges provide valuable information for understanding the Koipato Formation (Fig. 3.2). The two identified sections of the Rochester Rhyolite are primarily composed of banded rhyolite flows and rhyolite tuffs with minor amounts of tuff breccias and sedimentary deposits (Vikre, 1977; See "Geology" in Chapter Two). Alteration is present within both sections of the Rochester Rhyolite, but the degree of alteration is considerably less than that observed within the Limerick Greenstone (Burke, 1973; Vikre, 1977; See "Geology" in Chapter Two). Deposition of the Rochester Rhyolite is interpreted to have occurred in proximity to the same arc as the Limerick Greenstone, which had begun to erupt more compositionally mature volcanic products (Burke, 1973; Vikre, 1977). The Weaver Rhyolite will not be discussed in detail in this section.

Researchers have interpreted that the intrusive units present throughout the southern Humboldt Range are related to the same episode of magmatism as the older section of silicic volcanics within the Koipato Formation (Fig. 3.2) (Wallace et al.,

1969a; Silberling, 1973; Vikre, 1977; See “Discussion” in Chapter Two). The leucogranite is composed primarily of coarse feldspar and quartz grains, whereas the rhyolite porphyry dikes closely mirror the composition of the older section of the Rochester and Weaver Rhyolite flow units (Vikre, 1977; See “Geology” in Chapter Two). Burke (1973) and Vikre (1977) noted that it is difficult to differentiate the intrusive units in the field, which they attribute to a shared magmatic history. Vikre (1977) also concluded that these intrusive units were the cause of some of the pervasive alteration seen within the Limerick Greenstone and to a lesser degree in the older Rochester Rhyolite.

Geology

Fieldwork conducted during the summer and fall of 2009-2010 resulted in modifications to the original Wallace et al. (1969a, b) maps for the southern Humboldt Range (Fig. 3.2). The locations of samples collected during fieldwork and discussed in this section can be found on this map, Figure 3.3 and in Table 3.1. Rocks that are interpreted to be lava flows will be described as such, whereas rocks that are pyroclastic in origin will be described using pyroclastic rock terminology, such as tuff, ash-flow tuff, and tuff breccia after White and Houghton (2006). Sedimentary and metasedimentary units are described using sedimentary terminology, such as sandstone, shale, siltstone, etc. Sedimentary units composed of a large percentage of volcanic clasts will be described using terms such as volcanic sandstone and volcanic conglomerate. The term volcaniclastic will be used to describe volcanic rocks that have an unclear pyroclastic or epiclastic origin.

American Canyon

Observations made during fieldwork in American Canyon of the Humboldt Range focused on a section of the Limerick Greenstone and a rhyolite porphyry dike that cuts though the greenstone. The Limerick Greenstone forms a massive igneous complex that occupies the area from the base of American Canyon to the top of the first ridgeline to the south of the Canyon, with less extensive exposures on the north side of American Canyon (Fig. 3.2). Cutting through the Limerick Greenstone, in American Canyon, are several rhyolite porphyry dikes that stand out from the dark colored Limerick Greenstone. These dikes appear to be related to the leucogranite and dikes observed in Limerick Canyon (Fig. 3.2).

The Limerick Greenstone exposed in American Canyon is composed of porphyritic igneous units that have an intermediate composition and appear to represent a hypabyssal intrusive complex. Evidence for an intermediate composition includes the prevalence of hydrous ferromagnesian minerals and feldspar with little to no quartz. Feldspar and hornblende phenocrysts range from <1 mm to 6-7 mm in size. Outcrops in the field are massive and exhibit no bedding planes, but a pervasive foliation is present. All outcrops exhibit metamorphism to greenschist facies. The Limerick Greenstone clearly underlies what is mapped as the Rochester Rhyolite, but its relation to the Limerick Greenstone from Limerick Canyon is harder to define due to the lack of a stratigraphic continuity.

Two samples were collected from the Limerick Greenstone in American Canyon and analyzed for this study. The first sample (AC 09-13) is from a massive outcrop of the

Limerick Greenstone intrusion exposed on the north side of American Canyon (Fig. 3.2). It is interpreted to come from an intermediate hypabyssal intrusion that contains plagioclase, potassium feldspar, and biotite phenocrysts in a fine-grained matrix. Phenocrysts in the sample range in size from 0.5 to 3 mm, with the plagioclase grains representing the largest fraction. A small amount of sericite alteration of feldspar is evident along with minor amounts of calcite, quartz, and chlorite replacement.

The second sample (AC 09-22) was obtained from a massive exposure of the Limerick Greenstone intrusion along the south side of American Canyon (Fig. 3.2). The composition and texture of sample AC 09-22 is very similar to that described for AC 09-13, but this sample lacks any observable potassium feldspar and alteration of this unit is much more pervasive. Plagioclase grains have been completely altered to sericite and the sample exhibits extensive chlorite and calcite replacement.

Cutting through the Limerick Greenstone in American Canyon are several rhyolite porphyry dikes that stand out from the dark colored Limerick Greenstone. Based upon their similar composition and texture, it is interpreted that these dikes are related to the leucogranite intrusive observed in Limerick Canyon (09NV41) and that they probably acted as feeders off the large plutonic body. This interpretation is based on their similar composition and texture and the similarity in high precision U-Pb zircon ages of the two intrusive types (See “Geology” and “Geochronology” in Chapter Two). Sample AC 09-09 was obtained from one of these dikes close to the top of the first ridgeline to the south of American Canyon (Fig. 3.2). It is composed of plagioclase, potassium feldspar, and quartz phenocrysts ranging in size from ~0.5 to 6 mm in a microcrystalline groundmass.

Feldspar grains exhibit a minor amount of sericite alteration, but the sample is generally unmetamorphosed.

Hoffman Canyon, Tobin Range

No fieldwork was conducted in the Tobin Range during this study, but sample 00NV-17 was procured from a previous expedition and analyzed for this report (C.J. Northrup, personal communication). This sample originates from an outcrop of the Koipato Formation approximately 1 m above the unconformity with the underlying Havallah Formation of the Golconda Allochthon in Hoffman Canyon, which is the type location for the Sonoma Orogeny (Fig. 3.1 and 3.3) (Silberling and Roberts, 1962). The sample is classified as a rhyolite tuff breccia that is not welded and contains grains that range in size from 1 to 10 mm in an ashy matrix (C.J. Northrup, per. comm.). The presence of slightly rounded, non-volcanic lithic clasts does suggest that the sample was reworked prior to final deposition, but the degree of reworking is inferred not to have affected the overall sample composition and analysis (C.J. Northrup, per. comm.). Based on the unit description, mineral composition, and age, this sample would most likely have been procured from an exposure of the older Rochester Rhyolite (See “Geology” and “Geochronology” in Chapter Two).

Isotopic Geochemistry

Apatite and sphene populations numbering in the hundreds of grains were handpicked from samples for Rb-Sr and Sm-Nd isotopic analysis. Apatite and sphene were chosen so as to avoid the effects of greenschist facies alteration of the Koipato

Formation, which could modify their whole rock isotopic systematics. These accessory minerals are robust to metamorphic alteration or recrystallization, and contain both high concentrations of Sr and Nd. Apatite and sphene also have low Rb/Sr, thus minimizing the effects of age correction for estimating the initial Sr isotope composition of these Triassic rocks. The Nd and Sr isotopic data are reported in Table 3.1 and depicted graphically in Figures 3.4 and 3.5.

For this study, two samples from the Limerick Greenstone, one from the Rochester Rhyolite, and one from a rhyolite porphyry dike were analyzed for their $^{87}Rb/^{86}Sr$ – $^{87}Sr/^{86}Sr$ and $^{147}Sm/^{144}Nd$ – $^{143}Nd/^{144}Nd$ isotopic compositions. Limerick Greenstone samples AC 09-13 and AC 09-22, from the Humboldt Range, yielded initial $^{87}Sr/^{86}Sr$ values of 0.7120 and 0.7118 and initial εNd values of -9.73 and -10.34 (Table 3.1). Such values are characteristic of volcanics with a significantly old continental crust influence (Fig. 3.4) (DePaolo and Wasserburg, 1977; Farmer, 1988; Fleck, 1990).

Sample 00NV-17 of the Rochester Rhyolite exposed in Hoffman Canyon, Tobin Range has an initial $^{87}Sr/^{86}Sr$ of 0.7126 and an initial εNd of -12.89 (Table 3.1). These values are very close to those of the Limerick Greenstone in the Humboldt Range, which indicates that both the intermediate and felsic sections of the Koipato Formation were derived with contributions from the same age continental crust (Fig. 3.4).

The sample of the rhyolite porphyry dike from American Canyon was also analyzed for its Rb-Sr and Sm-Nd isotopic content. Sample AC 09-09 was analyzed using sphene grains and provides an initial $^{87}Sr/^{86}Sr$ of 0.7089 and an initial εNd of 3.43 (Table 3.1). The less radiogenic Sr and more radiogenic Nd isotope compositions for this unit

indicate a greater influence of mantle-derived magma in the production of the intrusive unit, although some continental influence is inferred due to the relatively high $^{87}Sr/^{86}Sr$ ratio (Fig. 3.4) (DePaolo and Wasserburg, 1977; Farmer and DePaolo, 1983; Farmer, 1988; Fleck, 1990).

Discussion

Rb-Sr and Sm-Nd Interpretations

Rb-Sr and Sm-Nd isotopic analyses of samples from the Koipato Formation reveal that the intermediate and felsic volcanic rocks are primarily derived through crustal and lithospheric mantle assimilation (DePaolo and Wasserburg, 1977; Farmer, 1988; Fleck, 1990). This conclusion is drawn from the relatively high $^{87}Sr/^{86}Sr$ and negative εNd values observed in most of the samples analyzed from the Koipato Formation (Table 3.1 and Fig. 3.4). Rb-Sr isotopic work conducted by Kistler and Speed (2000) on the Koipato Formation also yielded $^{87}Sr/^{86}Sr$ values around 0.714, consistent with the results obtained from this study.

Nd isotopic evolution for the samples was modeled using Sm/Nd crustal values obtained from the Geochemical Earth Reference Model database (Farmer and DePaolo, 1984; Bennett and DePaolo, 1987; Farmer, 1988; Rudnick and Fountain, 1995). The crustal Sm/Nd values used for this modeling were the averages for the upper and bulk continental crust (Rudnick and Fountain, 1995). Under the assumption that the most unradiogenic Koipato Formation volcanics represent pure crustal melts, modeling indicates that the crustal source separated from the depleted mantle around 1.7 to 2.4 Ga,

with the upper crustal model line yielding a robust minimum model age of 1.7 Ga (Fig. 3.5). This is a minimum age if the Koipato Formation volcanics have a mantle-derived component, as suggested by sample AC 09-09. This is an important finding because it indicates that the Koipato Formation volcanics are derived from crust of Paleoproterozoic age or older, consistent with melting of and eruption through the Precambrian rifted margin of western North America, rather than in an intraoceanic or proximal fringing arc setting. The derived model ages of the crustal source of the Koipato Formation volcanics are consistent with previous isotopic studies, which have found crust as old as 2 Ga beneath the Great Basin area of central Nevada (Bennett and DePaolo, 1987; Farmer, 1988; Farmer et al., 1989).

Based on this isotopic investigation, it can be deduced that the Golconda Allochthon was at least partially attached to the continental margin by the latest Permian to Early Triassic, which would allow the Koipato Formation to be deposited on top of the allochthonous package and exhibit the highly continental isotopic values discussed above. The findings discussed here do not confirm the idea that final movement of the Golconda Allochthon occurred pre-Koipato Formation, but leave open the possibility that movement continued after Koipato Formation deposition, sometime later in the Mesozoic, as supported by some authors (Ketner, 1984; Snyder and Brueckner, 1989; Northrup and Snyder, 2000; Dunston et al., 2001). More research is required to confirm these findings and definitively determine the age of final emplacement of the Golconda Allochthon and possibly the Koipato Formation.

Rb-Sr and Sm-Nd analysis of volcanic and intrusive samples from the Koipato Formation allows for the comparison of results and interpretations of the isotopic signatures of Mesozoic-Tertiary granites and volcanics and the inferred crustal structure of the Great Basin (DePaolo, 1981; Farmer and DePaolo, 1983, 1984; Samson et al., 1989; DePaolo and Daley, 2000). Figure 3.4 depicts a compilation of Mesozoic and Tertiary isotopic data for volcanic and granitic samples from the Great Basin area along with the four reported Koipato Formation samples from this study. Overall, the analyzed Triassic samples from the Koipato Formation yielded results with higher $^{87}Sr/^{86}Sr$ ratios and lower εNd values than earlier reported Triassic samples from the Great Basin area (Fig. 3.4). This may be due to older crustal material residing underneath the area of the Koipato Formation during its deposition or the fact that the few similar igneous Triassic rocks in Nevada, other than the Koipato Formation, have yet to be isotopically analyzed and reported. In support of the first hypothesis, Farmer and DePaolo (1983) and Farmer (1988) interpret that a tectonically thinned section of the Precambrian crust existed under the Great Basin area in the Triassic. If this was a localized feature, it could explain the anomalously evolved isotopic signature of the Triassic Koipato volcanics reported in this study compared to other Triassic samples from elsewhere in the Great Basin. The Jurassic granitic and volcanic samples show a more evolved signature than the Triassic samples and are more in line with the reported values from the Koipato Formation, whereas the Cretaceous and Tertiary volcanics and granites have a very similar isotopic signature to the Koipato Formation samples and a few of these samples have experienced a greater proportion of crustal contamination (Fig. 3.4). The patterns observed within the isotopic signatures of samples from the various time periods can be explained by differences in

crustal age, thickness, and the flux of mantle magma entering the crust (DePaolo and Farmer, 1984). The progressively younger reported samples likely experienced less mantle flux and travelled through thicker and older continental crust, which explains the increasing continental signature of these samples.

Tectonic Setting of Koipato Formation Deposition

Previous research interpreted the Koipato Formation to have been erupted as either a continental arc (e.g., Silberling and Roberts, 1962; Burke, 1973; Vikre, 1977; Speed and Sleep, 1982; Burchfiel et al., 1992; Dickinson, 2004, 2006), island arc (e.g., Dickinson, 1977; Speed, 1977; Burchfiel et al., 1992; Dunston et al., 2001; Wilkins, 2010), or, equivocally, either. These interpretations were based mainly on the lithology of the volcanic and sedimentary units that compose the Koipato Formation, with the interpretations also taking into consideration the sparse geochemical and unreliable geochronological data. The newly reported geochronology and isotopic data presented in this report allow for the interpretation that the volcanic and intrusive rocks of Koipato Formation record a period of continental back-arc magmatism and extension during the Early Triassic.

Burke and Silberling (1973) were the first to recognize the possibility of an Early Mesozoic back-arc basin to account for the Koipato Formation deposition, with the interpretation that the sedimentary Middle to Late Triassic Auld Lang Syne Group was deposited within the continuation of this back-arc basin. Rogers et al. (1974) further noticed that a Late Paleozoic island arc was separated from the continental margin by an oceanic back-arc basin. Speed (1979) expanded on these works and noted that following

the Sonoma Orogeny the allochthonous units began to cool and contract due to the loss of subduction-related heating after the subduction zone jumped outboard of the new continental margin, with the Koipato Formation having been deposited in a block-faulted terrane. The block-faulting may have produced the previously noted angular unconformity between the Limerick Greenstone and Rochester Rhyolite (See "Geologic Background" and "Discussion" in Chapter Two). This block-faulted terrane could have formed in a post-collisional extensional setting within the back-arc basin that produced the Koipato Formation rhyolites and a large basin, which limited the influx of volcanic arc sediment into the overlying marine strata (Speed, 1979). Ketner and Ross (1983) and Ketner (1984) supported the idea of a basin existing in Nevada during the Early Triassic by interpreting that slope and basin carbonate turbidites in the Adobe Range of northeastern Nevada were deposited either in a deep basin or trough that existed at the time of or immediately following the Sonoma Orogeny. Elison and Speed (1988, 1989) considered the Koipato Formation to possibly represent the initial vestiges of this Late Triassic-Jurassic back-arc basin in central Nevada, which consisted of a shelf, slope, and basin that was bounded to the west by a volcanic arc (the Klamath arc). The interpretations of these previous researchers are supported by the geochronology and isotopic data presented in this report, which documents a punctuated period of intermediate to felsic volcanism.

Correlating the Koipato Formation with Related Units along the Western US Cordillera

The importance of the Koipato Formation in the Early Triassic tectonic picture of western North America has been debated since its volcanic sequences were first observed

and described. The new data presented in this study has allowed for the interpretation that the volcanic and sedimentary units of the Koipato Formation represent a period of back-arc extensional magmatism and sedimentation during the Early Triassic following at least initial emplacement of the Golconda Allochthon. A better understanding of the Koipato Formation's importance to Early Triassic tectonics can be garnered by comparing its volcanic and sedimentary units to corresponding localities located along the western U.S. Cordillera (Fig. 3.6).

The closest temporal association to the Koipato Formation is the upper member of the Inskip Formation of the East Range, which Wilkins (2010) has determined to be a correlative to the Limerick Greenstone. The Inskip Formation is characterized by greenstone, phyllite, and quartzite with volcanic and sedimentary units more abundant in the lower sections (Wilkins, 2010). The lithologic similarities are not extensive, but Wilkins (2010) does provide ages for a few samples that overlap with the ages determined for the Koipato Formation in this study. A 249.27 ± 0.27 Ma deformed quartz diorite sill, from the lower Inskip Formation, overlaps with the intrusive units observed in the Humboldt Range, which indicates that silicic intrusive activity and possibly volcanism was occurring coevally (Wilkins, 2010; See "Geochronology" and "Discussion" in Chapter Two). For the upper Inskip Formation, a 249.14 ± 0.13 Ma tuffaceous phyllite indicates that deposition of this unit and the older sequence of silicic volcanism within the Koipato Formation were occurring coevally (Wilkins, 2010; See "Geochronology" and "Discussion" in Chapter Two). Wilkins (2010) has correlated the Inskip Formation to the Limerick Greenstone, but, after reviewing the reported ages, it

appears that his units are also temporally linked to the older sequence of the Rochester Rhyolite (See “Geochronology” and “Discussion” in Chapter Two). Sample RHC 10-03, of the older Rochester Rhyolite exposed in the East Range, has yielded an age of 249.18 Ma, which overlaps with the age reported for the upper Inskip Formation (See “Geochronology” in Chapter Two). These results allow for the correlation of the Inskip Formation to the older sequence of the Rochester Rhyolite and the Limerick Greenstone.

Farther afield from the Humboldt Range, the Yerington District of west-central Nevada is composed of metamorphosed Triassic and Jurassic volcanic and sedimentary rocks that may be a southern extension of the units observed in the Humboldt Range (Fig. 3.6D) (Proffett and Dilles, 2008). The lowermost unit exposed in the Yerington District is the pre-Late Triassic McConnell Canyon volcanics, which is composed of an andesitic lower member and a rhyolitic upper member (Proffett and Dilles, 2008). The minimum age of deposition of this unit is constrained by early Late Triassic (Late Carnian) ammonites in the overlying carbonate units and a 232.2 ± 2.3 Ma quartz porphyry intrusion (Proffett and Dilles, 2008). No ages have so far been reported either within or below the McConnell Canyon volcanics, which prevent determining the duration of volcanism. The lithology of this unit closely mirrors that of the Koipato Formation exposed in the Humboldt Range, but the lack of reliable internal age constraints on the timing and duration of volcanism of the McConnell Canyon volcanics preclude the definitive determination that volcanism in the Yerington District was coeval with Koipato Formation volcanism (Fig. 3.6). However, following the deposition of the McConnell Canyon volcanics, the Yerington District converted to mainly clastic and carbonate

deposition from the Late Triassic and into the Jurassic, which closely mirrors the depositional pattern observed within the Humboldt Range following the volcanism of the Koipato Formation (Fig. 3.6) (Proffett and Dilles, 2008). This may indicate that the back-arc basin that developed in the area of the Koipato Formation in the Early Triassic, discussed earlier in this report, was not a localized feature and extended to the south, with the Late Triassic to Jurassic shelf and basinal sedimentary units of the Yerington District acting as evidence of this (Fig. 3.6) (Proffett and Dilles, 2008).

To the north of the Humboldt Range are exposures near Quinn River, Nevada of two Paleozoic to Mesozoic terranes, which Crafford (2007) interpreted as equivalent to the Koipato Formation. The lowermost of these terranes, the Jackson terrane, is composed primarily of chert and sandstone below a Jurassic ash-flow tuff (Jones et al., 1988; Jones, 1990). The age of the sedimentary section of the Jackson terrane is hard to constrain, but must be younger than Devonian based on occurrence of Late Devonian chert pebbles and older than the Jurassic ash-flow tuff (Jones, 1990). A more concise age constraint is impossible due to the lack of identifiable fossil species within the Jackson terrane. The lack of reliable ages and absence of Early Triassic volcanics or volcaniclastic sediment in this predominately sedimentary terrane precludes the comparison of units within the Jackson terrane with the Koipato Formation.

Overlapping the Jackson terrane, along a thrust contact, is the Black Rock terrane, which is composed of the Permian Bilk Creek limestone, a sequence of volcaniclastic rocks, and the Late Permian to Middle Triassic Quinn River Formation (Jones, 1990). The Permian Bilk Creek limestone and Permian volcaniclastic rocks were most likely

deposited prior to Koipato Formation volcanism (Ketner and Wardlaw, 1981; Jones, 1990). It is possible that these two units extend into the Late Permian or even the Early Triassic due to the lack of reliable age constraints on their upper sections, but based on current information these formations cannot be adequately compared to the Koipato Formation. The uppermost formation of the Black Rock terrane, the Quinn River Formation, is composed of sedimentary and volcaniclastic units, with volcanogenic influence increasing towards the upper sections of the formation (Jones, 1990). Ketner and Wardlaw (1981), Silberling and Jones (1982), and Jones (1990) constrain the age of this formation using ammonites, which date from the Middle Permian (Wordian) to Middle Triassic (Anisian). More recent research conducted by Sperling and Ingle (2006) concluded that the Quinn River Formation actually represents a continuous stratigraphic section across the Permian-Triassic boundary, with this section representing the first deep-water Permian-Triassic boundary section along the western U.S. Cordillera. From this section, an ash-flow deposit has been dated to ~253 Ma (J.L. Crowley, personal communication), which coincides with the oldest age determined for the Koipato Formation from an inherited zircon population reported earlier in this study (09NV41; See “Geochronology” in Chapter Two). Based on the composition of this formation, the lack of volcanic units, and its age, the Quinn River Formation was deposited in a deeper water environment at the time of Koipato Formation volcanism, with little influence from the Koipato Formation volcanism. This deeper water environment may have been a northern extension of the back-arc basin where the Koipato Formation was erupted.

Three more distant stratigraphic sections may include Koipato age equivalent units; these are: the Wallowa terrane, eastern Klamath terrane, and Mojave Desert (Fig. 3.6). The Wallowa terrane is located in northeastern Oregon and is part of the Paleozoic-Mesozoic Blue Mountains Province. The Wallowa terrane is composed of Permian to Triassic plutonic, volcanic, and volcaniclastic rocks, which are thought to have formed close to a volcanic arc and within an adjoining sedimentary basin (Fig. 3.6B) (Dorsey and LaMaskin, 2007). The commonly accepted notion of volcanism within the Wallowa terrane is that there is a marked period of quiescence that lasts from the early Middle Permian to the Middle Triassic (Fig. 3.6B) (Dorsey and LaMaskin, 2007). However, recent research within the Cougar Creek Complex of the Wallowa Arc terrane has shed new light on this period of supposed quiescence. The Cougar Creek Complex is a Late Permian to Triassic intrusive suite, which evolved from felsic to mafic over its lifetime (Kurz, 2010). Within the Cougar Creek Complex, the Triangle Mountain pluton has yielded a 254.21 ± 0.14 Ma age, which overlaps with the 254.08 ± 0.18 Ma inherited zircons from the leucogranite (09NV41) related to the Koipato Formation (Kurz, 2010; See “Geochronology” in Chapter Two). If the ~254 Ma age of inherited zircons from the leucogranite, of the southern Humboldt Range, is taken as representing the initial stages of Koipato volcanism, then the Triangle Mountain pluton of the Cougar Creek Complex can be inferred as a coeval unit to these earliest volcanics. Further evidence for a temporal correlation is provided by the upper sections of the Trudy Mountain Gneissose Unit of the Cougar Creek Complex, which yields a crystallization age of 248.75 ± 0.08 Ma (Kurz, 2010). This crystallization age is coeval with the age determined for the upper Weaver Rhyolite (TC 10-01), within the younger volcanic succession of the Koipato

Formation, which yielded an age of 248.62 ± 0.08 Ma (See “Geochronology” in Chapter Two). This sample of the Trudy Mountain Gneissose Unit also yielded inherited zircons, which returned an age of 249.14 ± 0.07 Ma (Kurz, 2010). These inherited zircons overlap with Koipato Formation samples from the older Rochester Rhyolite in both the East Range (RHC 10-03) and Hoffman Canyon (00NV-17), which yielded ages of 249.18 ± 0.07 Ma and 249.14 ± 0.14 Ma, respectively (See “Geochronology” in Chapter Two). More research needs to be conducted in order to determine whether there are more Late Permian to Early Triassic units within the Wallowa terrane, but based on the recent research of Kurz (2010), it does appear that there are coeval volcanic assemblages with the Koipato Formation within the Wallowa terrane.

The eastern Klamath terrane is located in northern California and is composed of Devonian to Middle Jurassic volcanic, volcaniclastic, and basinal units (Fig. 3.6A) (Miller and Harwood, 1990). Figure 3.6A shows that the commonly accepted notion for the eastern Klamath terrane is that an unconformity exists from the Middle Permian to Middle Triassic. However, the age of the Triassic Pit Formation is poorly constrained due to the fact that the unit is sparsely fossiliferous; nevertheless, it is interpreted that Upper Permian to Lower Triassic rocks are missing within the eastern Klamath terrane (Miller and Harwood, 1990). Miller (1988) and Miller and Harwood (1990) interpreted this hiatus to represent a structural break during deposition of the eastern Klamath terrane. During this hiatus within the eastern Klamath terrane, the Koipato Formation was erupted to the east and records the time frame that is missing within the eastern Klamath terrane (Fig. 3.6). During the Middle to Late Triassic, the eastern Klamath terrane is dominated

by volcanic and volcaniclastic units, which indicate that a volcanic arc had formed in the area by this time (Fig. 3.6A) (Miller and Harwood, 1990). This is markedly different from the sedimentation occurring within the basin to the east, where the carbonate Star Peak Group was deposited (Fig. 3.6). During the Middle to Late Triassic, the eastern Klamath terrane likely acted as a bounding volcanic arc to the west of the back-arc basin within which the Koipato Formation was deposited.

The Mojave Desert is located in southeastern California and is composed of Paleozoic platformal and eugeoclinal units along with Mesozoic volcanic and continental sedimentary units (Saleeby and Busby-Spera, 1992; Miller et al., 1995). The Mojave Desert marks the southern terminus of Sonoma Orogeny tectonism and therefore the Triassic igneous rocks there may be an extension of the magmatic activity that produced the Koipato Formation volcanism (Miller and Cameron, 1982; Saleeby and Busby-Spera, 1992). However, there is no definitive evidence that Late Permian-Early Triassic units are preserved in the Mojave Desert area (Fig. 3.6). Miller et al. (1995) dated plutons in the El Paso Mountains and northern Mojave Desert area, which returned ages between 260 to 240 Ma (Fig. 3.6C). These ages have a large amount of uncertainty (some cases exceed 5 Ma) and scatter within the zircon population of most dated samples, which inhibit a definitive age determination of these plutons (Miller et al., 1995). Further research is required to more definitively determine the age of the Mojave plutons, resolve whether Late Permian-Early Triassic units are exposed in this locality, and to establish the relationship to the Koipato Formation.

Conclusions

The Koipato Formation is important because it apparently preserves Late Permian to Early Triassic volcanic and intrusive units not yet identified elsewhere in the western U.S. Sr and Nd isotopic analyses indicate that the volcanics of the Koipato Formation were sourced from continentally derived material due to the relatively high $^{87}Sr/^{86}Sr$ and fairly negative εNd values. Along with these results, modeling of the progressive Nd isotopic evolution for the samples revealed that the Koipato Formation was likely sourced from approximately 2 Ga old continental crust. Thus, the Koipato Formation was likely erupted within a newly developed back-arc basin and not as part of an offshore island arc as some authors have postulated (e.g., Speed, 1977; Burchfiel et al., 1992). These conclusions, combined with field evidence, indicate that the Golconda Allochthon was likely attached to the continental margin by the Early Triassic. However, this does not signify that the Golconda Allochthon was fully emplaced onto the continental margin, as final movement may have occurred at a later time in the Mesozoic.

The relationship of the Koipato to other Mesozoic igneous provinces in the western U.S. is less clear. To the east of the Humboldt Range, the Koipato Formation, specifically the Rochester Rhyolite and Limerick Greenstone, is temporally linked to the Inskip Formation identified in the East Range and they are most likely part of the same magmatic-sedimentary complex. To the north, the Quinn River Formation and possibly the Cougar Creek Complex of the Wallowa terrane have been shown to preserve Late Permian to Early Triassic units. The units preserved in the Quinn River Formation are basinal and shelfal sedimentary deposits, which may have been deposited into the same

back-arc basin that the Koipato Formation was erupted within. However, the relationship between the Wallowa terrane and the Koipato Formation is still poorly defined. To the west and south of the Humboldt Range, the eastern Klamath terrane and Yerington District display a marked unconformity during the time of Koipato Formation volcanism, while poorly constrained plutons from the Mojave Desert area may have been emplaced sometime in the Late Permian-Early Triassic. More research is required to determine the full extent of this Early Mesozoic back-arc basin.

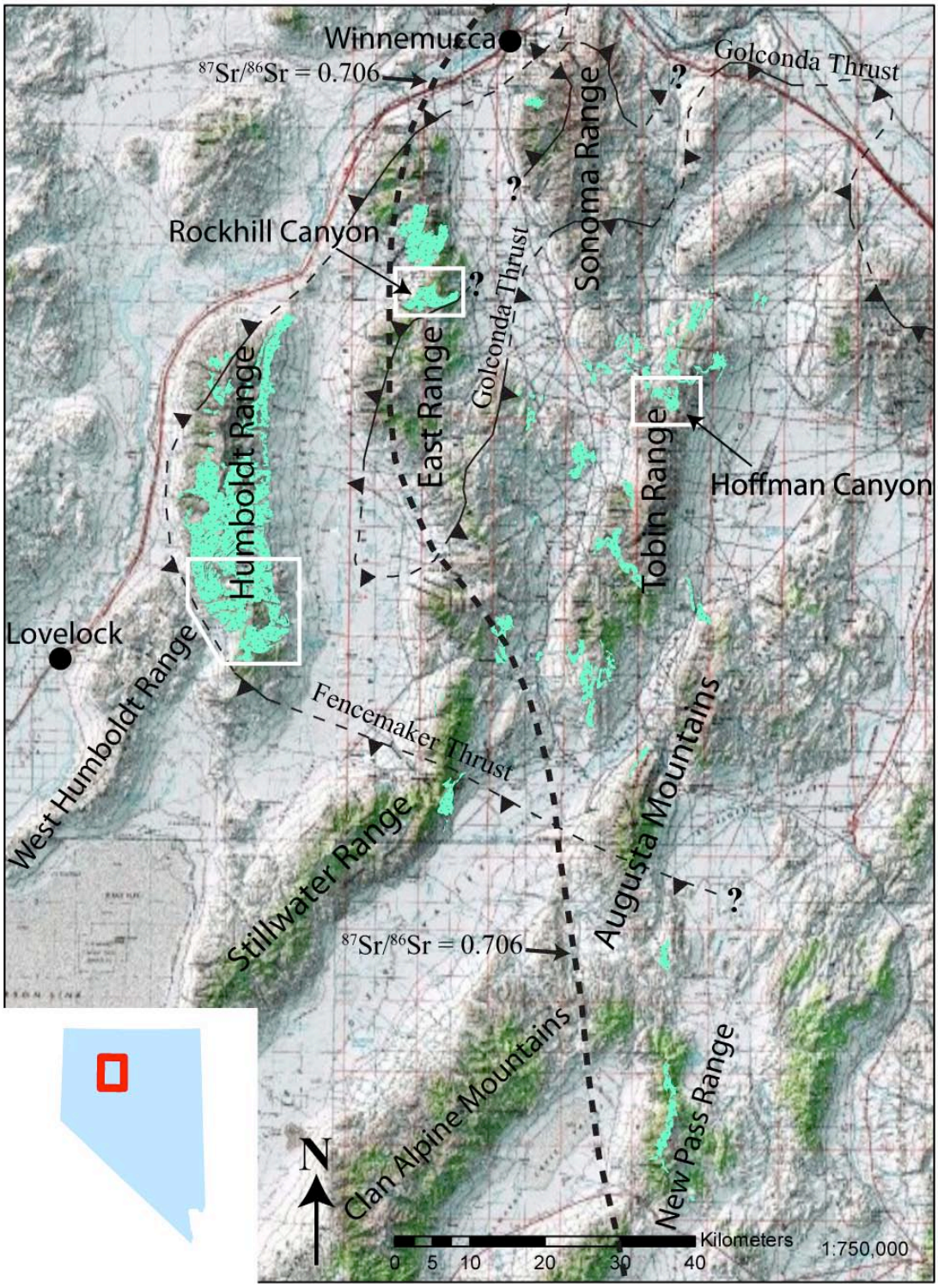

Figure 3.1. Topographic map of central Nevada showing the location of outcrops of the Koipato Formation and related units (bright green). Important mountain ranges and canyons are noted. White boxes outline the main field areas discussed in this report. Golconda and Fencemaker Thrust trends from Wilkins (2010). The $^{87}Sr/^{86}Sr = 0.706$ line is from Elison et al. (1990). Modified from Crafford (2007).

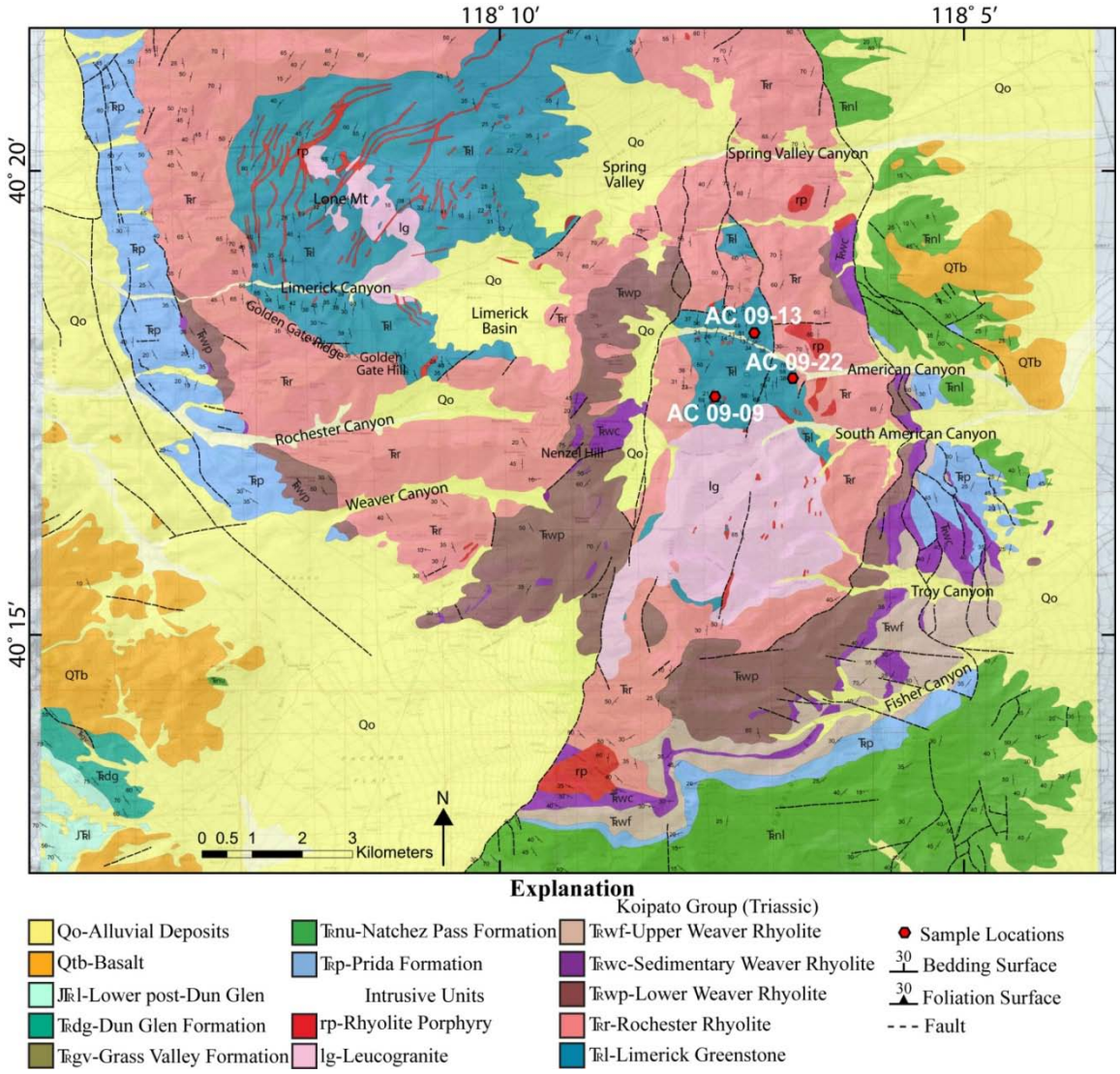

Figure 3.2. Geologic map of the southern Humboldt Range slightly modified from Wallace et al. (1969a, b). Map depicts sample locations analyzed in this study and geologic units discussed in the text.

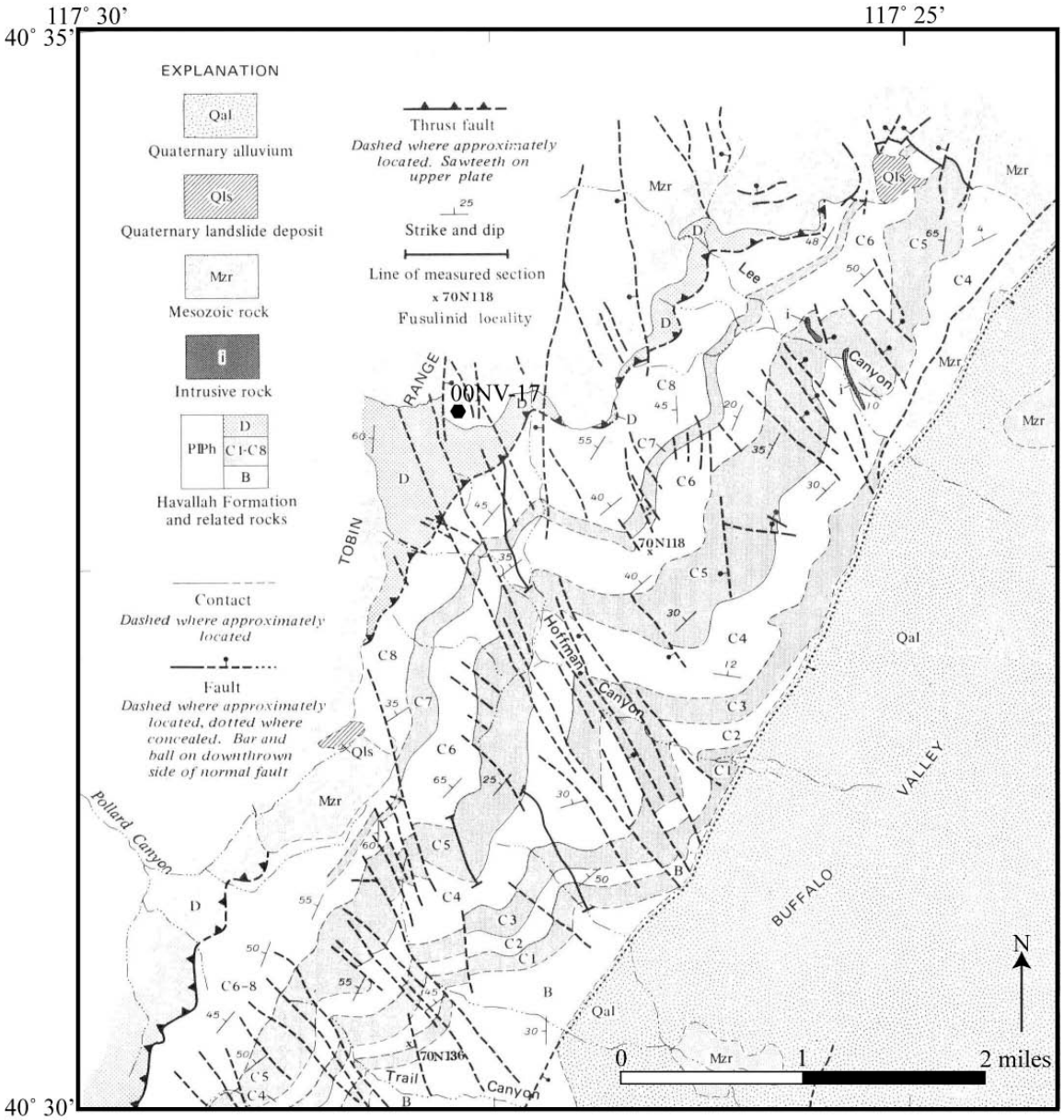

Figure 3.3. Geologic map of Hoffman Canyon in the Tobin Range from Stewart et al. (1977). Location of sample 00NV-17 is approximated on the map.

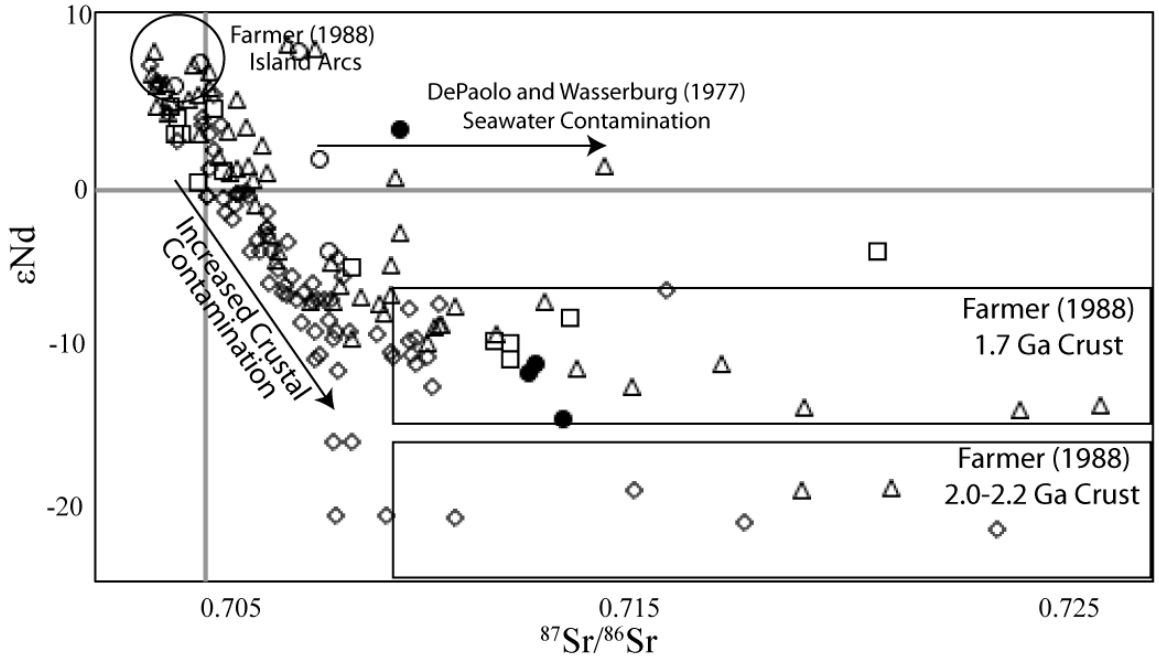

Figure. 3.4. εNd vs. $^{87}Sr/^{86}Sr$ plot showing the values of four samples (solid circles) from the Koipato Formation reported in this study and other Mesozoic and Tertiary samples from DePaolo (1981), Farmer and DePaolo (1983; 1984), Samson et al. (1989), and DePaolo and Daley (2000). Open circles = Triassic, open squares = Jurassic, open triangles = Cretaceous, and open diamonds = Tertiary. Arrow showing increased crustal contamination is taken from Farmer (1988).

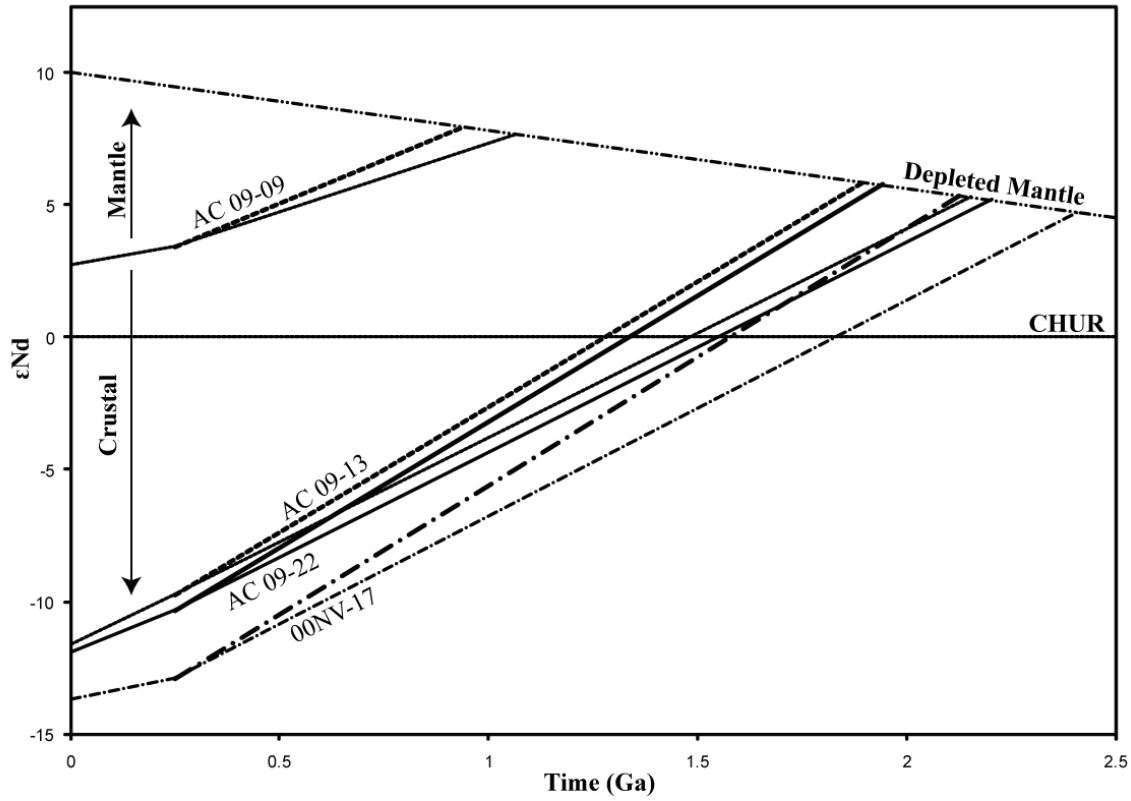

Figure 3.5. εNd isotopic evolution for samples from the Koipato Formation analyzed in this report. εNd evolution models are based upon average bulk (thin lines) and upper (thick lines) continental crustal compositions from Rudnick and Fountain (1995). All modeling is conducted after time of deposition of units, which is pinpointed at 249 Ma.

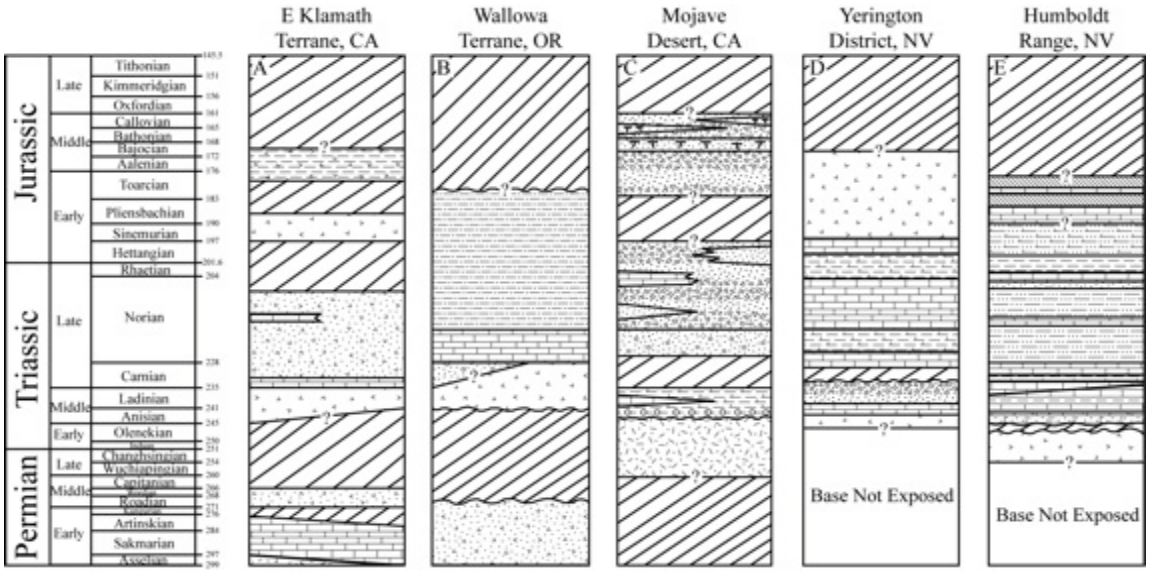

Figure 3.6. Comparison of generalized stratigraphic columns from Eastern Klamath terrane, Wallowa terrane, Mojave Desert area, Yerington District, and the Humboldt Range. (A) Data are from (Watkins, 1985; Miller and Harwood, 1990) adjusted to most recent timescale. (B) Data are from (Brooks and Vallier, 1978; Dorsey and LaMaskin, 2007; Tumpane, 2010) adjusted to most recent timescale. (C) Data are from (Saleeby and Busby-Spera, 1992; Miller et al., 1995) adjusted to most recent timescale. (D) Data are from (Hardyman, 1980; Stewart, 1997; Proffett and Dilles, 2008) adjusted to most recent timescale. (E) Data are from (Silberling and Wallace, 1969; Johnson, 1977; Elison and Speed, 1988; Saleeby and Busby-Spera, 1992; Proffett and Dilles, 2008) adjusted to most recent timescale and with the new ages for the duration of Koipato Formation volcanism as determined in this study.

Table 3.1. Summary of Sample Locations, Ages, and Sr and Sm-Nd Isotopic Data

Sample Name	Lithology	Formation	Latitude	Longitude	$^{206}Pb/^{238}U$ Age (Ma)	Sr ppm	87Sr/86Sr(T)	± 2σ [abs]	[Sm] ppm	[Nd] ppm	147Sm/144Nd	143Nd/144Nd	± 2σ [abs]	εNd (T)
AC 09-09	Rhyolite porphyry	Dike	40.292	-118.128	249.07 ± 0.14	46.8	0.708912	9	80.0	276.8	0.1747	0.512778	7	3.43
00NV-17	Rhyolite tuff breccia	Rochester	40.553	-117.460	249.14 ± 0.14	1569	0.712625	6	756.8	2660	0.1720	0.511937	5	-12.89
AC 09-22	Intermediate intrusive	Limerick	40.295	-118.114	249.37 ± 0.10	1621	0.711839	7	661.2	2720	0.1469	0.512027	4	-10.34
AC 09-13	Intermediate intrusive	Limerick	40.302	-118.121	249.59 ± 0.08	962.2	0.711996	8	554.3	2421	0.1384	0.512044	4	-9.73

Notes: Lat/Long coordinates are in WGS 1984 datum.
-Sr and Sm-Nd measurements were made on a GV Isoprobe-T multicollector thermal ionization mass spectrometer in either static or dynamic Faraday mode.
-Errors on 147Sm/144Nd measurement at 2σ are 0.0003.
-2σ errors on 143Nd/144Nd are in the 6th decimal place, e.g. 0.000004.
-2σ errors on 87Sr/86Sr are in the 6th decimal place, e.g. 0.000006.

References Cited

Bennett, V.C., and DePaolo, D.J., 1987, Proterozoic crustal history of the western United States as determined by neodymium isotopic mapping: Geological Society of America Bulletin, v. 99, p. 674-685.

Brooks, H.C., and Vallier, T.L., 1978, Mesozoic rocks and tectonic evolution of eastern Oregon and western Idaho, in Howell, D.G., and McDougall, K.A., eds., Mesozoic paleogeography of the Western United States, Pacific Coast Paleogeography Symposium 2: Los Angeles, Pacific Section, Society of Economic Paleontologists and Mineralogists, p. 133-146.

Burchfiel, B.C., Cowan, D.S., and Davis, G.A., 1992, Tectonic overview of the Cordilleran orogen in the western United States, in Burchfiel, B.C., Lipman, P.W., and Zoback, M.L., eds., The Cordilleran Orogen: Conterminous U.S., Volume G-3: The Geology of North America: Boulder, Colorado, Geological Society of America, p. 407-479.

Burke, D.B., 1973, Reinterpretation of the Tobin thrust – Pre-Tertiary geology of the southern Tobin Range, Pershing County, Nevada: Ph.D. thesis, Stanford University, Stanford, California, 82 p.

Burke, D.B., and Silberling, N.J., 1973, The Auld Lang Syne Group, of Late Triassic and Jurassic (?) age, north-central Nevada: U.S. Geological Survey Bulletin 1394-E, 14 p.

Crafford, A.E.J., 2007, Geologic Map of Nevada: U.S. Geological Survey Data Series 249.

DePaolo, D.J., 1981, A Neodymium and Strontium Isotopic Study of the Mesozoic Calc-Alkaline Granitic Batholiths of the Sierra Nevada and Peninsular Ranges, California: Journal of Geophysical Research, v. 86, no. B11, p. 10470-10488.

DePaolo, D.J., and Farmer, G.L., 1984, Isotopic data bearing on the origin of Mesozoic and Tertiary granitic rocks in the western United States: Phil. Trans. R. Soc. London, A 310, p. 743-753.

DePaolo, D.J., and Wasserburg, G.J., 1977, The sources of island arcs as indicated by Nd and Sr isotopic studies: Geophysical Research Letters, v. 4, no. 10, p. 465-468.

DePaolo, D.J., and Daley, E.E., 2000, Neodymium isotopes in basalts of the southwest basin and range and lithospheric thinning during continental extension: Chemical Geology, v. 169, p. 157-185.

Dickinson, W.R., 1977, Paleozoic plate tectonics and the evolution of the Cordilleran continental margin, in Stewart, J.H., Stevens, C.H., and Fritsche, A.E., eds., Paleozoic paleogeography of the western United States: Pacific Coast Paleogeography Symposium 1: Los Angeles, Society of Economic Paleontologists and Mineralogists, Pacific Section, p. 137-155.

—, 2004, Evolution of the North American Cordillera: Annual Review of Earth and Planetary Sciences, v. 32, p. 13-45.

—, 2006, Geotectonic evolution of the Great Basin: Geosphere, v. 2, p. 353–368.

Dorsey, R.J., and LaMaskin, T.A., 2007, Stratigraphic record of Triassic-Jurassic collisional tectonics in the Blue Mountains Province, northeastern Oregon: American Journal of Science, v. 307, p. 1167-1193.

Dunston, J.R., Northrup, C.J., and Snyder, W.S., 2001, Post-Latest Triassic thrust emplacement of the Golconda Allochthon, Sonoma Range, Nevada [abs.]: GSA Annual Meeting.

Elison, M.W., and Speed, R.C., 1988, Triassic flysch of the Fencemaker allochthon: fan facies and provenance: Geological Society of America Bulletin, v. 100, p. 185-199.

—, 1989, Structural development during flysch basin collapse: the Fencemaker allochthon, East Range, Nevada: Journal of Structural Geology, v. 11, no. 5, p. 523-538.

Elison, M.W., Speed, R.C., and Kistler, R.W., 1990, Geologic and isotopic constraints on the crustal structure of the northern Great Basin: Geological Society of America Bulletin, v. 102, p. 1077-1092.

Farmer, G.L., 1988, Isotope geochemistry of Mesozoic and Tertiary igneous rocks in the western United States and implications for the structure and composition of the deep continental lithosphere, in Ernst, W.G., ed., Metamorphism and crustal evolution of the western United States: W.W. Rubey v. VII, p. 87-109.

Farmer, G.L., and DePaolo, D.J., 1983, Origin of Mesozoic and tertiary granite in the western United States and implications for pre-Mesozoic crustal structure: 1. Nd

and Sr isotopic studies in the geosyncline of the northern Great Basin: Journal of Geophysical Research, v. 88, p. 3379-3401.

—, 1984, Origin of Mesozoic and tertiary granite in the western United States and implications for pre-Mesozoic crustal structure: 2. Nd and Sr isotopic studies of unmineralized and Cu- and Mo- mineralized granite in the Precambrian craton: Journal of Geophysical Research, v. 89, p. 10141-10160.

Farmer, G.L., Perry, F.V., Semken, S., Crowe, B., Curtis, D., and DePaolo, D.J., 1989, Isotopic Evidence on the Structure and Origin of Subcontinental Lithospheric Mantle in Southern Nevada: Journal of Geophysical Research, v. 94, no. B6, p. 7885-7898.

Ferguson, H.G., Roberts, R.J., and Muller, S.W., 1952, Geology of the Golconda quadrangle, Nevada: U.S. Geological Survey Geologic Quadrangle Map GQ-15.

Fleck, R.J., 1990, Neodymium, strontium, and trace element evidence of crustal anatexis and magma mixing in the Idaho batholith, in Anderson, J.L., ed., The nature and origin of Cordilleran magmatism: Geological Society of America Memoir 174, p. 359-373.

Hardyman, R.F., 1980, Geologic Map of the Gillis Canyon Quadrangle, Mineral County, Nevada: U.S. Geological Survey Miscellaneous Investigations Map I-1237.

Johnson, M.G., 1977, Geology and Mineral Deposits of Pershing County, Nevada: Nevada Bureau of Mines and Geology Bulletin 89, 115 p.

Jones, A.E., 1990, Geology and tectonic significance of terranes near Quinn River Crossing, Nevada, in Harwood, D.S. and Miller, M.M. eds., Paleozoic and Mesozoic Paleogeographic Relations: Sierra Nevada, Klamath Mountains, and Related Terranes: Geological Society of America Special Paper 225, p. 239-253.

Jones, A.E., Langenheim, V.E., Jones, D.L., and Renne, P., 1988, new age data from Quinn River Crossing, Humboldt County, Nevada: Implications for Paleozoic and Mesozoic tectonics: Geological Society of America Abstracts with programs, v. 20, p. A109-A110.

Ketner, K.B., 1984, Recent studies indicate that major structures in northwestern Nevada and the Golconda thrust in north-central Nevada are of Jurassic or Cretaceous age: Geology, v. 12, p. 483-486.

Ketner, K.B., and Ross, R.J., Jr., 1983, Preliminary geologic map of the northern Adobe Range, Elko County, Nevada: U.S. Geological Survey Open-File Map 83-290.

Ketner, K.B., and Wardlaw, B.R., 1981, Permian and Triassic rocks near Quinn River Crossing, Humboldt Country Nevada: Geology, v. 10, p. 298-303.

Kistler, R.W., and Speed, R.C., 2000, $^{40}Ar/^{39}Ar$, K-Ar, Rb-Sr Whole-Rock and Mineral Ages, Chemical Composition, Strontium, Oxygen and Hydrogen Isotopic Systematics of Jurassic Humboldt Lopolith and Permian(?) and Triassic Koipato Group rocks, Pershing and Churchill Counties, Nevada: U.S. Geological Survey Open-File Report 00-217, 14p.

Knopf, A., 1924, Geology and ore deposits of the Rochester District, Nevada, U.S. Geological Survey Bulletin 762.

Kurz, G., 2010, Geochemical, Isotopic, and U-Pb Geochronologic Investigations of Intrusive Basement Rocks from the Wallowa and Olds Ferry Arc Terranes, Blue Mountains Province, Oregon-Idaho: Ph.D. thesis, Boise State University, Boise, Idaho, 278 p.

MacMillan, J.R., 1972, Late Paleozoic and Mesozoic Tectonic events in west central Nevada: Ph.D. thesis, Northwestern University, Evanston, Illinois, 146 p.

Miller, E.L., and Cameron, C.S., 1982, Late Precambrian to Late Cretaceous evolution of the southwestern Mojave Desert, California, in Cooper, J.D., Troxel, B.W., and Wright, L.A., eds., Geology of selected areas in the San Bernardino Mountains, western Mojave Desert and southern Great Basin, California: Geological Society of America Volume and Guidebook, Shoshone, California, Death Valley Publishing Company, p. 21-34.

Miller, J.S., Glazner, A.F., Walker, J.D., and Martin, M.W., 1995, Geochronologic and isotopic evidence for Triassic-Jurassic emplacement of the eugeoclinal allochthon in the Mojave Desert region, California: Geological Society of America Bulletin, v. 107, no. 12, p. 1441-1457.

Miller, M.M., 1988, Permo-Triassic(?) deformation within the eastern Klamath terrane, northern California: Geological Society of America Abstracts with Programs, v. 20, p. 216.

Miller, M.M., and Harwood, D.S., 1990, Paleogeographic setting of upper Paleozoic rocks in the northern Sierra and eastern Klamath terranes, northern California, in Harwood, D.S., and Miller, M.M., eds., Paleozoic and early Mesozoic

paleogeographic relations; Sierra Nevada, Klamath Mountains, and related terranes: Geological Society of America Special Paper 255, p. 175-192.

Northrup, C.J., and Snyder, W.S., 2000, Significance of the Sonoma Orogeny, Western U.S.: What, Where, and When? Geological Society of Nevada Symposium 2000, Program with Abstracts, p. 66-67.

Proffett, J.M., and Dilles, J.H., 2008, Lower Mesozoic sedimentary and volcanic rocks of the Yerington region, Nevada, and their regional context, in Wright, J.E., and Shervais, J.W., eds., Ophiolites, Arcs, and Batholiths: A Tribute to Cliff Hopson: Geological Society of America Special Paper 438, p. 251–288.

Roberts, R.J., Hotz, P E., Gilluly, J., and Ferguson, H.G., 1958, Paleozoic rocks of north-central Nevada: American Association of Petroleum Geologists Bulletin, v. 42, p. 2813-2857.

Rogers, J.J., Burchfiel, B.C., Abbott, E.W., Anepohl, J.K., Ewing, A.H., Koehnken, J.M., Novitsky-Evans, J.M., and Talukdar, S.C., 1974, Paleozoic and lower Mesozoic volcanism and continental growth in the western United States: Geological Society of America Bulletin, v. 85, p. 1913-1924.

Rudnick, R.L., and Fountain, D.M., 1995, Nature and Composition of the Continetal Crust: A Lower Crustal Perspective: Reviews of geophysics, v. 33, p. 267-309.

Saleeby, J.B., and Busby-Spera, C., 1992, Early Mesozoic tectonic evolution of the western U.S. Cordillera, in Burchfiel, B.C., Lipman, P.W., and Zoback, M.L., eds., The Cordilleran Orogen: Conterminous U.S., Volume G-3: The Geology of North America: Boulder, Colorado, Geological Society of America, p. 107-168.

Samson, S.D., McClelland, W.C., Patchett, P.J., Gehrels, G.E., and Anderson, R.G., 1989, Evidence from neodymium isotopes for mantle contributions to Phanerozoic crustal genesis in the Canadian Cordillera: Nature, v. 337, p. 705-709.

Silberling, N.J., 1973, Geologic events during the Permian-Triassic time along the Pacific margin of the United States, in Logan, A., and Hills, L.V., eds. The Permian and Triassic systems and their mutual boundary: Canada Society of Petroleum Geologists Memoir 2, p. 345-362.

Silberling, N.J. and Roberts, R.J., 1962, Pre-Tertiary stratigraphy and structure of northwestern Nevada: Geological Society of America, Special Paper 72, 58 p.

Silberling, N.J., and Wallace, R.E., 1969, Stratigraphy of the Star Peak Group (Triassic) and overlying Mesozoic rocks, Humboldt Range, Nevada: U.S. Geological Survey, Profesional Paper 592, 50 p.

Silberling, N.J., and Jones, D.L., 1982, Tectonic significance of Permian-Triassic strata in northwestern Nevada and northern California: Geological Society of America Abstracts with Programs, v. 14, p. 234.

Snyder, W.S., and Brueckner, H.K., 1983, Tectonic evolution of the Golconda allochthon, Nevada: Problems and perspectives, in Stevens, C.H., ed., Pre-Jurassic rocks in western North American suspect terranes: Society of Economic Paleontologists and Mineralogists, Pacific Section, p. 103-123.

—, 1989, Permian-Carboniferous tectonics of the Golconda Allochthon; an accreted terrane in the Western United States: Compte Rendu 4 – XI Congres International de Stratigraphie et de Geologie du Carbonifere, p. 294-312.

Speed, R.C., 1977, Island-arc and other paleogeographic terranes of late Paleozoic age in the western Great Basin, in Stewart, J.H., Stevens, C.H., and Fritsche, A.E., eds., Paleozoic paleogeography of the western United States: Pacific Coast Paleogeography Symposium 1: Los Angeles, Society of Economic Paleontologists and Mineralogists, Pacific Section, p. 349-362.

—, 1979, Collided Paleozoic microplate in the western United States: Journal of Geology, v. 87, p. 279-292.

Speed, R.C., and Sleep, N.H., 1982, Antler orogeny and foreland basin: A model: Geological Society of America Bulletin, v. 93, p. 815-828.

Sperling, E.A., and Ingle, J.C., Jr., 2006, A Permian–Triassic boundary section at Quinn River Crossing, northwestern Nevada, and implications for the cause of the Early Triassic chert gap on the western Pangean margin: Geological Society of America Bulletin, v. 118, no. 5/6, p. 733-746.

Stewart, J.H., 1997, Triassic and Jurassic Stratigraphy and Paleogeography of West-Central Nevada and Eastern California with a Correlation Diagram of Triassic and Jurassic Rocks by Stewart, J.H., Silberling, N.J., and Harwood, D.S.: U.S. Geological Survey Open-File Report 97-0495, 57 p.

Stewart, J.H., MacMillan, J.R., Nichols, K.M., and Stevens, C.H., 1977, Deep-water upper Paleozoic rocks in north-central Nevada – A study of the type area of the Havallah Formation, in Stewart, J.H., Stevens, C.H., and Fritsche, A.E., eds.,

Paleozoic paleogeography of the western United States: Pacific Coast Paleogeography Symposium 1: Los Angeles, Society of Economic Paleontologists and Mineralogists, Pacific Section, p. 337-347.

Tumpane, K.P., 2010, Age and isotopic investigations of the Olds Ferry terrane and its relations to other terranes of the Blue Mountains province, eastern Oregon and west-central Idaho: M.S. thesis, Boise State University, Boise, Idaho, 220 p.

Vikre, P.G., 1977, Geology and Silver Mineralization of the Rochester District, Pershing County, Nevada: Ph.D. thesis, Stanford University, Stanford, California, 404 p.

Wallace, R.E., Tatlock, D.B., Silberling, N.J., and Irwin, W.P., 1969a, Geologic map of the Unionville Quadrangle, Pershing County, NV: U.S. Geological Survey Geologic Quadrangle Map GQ-820.

Wallace, R.E., Silberling, N.J., Irwin, W.P., and Tatlock, D.B., 1969b, Geologic map of the Buffalo Mountain Quadrangle, Pershing and Churchill Counties, NV: U.S. Geological Survey Geologic Quadrangle Map GQ-821.

Watkins, R., 1985, Volcaniclastic and carbonate sedimentation in late Paleozoic island-arc deposits, eastern Klamath Mountains, California: Geology, v. 13, p. 709-713.

Wheeler, H.E., 1939, Helicoprion in the Anthracolithic (Late Paleozoic) of Nevada and California, and its stratigraphic significance: Journal of Paleontology, v. 13, no. 1, p. 103–114.

White, J.D.L., and Houghton, B.F., 2006, Primary volcaniclastic rocks: Geology, v. 34, no. 8, p. 677-680.

Wilkins, J., 2010, Structural and Stratigraphic Age Constraints of the Inskip Formation, East Range, Nevada: Implications for Mesozoic Tectonics of Western North America: M.S. thesis, Boise State University, Boise, Idaho, 117 p.

Williams, H., 1939, The history and character of volcanic domes: University of California Publications, Bulletin of the Department of Geologic Science, v. 21, p. 51-146.